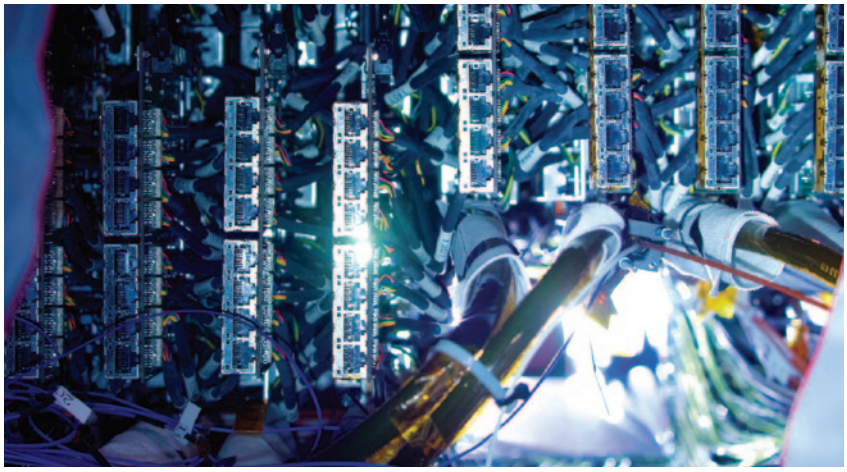

J-PARC

ANNUAL REPORT 2018

Vol.1: Highlight

Editorial Board (April 2019 – March 2020)

 Hideaki HOTCHI *(Accelerator Division)*

 Takayuki YAMAZAKI *(Materials and Life Science Division)*

 Masaharu IEIRI *(Particle and Nuclear Physics Division)*

 Kazuo GORAI *(Information System Section)*

 Shigeru SAITO *(Transmutation Division)*

 Fumihiro SAITO *(Safety Division)*

 Shinji NAMIKI *(Users Office Team)*

 Naomi EBISAWA *(Public Relations Section)*

Cover photographs

 Photograph ① : KOTO circuits, output connectors
Image credit: Masahiko UOTA

 Photograph ② : Extremely cold world
Image credit: Koji NUNOMURA

 Photograph ③ : Neutrino Experimental Facility
Image credit: Hiroshi ITO

J-PARC Annual Report 2018

Contents

Preface

This volume describes the progress made at J-PARC in fiscal year 2018, from April 2018 through March 2019.

We have been steadily improving the stability and beam power of the facilities towards the design power of 1 MW at the Material and Life Sciences Experimental Facility (MLF) and 0.75 MW for Fast Extraction (FX) and 0.1 MW for Slow Extraction (SX) at the Main Ring (MR).

At MLF, we were able to perform a continuous operation at 1 MW[1] for more than an hour. It provided a confidence to operate the MLF with the design power in a foreseeable future.

At the MR, we were able to provide a highest possible beam power operation within the current limitation of hardware, both in FX and SX mode. However, to our deepest regret, the SX beam time was cut short due to a malfunction of one of the bending magnets in the beam-transport line, 3-50BT, which transports the beam from the Rapid Cycle Synchrotron (RCS) to the MR. It clearly represented one of our weak points in the maintenance scenario, which will be improved soon.

[1] The operation at 1 MW means, the beam power at the RSC is 1 MW, and the extracted beam power to the MLF was 932 kW, due to beam bunches planned for an MR injection.

The continuous efforts to maintain the facilities with high availability and high beam power have resulted in many impactful scientific results produced with the users from both domestic and oversea research institutions and industries. Those results are described in this volume. Some of them were also shared with the community and society through press releases at a rate of more than one per month. We will continue this high level physics production mode by deepening and widening the collaborations with the users from all over the world, across the fields.

As was done in the previous years, we have been enhancing the collaboration with domestic universities, oversea institutions, and industrial sectors. We hope that deeper and wider collaboration will provide more impactful outcomes. It also helps creation of the future not only by expanding the frontier of academic knowledge and the variety of materials, but also by fostering the next generation of researchers with an extensive experience in cutting-edge facility operation, who can, in turn, produce the next generation of research facility for the future.

"High power beams for the next stage of our life!"

Naohito SAITO
On behalf of the J-PARC staff members,
Director of J-PARC Center

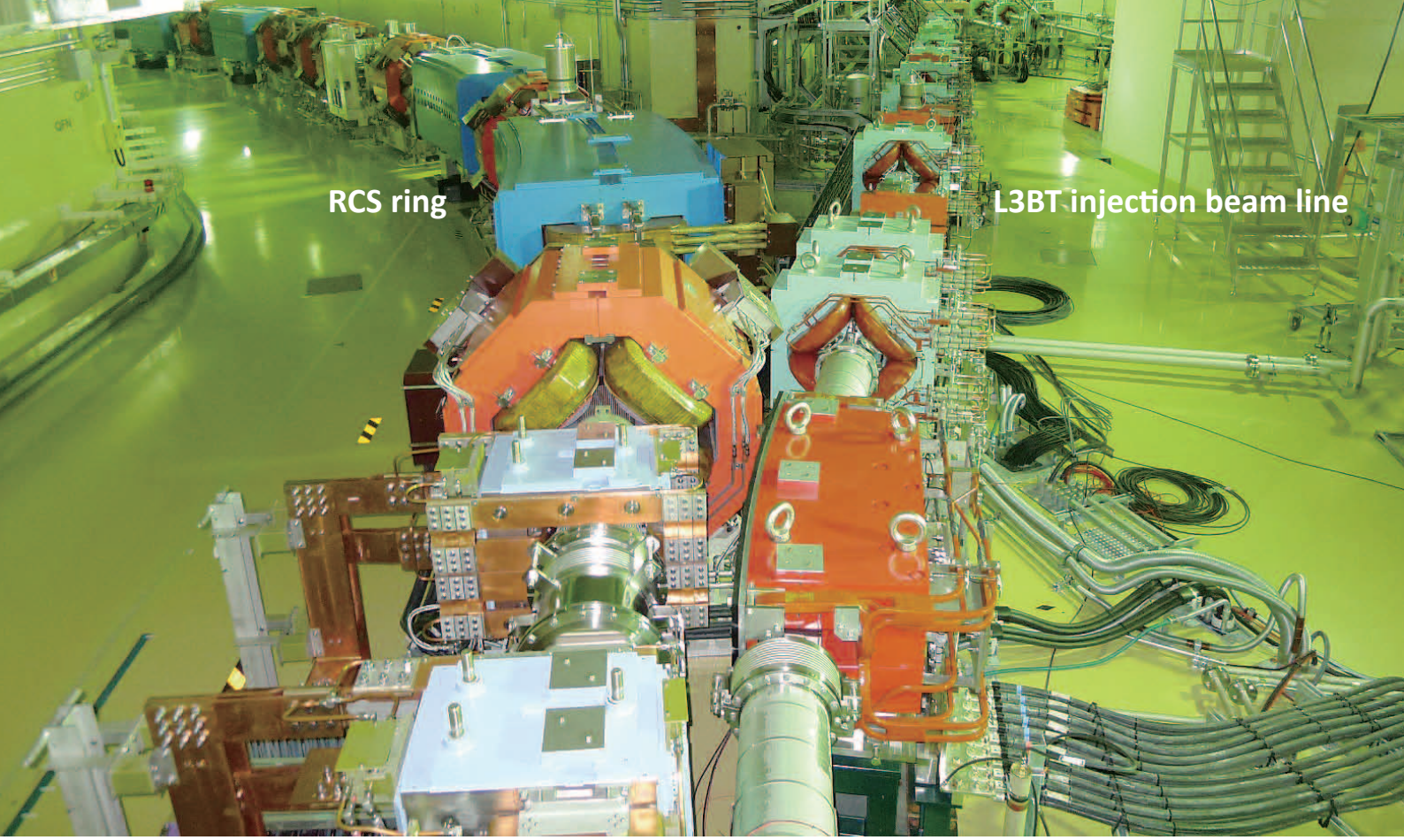

Accelerators

Overview of the Accelerator

The J-PARC accelerator complex consists of a 400 MeV linac, a 3 GeV Rapid Cycling Synchrotron (RCS) and a Main Ring Synchrotron (MR, 30 GeV). A proton beam from the RCS is injected to the Materials and Life Science Experimental Facility (MLF) for neutron and muon experiments. The MR has two beam extraction modes: fast extraction (FX) for the Neutrino experimental facility (NU) and slow extraction (SX) for the Hadron experimental facility (HD).

The operation in FY2018 is illustrated in Fig. 1. The topics related to the beam operation are as follows:

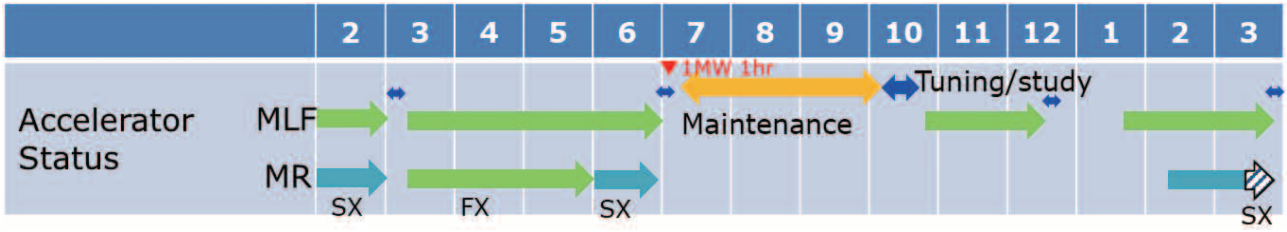

Fig. 1. Accelerator operation in FY2018 (includes a short period at the end of FY2017).

(1) Operation for the MLF

We started a new operation run on April 4, 2018 at 400-kW beam power for the MLF user operation. The beam power increased to 500 kW on April 19. The same beam power was maintained during FY2018 except for the startup and tuning/study.

After completion of the user operation before the summer shutdown, we had a study time in the beginning of July 2018. During that time, we successfully demonstrated 1 MW equivalent (8.3×10^{13} protons per pulse and 25 Hz) and one-hour duration operation for the MLF. The 1-MW demonstration took place for the first time in January 2015 as a single shot operation. Those results were the starting point of our work to achieve a continuous 1 MW operation.

Although the MLF beam power remained at 500 kW before and after the summer shutdown, the linac beam current was increased from 40 to 50 mA, which was a nominal current for 1 MW operation.

The shutdown period before and after the new year holidays was slightly longer than normal and continued from the end of December to mid-January. We had a power outage in the end of December due to refurbishment of an old power station of the Nuclear Science Research Institute of the Japan Atomic Energy Agency, to which our power line is connected. In mid-January, the MLF did not accept the beam because of the transportation of a used neutron production target to the storage building. We started the linac tuning on January 18, followed by the RCS and the MR tuning. The MLF user program started on January 23 and ended on March 26, as scheduled.

(2) Operation of the MR for the Neutrino Experiments (FX mode) and Hadron Experiment (SX mode)

The operation of the MR before the summer shutdown in 2018 was stable. The MR delivered beams to the NU at about 490 kW by the end of May. Then we switched the extraction mode from FX to SX and started tuning for the HD. We smoothly ramped up the power to 51 kW and the user program ended on June 29 before the summer shutdown.

The beam operation of the MR was suspended in the period from October to December due to improvement work on the experimental facilities: refurbishment of the Super-Kamiokande detector for the Neutrino experiment, and maintenance and upgrade work on the HD facility. During the beam suspension, a realistic test was carried out for a new magnet power supply for a future upgrade.

In January, we had a short (3-day long) machine study of the FX. Then, the beam tuning for the HD started in February, followed by the user program. The beam power was 51 kW as in the previous HD run in June 2018. The user program ran smoothly until March 18, when one of the bending magnets (named B15D) had a failure in the beam transport line from the RCS to the MR. The cause of the failure was a layer short of a coil.

The operation statistics for FY2018 (from April 2018 to March 2019) are shown in Table 1 and Fig. 2. The total operation time, which was defined as the shift leaders' on-duty time at the control room, including startup and RF conditioning, was 5,824 hours. The net user operation hours and the beam availability rate for each experimental facility were as follows: 4,129 hours (94%) for MLF; 1,053 hours (86%) for NU; and 1,089 hours (74%) for HD. These statistics show that the linac and the RCS operated properly. The cause of the low availability for the HD was the B15D trouble in March 2019.

The downtime by components is shown in Fig. 3. There were several causes of the downtimes. Over the last few years, we have taken many countermeasures against troubles at the linac: stabilization of the cooling water flow, inside cleaning of some SDTL cavities, replacement of old bias power supplies for the klystron high voltage power supply system (HVDC). We still had a long HVDC down time, due to a failure of the old 324 MHz klystron.

There were no serious downtime events at the RCS. Discharges in the high voltage cables in the kicker magnet system were one of the major causes for the occasional minor interruptions.

The MR had several troubles: cooling water flow drop (QM), timing signal distribution system trouble (BM), vacuum tube failures (RF), oil leakage at the outside transformer (Injection). The longest down time (324 hours, out of the range) was due to a problem with the B15D magnet in the "Others" category.

Most of the improvement and upgrade work was carried out during the summer shutdown. These improved items, major causes for downtime, and beam power history are described in further chapters.

Table 1. Operation statistics in hours for FY2018. Figures in the parentheses in trouble columns show the lost time as a percentage.

Facility	User Time (hours)	Trouble, Acc.only (hours)	Trouble, Fac.only (hours)	Net Time (hours)	Availability, Total (%)
MLF	4,388	252 (5.7%)	6 (0.1%)	4,129	94.1
Neutrino (FX)	1,224	149 (12.2%)	22 (1.8%)	1,053	86.0
Hadron (SX)	1,477	366 (24.8%)	22 (1.5%)	1,089	73.7

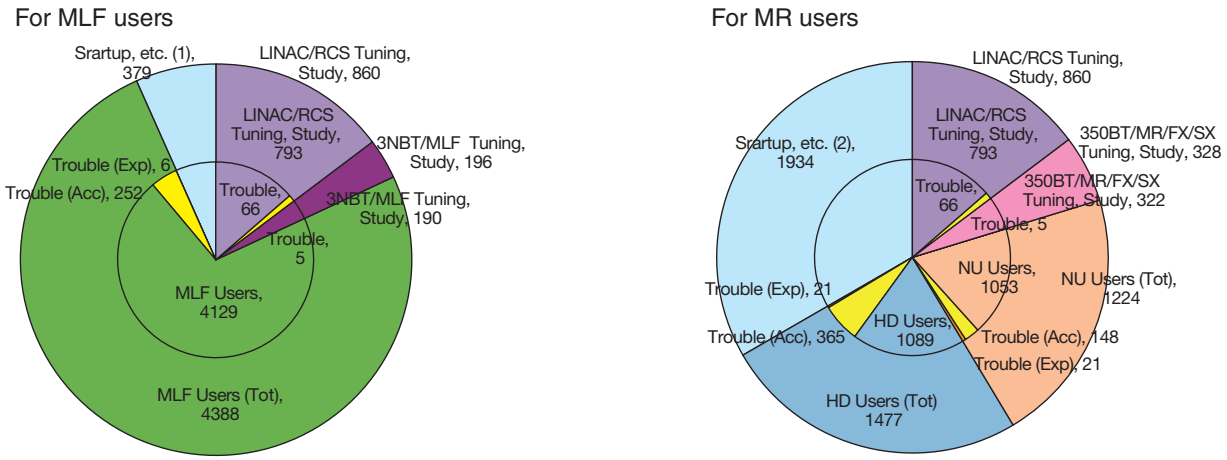

Fig. 2. Operation statistics for FY2018. The total operation time was 5,824 hours.

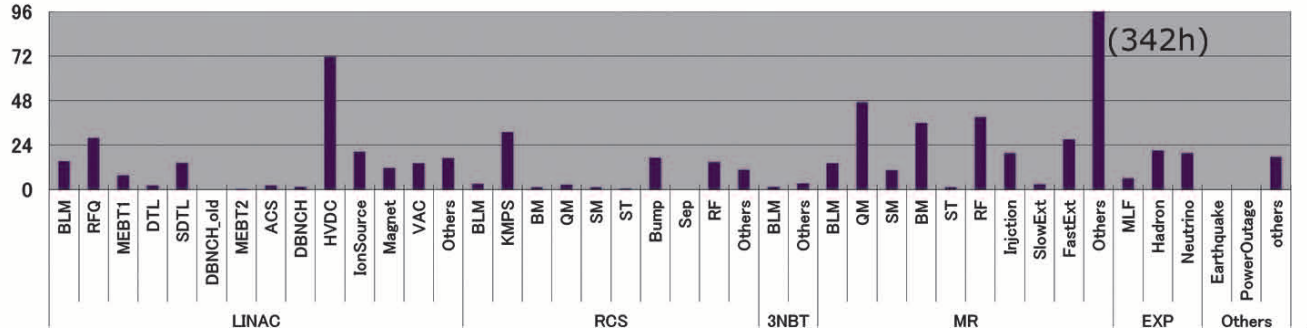

Fig. 3. Downtime by components in FY2018.

Linac

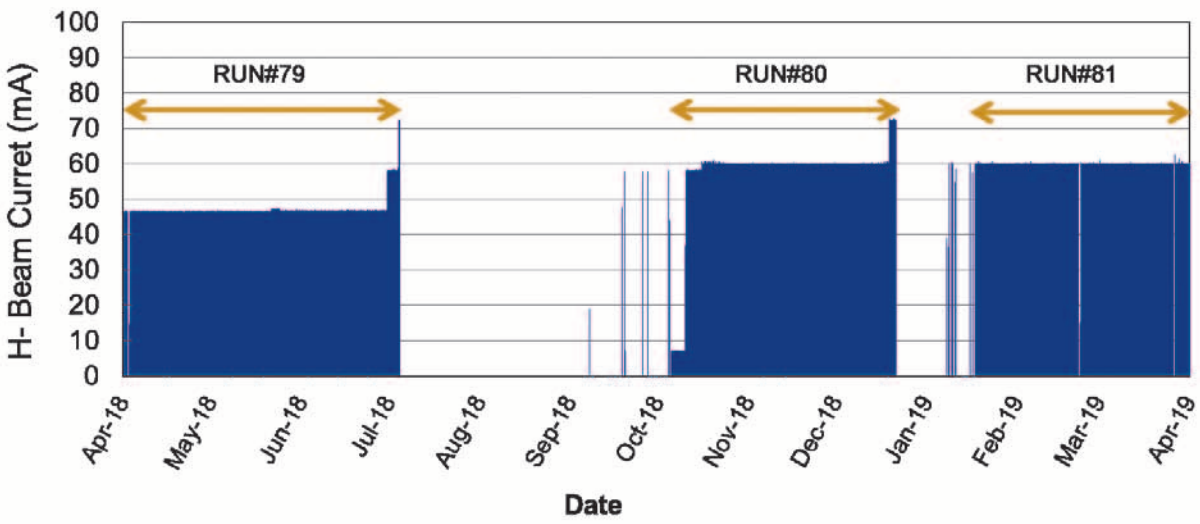

Fig. 4. Operation history of the ion source in FY2018.

Overview

The J-PARC linac has been operated with a nominal peak beam current of 50 mA since October 2018. High availability of approximately 94% (to the MLF) was achieved during FY2018 at the linac. Three 10-hour long beam stop events occurred due to the failure of a 324-MHz klystron, an ion source antenna and a klystron anode modulator. The number of trips due to the RFQ and the beam loss monitor (BLM) was still higher than that of other components. In the summer of 2018, we reconsidered the high voltage and the impedance of proportional counters for the BLM not to detect the event considered to be misfired (e.g.: fired by only one BLM). As a result, the trip rate due to the BLM decreased dramatically from 15-20 a day to a few a day. No increase in the activation of the accelerator components caused by this measure was observed.

Accelerator components status

The operation history of the ion source in FY2018 is shown in Fig. 4. We have gradually increased the continuous operation time of the ion source. In RUN#79, a continuous operation of approximately 2,200 hours was achieved with the typical beam current, pulse length and repetition rate of 47 mA, 300 μs and 25 Hz, respectively. After the 2018 summer shutdown, the peak current from the ion source increased to 60 mA so that the linac could inject the beam current of 50 mA into the RCS. At the end of RUN#79 and RUN#80, the ion source extracted stable 72 mA beams for high- intensity beam studies at the linac. In the RUN#81, unscheduled ion source replacement was performed due to an antenna malfunction during the operation.

Figure 5 shows the time variation of number of RFQ trips. We suppose the origin of the trip is the sparking between vane tips, which had been contaminated by carbon-related contaminants. Since the cryopumps installed at the RFQ have the potential to improve the vacuum condition, the vacuum ducts for the cryopumps were changed to manifold-type configurations in the 2018 summer shutdown. As a result, the vacuum pressure in the RFQ decreased by 20%. No significant improvement in the trip rate has been seen so far, but we will observe the trend in a long-term operation.

After the Great East Japan Earthquake in 2011, we could not input the design rf power into some SDTL cavities due to the multipactor effect. To improve this situation, we have polished the inside of the cavities by using acetone during the summer shutdown since 2015. After the treatment, the multipactor region disappeared completely, except in the SDTL05A cavity. We think that the SDTL05A was not cleaned up sufficiently, therefore we are going to retry the cavity cleaning of the SDTL05A in the summer of 2019.

The operation of the ACS cavities was more stable than the one of the other cavities. The number of trips of all the ACS cavities was less than once per day. In the summer of 2018, we replaced an RF window of one ACS cavity with a brand-new one in order to check the surface condition of the RF window, which has been used

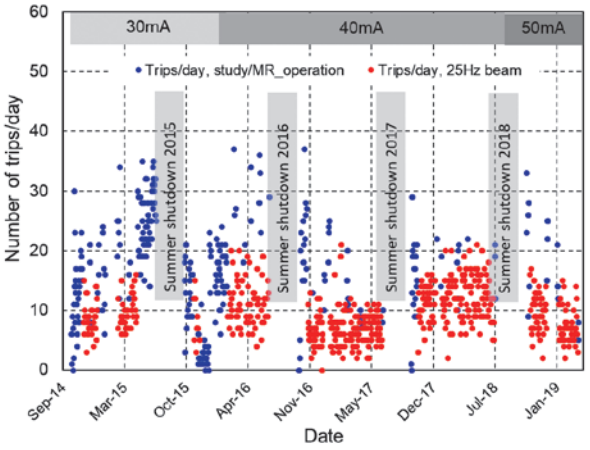

Fig. 5. Time variation of the number of RFQ RF-trips.

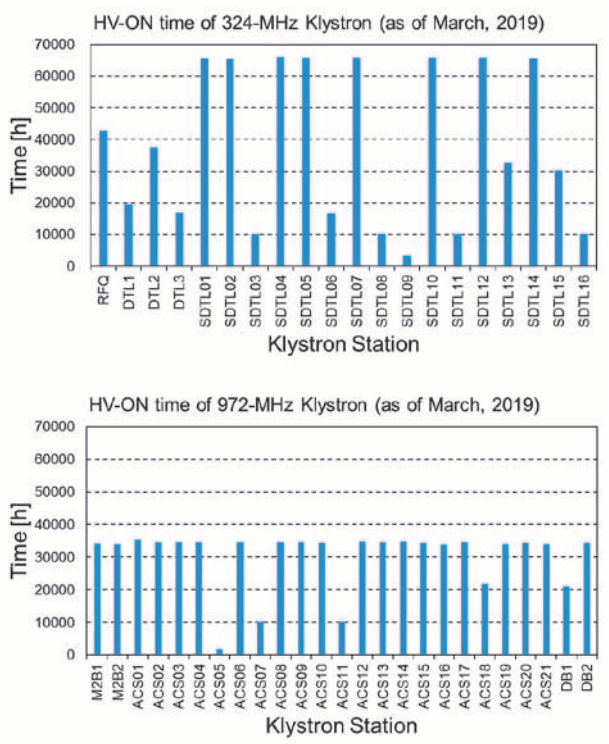

Fig. 6. The operation time of the 324-MHz klystron (upper) and 972-MHz klystron (lower) as of March 2019.

for about five years. The visual observation confirmed that the window has remained in good condition. We think that a periodical replacement of the ACS RF window will not be necessary for the next few years.

The RF chopper system, which is installed just after the RFQ, consists of two RF-deflecting cavities and a beam scraper. During every summer shutdown, we removed the used scraper from the beam line and measured the depth of damaged area using a laser microscope. After a 300-kW single bunch 2-month operation and a 400-kW single bunch 3-month operation, the depth of the damaged area was observed to be 0.7 mm. The result shows the depth can be evaluated to be approximately 1 mm in the case of a 9-month continuous 1-MW operation. This is tolerable level because the beam axis thickness of the scraper is 40 mm.

Klystron system status

We have been using two types of klystrons, such as a 324-MHz klystron and a 972-MHz one. The operation times of the two types of klystrons as of March 2019, are shown in Fig. 6. Eight out of twenty 324-MHz klystrons reached approximately 65,000 hours of operation, which has been the entire period since the linac operation was started. Most of the 972-MHz klystrons exceeded 30,000 hours of operation. In FY2018, one of each type of klystrons was replaced due to their performance degradation. A test-stand for the klystrons was built to perform off-line conditioning before installation in order to save replacement time. The test-stand will start to operate at full capacity in FY2019.

Beam monitor development

For higher intensity beam measurement, we have focused on a carbon nanotube (CNT) wire with its high

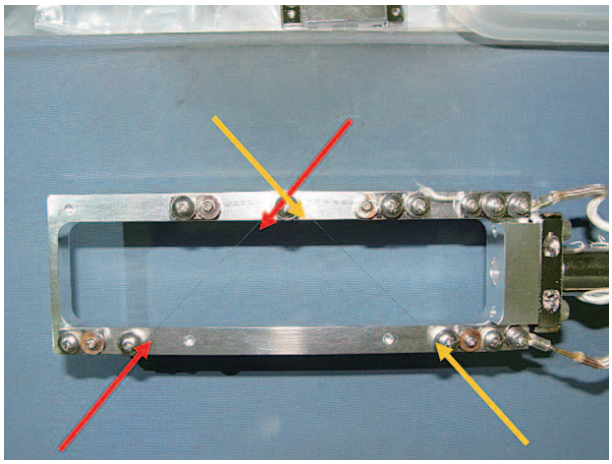

Fig. 7. Wire scanner monitor head equipped with a CNT wire.

tensile strength and electric conductivity. A new wire scanner monitor (WSM) based on the CNT wire (CNT-WSM) was developed, as shown in Fig. 7. The result of the off-line beam test showed that the CNT-WSM had the same dynamic range as the carbon-wire-type WSM, which has been used at a beam transport between the RFQ and the DTL. In the summer of 2018, we installed the CNT-WSM at the MEBT1 section. Currently, the CNT-WSM works without any issues at the beam line.

To conduct more precise beam studies by measuring a longitudinal beam profile, since 2016 we have

implemented the plan to install three bunch shape monitors (BSMs) at the ACS section. The last BSM was installed in the summer of 2018, and the installation program at the ACS section was completed.

Beam study

The beam studies have been performed to resolve some issues such as the Intra-Beam Stripping (IBSt) mitigation in the ACS section, the momentum stability at the linac exit, the precise beam measurement at the MEBT1, and so on.

The dominant source of the beam loss is found to be IBSt in H^- beam in the ACS section. Because the loss rate by the IBSt can be affected only by a beam optics, some optics with the different temperature ratio between transverse and longitudinal planes (Tx/Tz) were examined. Numerical simulations and the beam study results showed that the loss rate with Tx/Tz=0.7 optics was 40% lower than that with Tx/Tz=1.0, which is the J-PARC linac baseline design based on the equipartitioning setting. The Tx/Tz=0.7 optics will be applied to the operation from April 2019.

We are considering a further upgrade plan to increase the RCS beam power to 1.5 MW. To realize the upgrade plan, the beam current and the beam pulse length must increase to 60 mA and 600 μs respectively. The first 400-MeV and 56-mA beam at the linac exit was demonstrated in December 2017. In this demonstration, a significant decrease of the beam transmission was observed in the RFQ and the beam scraper of the RF chopper system. At the second demonstration, which was conducted in July 2018, we increased the RFQ tank level and expanded the scraper gap without affecting the extinction in order to improve the beam transmission. At the demonstration, the beam current from the ion source was also increased from 68 mA to 72 mA. By applying these measures, we successfully obtained 400-MeV and 62-mA beam at the linac exit, as shown in Fig. 8. A numerical simulation showed that the reduction of the beam halo from the ion source was effective in improving the RFQ transmission. Further high-intensity beam studies will be conducted.

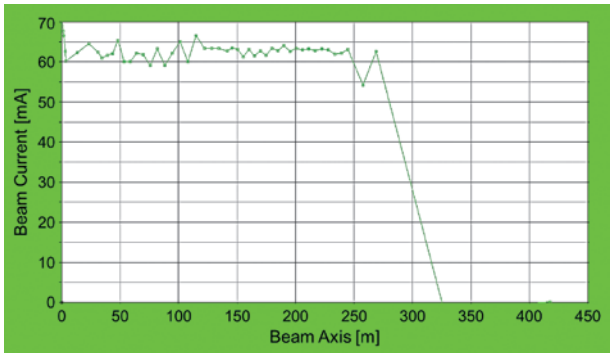

Fig. 8. Result of a 400-MeV and 60-mA demonstration at the linac.

RCS

Operational status

In JFY 2018, the operation beam power of RCS was started at 400 kW for the MLF. It was immediately increased to 500 kW at the end of April and maintained at that level during JFY 2018, except in the beginning of October. Meanwhile, the MR output power was steadily increased as the MR commissioning progressed. Figure 9 shows the change in the RCS output power with respect to time.

This year, there were no serious problems in the RCS. The major problems were the discharge of Pulse Forming Network (PFN) cables in the kicker magnet system. The discharges occurred twice, and we were not able to recover quickly. Therefore, after the second discharge incident the bump orbit made by the correction magnets near the extraction area compensated the shortage of the kick angle. Although the loss at the septum magnets increased several times over the usual operation, the dose rate was usually 100 μSv / h or lower, so we considered it acceptable and continued the operation under this condition. The dose after the operation was within the expectations.

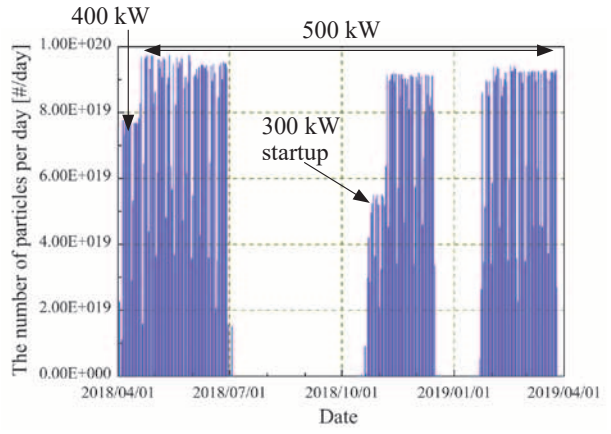

Fig. 9. Changes in the RCS output particles over time.

The availability of the RCS was summarized in the Table 2. The operation time for the MLF over the year was approximately 4130 h, excluding the commissioning time, and downtime of approximately 54 h; therefore, its overall availability was 98.4%. For the Neutrino and Hadron users, the availability of RCS was almost the same as in the MLF case and the availability value was around 99%.

Table 2. Summary of the availability

Facility	User time (hr)	Trouble in RCS (hr)	Availability of RCS (%)
MLF	4129:46	53:52	98.4
Neutrino	1053:32	8:28	99.2
Hadron	1089:28	3:06	98.9

Maintenance and improvements

1) Foil production

In J-PARC RCS, The Hybrid type thick Boron-doped Carbon (HBC) foil was used for charge exchange injection. It had been produced in KEK laboratory since the beginning of RCS commissioning. However, due to the retirement of the expert of the HBC foil production, the further manufacturing of the HBC foil in KEK became problematic. Therefore, the foil deposition system in KEK was moved to the J-PARC site to continue the HBC foil production. By using this system, we started research and development to produce more robust foil.

With some trial-and-errors, we produced new HBC foil. The performance of the new HBC foil was evaluated by using the heavy ion beam facilities in Takasaki Advanced Radiation Research Institute of National Institute for Quantum and Radiological Science and Technology before installing it in the RCS. The test result indicated that the new HBC foil would be almost as durable as the original KEK HBC foil. Finally, one new foil was tested during a 10-day user operation on June 2018, and it endured during this period. As a result, we have been using this new HBC foil from October for the full user operation. Figure 10 shows the new HBC foil before and after a 2-month operation.

2) Movable collimator installation

The beam collimation system removes the beam halo and localizes the beam loss to preserve the other accelerator components. The collimation system comprises one primary collimator, which scatters the halo particles, and five secondary collimators, which absorb those scattered particles. The radiation shielding around the collimator chamber was designed in a way that allowed the collimator system to absorb a halo of up to 4 kW.

In April 2016, a malfunction occurred in the VME system, i.e., the collimator's control system, and this malfunction caused a vacuum leak.

After an investigation, it was found that the fifth secondary collimator was the source of the leak, which

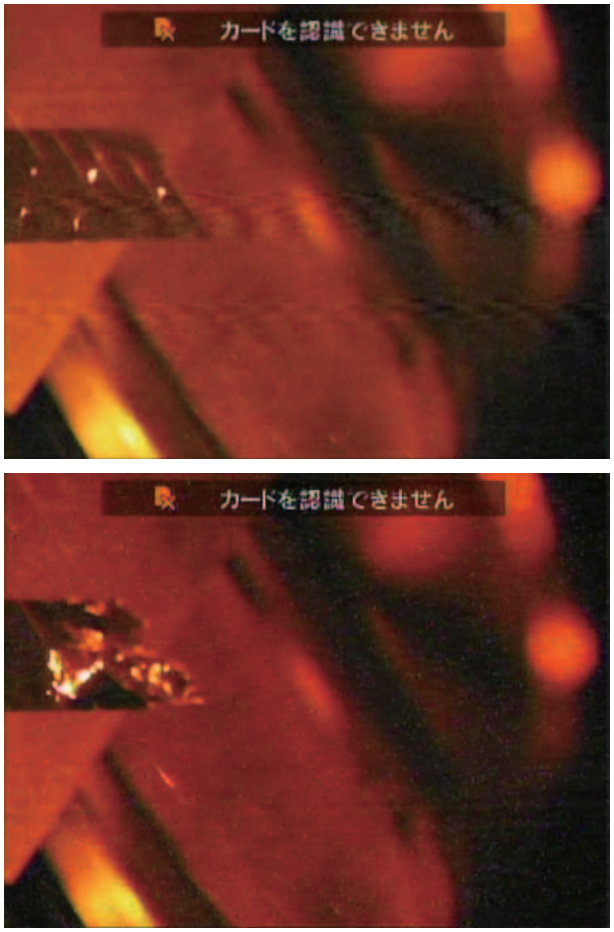

Fig. 10. The new HBC foil before (upper) and after a 2-month operation (lower).

was caused by a collision of the collimator blocks. We installed a spare straight duct, instead of repairing the broken collimator, for quick recovery.

After the user operation resumed, the residual dose was not as high as expected. Thus, we continued the user operation until the summer shutdown in 2016 under this condition. Following our temporary repair, we made a fixed collimator to replace the spare duct, and installed it during the summer shutdown period in 2016. During JFY2017, we improved significantly the reliability of the collimator moving system. The control system was changed from VME to PLC, and it included a redundant limit (software and hardware). The hardware was also improved to separate support point and vacuum boundary, and horizontal and vertical collimator positions are alternating to prevent hitting each of the collimator blocks. Finally, we installed a new fifth movable collimator system in the summer shutdown period in 2018.

Residual dose distribution and exposure during maintenance

Since the output power to the MLF was increased, the residual doses in the RCS were relatively larger than those in previous years.

Table 3 summarizes the radiation doses received by the workers during the summer shutdown period in 2018. A total of 49 workers were exposed to doses of more than 0.01 mSv, and their collective dose was 2.50 man-mSv. Eight workers were exposed to residual doses of more than 0.1 mSv, and the maximum dose received by any one worker was 0.24 mSv. Both the collective and maximum doses increased compared to previous years.

Table 3. Summary of worker radiation doses during the summer shutdown period in 2018.

Dose (mSv)	Number of workers
0.01–0.05	36
0.06–0.10	5
0.11–0.20	6
0.21–	2

1-MW TRIAL

At the beginning of July 2018, we carried out the trial of the 1-MW continuous operation. As a matter of fact, just before the 1-MW trial, we had a failure of the turbo molecular pump (TMP) at the arc section. This trouble caused contamination near the TMP failure point. Therefore, at the 1-MW operation, the pressure rises were slightly more than one order of magnitude, but three orders of pressure rise were found at the TMP failure point. Because of this vacuum deterioration, the signals of the beam loss monitors around the TMP failure point increased, and sometimes the beam was stopped due to the machine protection system. However, those signals were actually caused by the interaction between the beam and gas. Thus, there were no significant changes of the residual dose values before and after the 1-MW operation. Figure 11 shows the residual dose around the RCS tunnel before and after the 1-MW continuous operation.

Beyond 1-MW: Beam injection study

The result of the 1-MW demonstration showed that the beam loss in RCS was well controlled and RCS would have enough potential to accelerate a beam with power of more than 1 MW. Therefore, we carried out the trials beyond the 1-MW acceleration. However, the RF system in RCS does not have enough capacity to completely accelerate a beam more powerful than

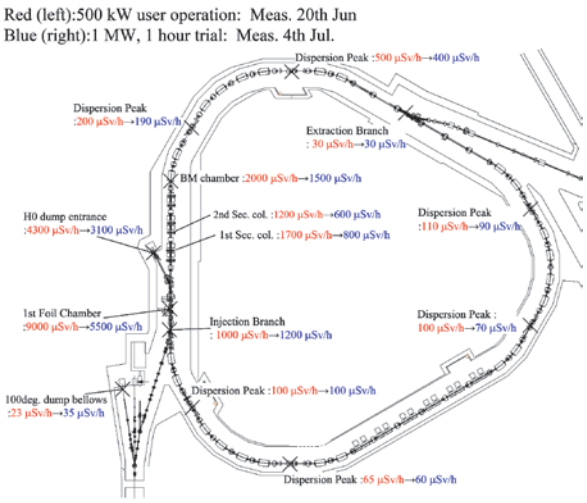

Fig. 11. Residual doses in RCS before and after the 1-MW demonstration.

1 MW. The simulation results indicated that the present RF system can accelerate stably only a 1.2-MW beam just in the first 10 ms.

Thus, in JFY2018, we carried out the 1.2-MW beam trial with acceleration energy of 1 GeV. In this case, the beam was accelerated during the first 6.75 ms and immediately extracted after acceleration. After fine tuning under this condition, we obtained enough low-loss beam condition. Figure 12 shows the beam loss monitor signals with various beam power. This figure indicated that the signal intensities are almost proportional to the beam power.

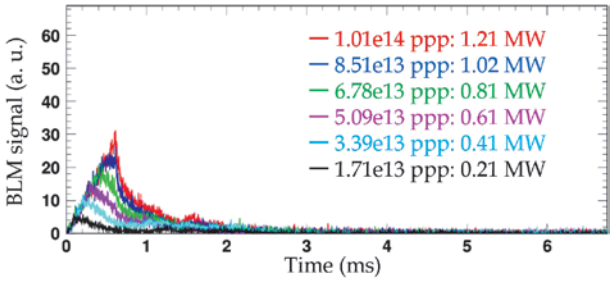

Fig. 12. Beam loss monitor signals observed at the collimator section.

Summary

The user operation at RCS has been enough stable. At present, RCS delivers 4.4e13 ppp, which were equivalent to 500-kW beam to the MLF and 6.5e13 ppp (780-kW equivalent in RCS) beam to the MR. It will be further increased step by step with carefully monitoring the neutron target status and the beam loss.

We achieved a 1-MW, 1-hr continuous operation in the beginning of July 2018. The 1-MW trial indicated some issues hindering a stable 1-MW operation. We will resolve those issues.

Trials beyond 1-MW were carried out. The results indicated that RCS had enough capability to accelerate a 1.2-MW beam if the RF system would be reinforced. Currently, we have been working on improvements of our RF system.

MR

Overview

The Main Ring synchrotron (MR) of J-PARC accelerates the 3-GeV beam injected from RCS up to 30 GeV. The 30-GeV proton beam is supplied alternatively to the neutrino experimental facility in a 2.48-s period, which is called fast-beam extraction (FX) mode, and also to the hadron experimental facility in a 5.20-s period, which is called slow-beam extraction (SX) mode.

The operation of MR was stable before the summer shutdown period in 2018. For the neutrino experiment in the FX-mode, MR successfully maintained the 490-kW stable operation and delivered a 500-kW, 50-shots trial with an acceptable beam loss. For the hadron experiment in the SX-mode, MR also achieved a 51-kW stable operation.

The MR operation after the maintenance period was resumed from January 2019. After the 3-day beam study in the FX-mode, the user operation with the SX-mode was started by using the 50-kW beam. The stability of the beam was satisfactory. However, a problem occurred in the bending magnet of the beam transport line from RCS to MR on March 18, 2019, caused by a short circuit between the layers of the magnet coil. It was fixed temporarily by making a bypass circuit for the shorted layer. (However, the beam operation was suspended in April again because another short circuit happened in other coil layers after three weeks of operation. Thus, MR has been suspended until the arrival of a new coil. It will be delivered in September 2019.)

As part of our plan for the future beam upgrade at MR, we continued the testing of a new bending-magnet power supply with higher repetition rate by using the real magnets in the MR tunnel. The test was conducted during the shutdown period in 2018, which was approximately twice as along as the usual one due to additional work to improve the experimental facilities. The long shutdown period is shown in Fig. 13 as the blank in the MR beam power history.

The details of the subjects described above are explained in the following section.

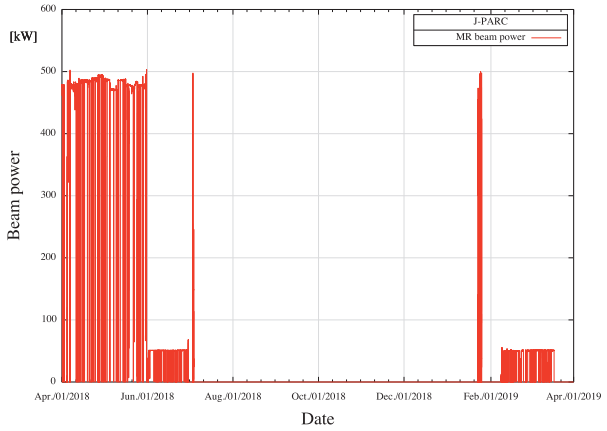

Fig. 13. MR beam power history (JFY2018)
(JFY2018: April 2018 – March 2019)
There was a long shutdown period from July to December of 2018.

B15D magnet trouble

The bending magnet B15D in the 3-50BT line between the RCS and the MR had a layer short-circuit on March 18, 2018. It was noticed by the beam loss induced by the horizontal beam orbit deviation measured at the spot just after the B15D magnet. As the magnet current did not change at that time, a coil problem was suspected because the beam orbit was shifted by the change of the magnetic field in the magnet.

The B15D magnet is shown in the Fig. 14. B15D has two coils, an upper and a lower. Each of the coils consists of 5-unit coils. The unit coil is composed of two layers of 12 turns hollow conductor, as shown in Fig. 15. It was confirmed that the first unit of the lower coil has a different impedance from that of the others. Thus, an electric terminal, which bypasses the first unit, was connected as a temporary repair. (As a result, we could start the SX-mode operation. However, the second unit had the same problem in the end of the following month.) It was assumed that the short circuit was induced by the water leakage from the joint of the hollow coils. The assumption will be verified after removing the coil.

The user operation period suspended by the B15U trouble will be compensated after the summer shutdown in 2019.

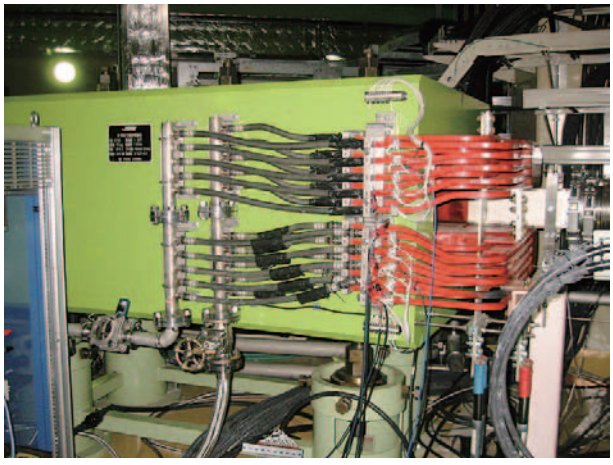

Fig. 14. B15D bending magnet

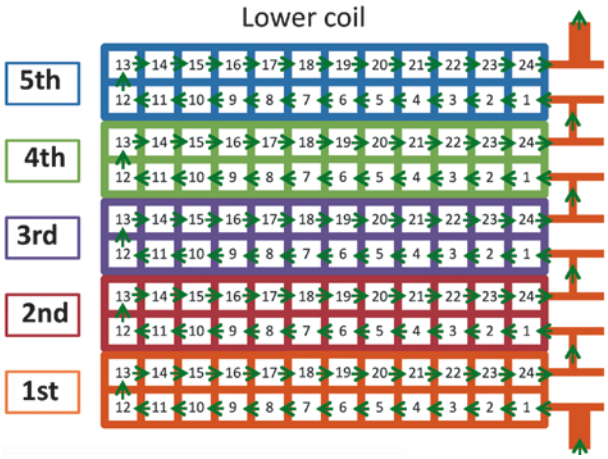

Fig. 15. Schematic view of the coil structure

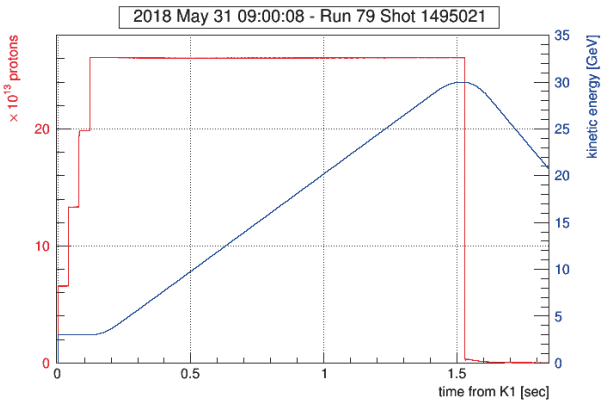

Fig. 16. DCCT output of the 500-kW beam

SX-mode operation

The SX-mode operation of JFY2018 was stable except for the trouble with the B15D magnet. The beam power of 50-51 kW was maintained.

The spill duty factor, which is a very important parameter for the hadron experiments, has been improved from 50% to 55% by fine tuning of the transvers RF pattern, which makes the beam distribution uniform.

FX-mode operation

The beam power of 490 kW was achieved for the FX-mode user operation. The beam loss of the 490-kW operation was approximately 50 W along the 3-50BT line and 480 W in the ring. These values are sufficiently small.

A 500-kW trial was carried out as a beam study. 50 shots of 500-kW beam were successfully accelerated and extracted to the neutrino facility. The observed beam loss in the ring was 700 W. An example of the DCCT data for the 500-kW beam is shown in Fig. 16. The red line shows the number of protons in the ring. It keeps a constant value after the injection, which means that there is no significant beam loss. Although the amount of the loss may be acceptable, it is planned to perform the iterative tunings of several parameters for less losses and better loss localization.

New magnet power supply

Three of the new power supplies for the MR bending magnet have been installed in the new power supply buildings.

Each of them supplies the current to 16 magnets, which are 1/6 of the bending magnets in MR. The basic test of every component has been done. Then, the realistic test was carried out by using the real bending magnets in the tunnel in JFY2018.

The examples of the data are shown in Fig. 17 for the FX-mode and in Fig. 18 for the SX-mode, respectively. Blue lines in the figures show the output current pattern of the power supply. For the FX-mode, the designed repetition period of 1.32 s was achieved. It is required to increase the beam power for the FX-mode

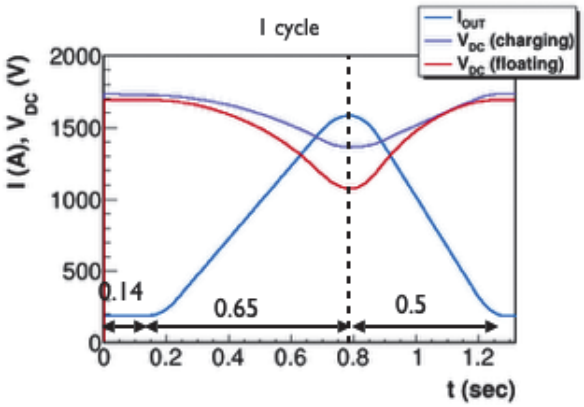

Fig. 17. Observed FX mode current pattern Repetition period is 1.32 s.

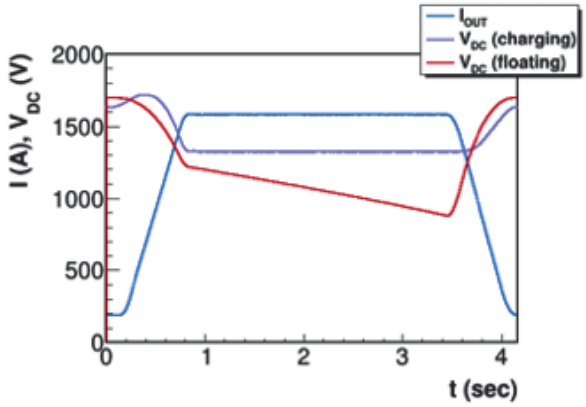

Fig. 18. Observed SX-mode current pattern The repetition period is 4.16 s.

up to the original design beam power of 750 kW and more. For the SX-mode, it was confirmed that the current ripple on the flat top was approximately one order smaller than that of the present power supply. It is sufficiently small for the hadron experiment. In the next step, the durability of the power supply will be checked by long time operation.

Summary

For the FX-mode, the beam power of 490 kW was maintained for the user operation and 50 shots of the 500-kW beam were achieved by the beam study. For the SX-mode, the beam power of 51 kW was achieved for the users.

However, the MR operation has been suspended by the coil trouble of the bending magnet in 3-50BT line. The operation will be resumed after the summer shutdown period in 2019.

The work on mass production of magnet power supply has advanced. The results of test operation of the new power supply for the bending magnet, using the real magnets in the MR tunnel, show the sufficient power and stability we expected.

Materials and Life Science Experimental Facility

Overview

In fiscal year 2018, the operation of Materials and Life Science Experimental Facility (MLF) started with the neutron production mercury target (#8), which had helium bubbling system. On April 19, the proton beam power delivered to the target was increased from 400 kW to 500 kW and the operation continued very stably until July 2, 2018, followed by a 1-MW test operation for one hour on July 3. The beam availability of the target (#8) to the scheduled beam time was 93%. In the summer maintenance period, the target was replaced from #8 to #9 and the neutron production started on October 22 and continued stably until March 26, 2019.

The muon rotating target system has been delivering a stable muon beam to users without trouble since 2014. However, the potential damage of a flexible joint for transferring motor rotation to the graphite disk target has been a cause for concern. Some measures were taken to minimize the potential hazards expected in case of suspended target rotation. By ensuring that those measures were effective, the muon user program was resumed in the beginning of November after two weeks delay behind the original schedule. The operation continued until March 26, 2019, without troubles.

Due to the stable operation of the facility, the MLF was able to produce many excellent outcomes in various research fields, such as hard matter, soft matter, energy materials, engineering materials, biomaterials and so on. In addition to the research outcomes, there were many activities in the MLF in 2018 to enhance the collaboration with international/ domestic users in academia and various industries. The Annual meeting of industrial application at J-PARC MLF was held on July 23 and 24 at Akihabara Convention Hall. The 3rd Neutron and Muon School was held from November 20 to 24. The 3rd ESS-J-PARC Workshop was held from November 13 to 15. On the first day of the workshop, the Swedish

Ambassador Magnus Robach delivered his greetings. Quantum Beam Science Festa which is a conference mainly for domestic users for MLF J-PARC and IMSS KEK was held in Tsukuba on March 12 and 13.

In the annual report, the research highlights, the technical developments and the collaboration activities with users in 2018 are described in detail.

Progress of the Neutron Source Section

Fiscal year 2018 started with a beam operation of 500 kW, which had been recognized as an important milestone to reach the final goal of 1 MW, because two targets failed consecutively during 500 kW beam operation in 2015 and, since then, considerable efforts were put into the design improvements of the next mercury target, target #8, to make it more robust and reliable during a high-power operation. Target #8 had been used at 300 kW and 400 kW since the last fiscal year and completed its user beam operation successfully on June 30, 2018, after a 3-month operation at 500 kW, which demonstrated the validity of the design improvement. In addition to that, target #8 was operated with 935 kW for one hour at the high-power beam study held on July 3. Reaching almost 1 MW within practical duration time was a great achievement of the J-PARC.

Gas-micro-bubbles injection into mercury and the high-speed mercury flow in a narrow channel formed by the double walled structure, shown schematically in Fig. 1, are the key measures to mitigate the pitting damage at the beam window which is the front end of the target vessel. At the high-power beam study, the vibration of the target vessel under the beam operation condition of 25 Hz was measured at almost 1 MW for the first time, as shown in Fig. 2. The displacement velocity on the top side of the target vessel at 935 kW remained on the same trend line with that measured at a lower beam power. It shows the efficacy of gas-micro-bubble injection to reduce the displacement velocity at the 1-MW operation.

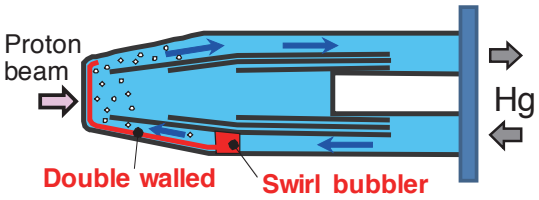

Fig. 1. Measures to mitigate the pitting damage equipped in target #8

The specimens were taken out of the used target #8 and the maximum depth of pitting damage on the inner side of the beam window was 18 μm, which was less than anticipated. This fact demonstrated the effectiveness of the present measures to mitigate the pitting damage. Then, target #8 was replaced with target #9, which has the same structure as target #8. The beam operation of target #9 had continued well at 500 kW with the high average availability of 93.5% as of the end of fiscal year 2018.

An important event was the transportation of the used target vessel from the MLF (Materials and Life Science Experimental Facility) to the RAM (Radio Activated Materials) building to save the limited space of the used components storage room in the MLF. A shielding container, 200 mm in wall thickness and 44 tons in total weight, was fabricated, and used in combination with the shipping container fabricated in 2017.

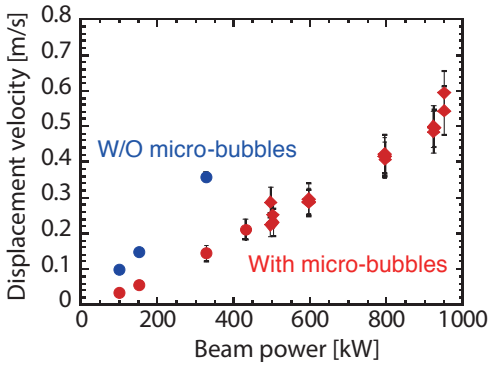

Fig. 2. Displacement velocity at the top side of target vessel #8 at beam study

Fig. 3. Transportation of a used target vessel

The preparation and rehearsal took almost a month and the used target vessel was transported successfully to the RAM building for the first time on January 16, 2019. The transportation is going to be held every year.

Neutron Science Section

1. User program

For the general-proposal round for 2018A, 175 general proposals and 5 new user promotion (NUP) proposals were approved from 260 submissions. Among them, 174 approved experiments and 9 reserved ones were executed. For 2018B, 190 general proposals and 8 NUP proposals were approved from 285 submissions. Among them, 178 approved experiments and 13 reserved ones were executed. Additionally, four newly approved long-term proposals started a 3-year project in the 2018B term. Fast Track Proposal, which is a mail-in program, has just started from the end of JFY2017 for Super HRPD at BL08 and NOVA at BL21. In 2018, 3 experiments were executed at BL08 and 2 experiments were done at BL21.

2. Instruments

This year, the MLF was stably operated with power of 500 kW. On July 3, a test operation with 1 MW power was performed for one hour. The high power was experienced in each beam line. On 4SEASONS and AMATERAS, inelastic neutron scattering from S=1/2 one-dimensional antiferromagnets were measured by using small samples of 0.3~0.5 cm^3. The dispersion relation of the spin excitations could be identified in the measurement for a few minutes, and well-analyzable data were obtained for only one hour.

After the beginning of the user program in the MIEZE part of the neutron spin-echo suit VIN ROSE at BL06 in 2017, scientific outcomes are starting to emerge. An experiment was performed in MnSi, where various spin structures, such as helical spin structure, conical spin structure, and skyrmions, were expected below the transition temperature. Clear spin relaxation was successfully observed just above the transition temperature.

3. International activities

The 3rd Neutron and Muon School was held from November 20 to 24. 35 young researchers and graduate students from China, India, Korea, Tahiland, Russia, United Kingdum, as well as Japan, participated in the school. The neutron science group contributed 9 neutron instruments for hands-on experiments (Fig. 4).

The J-PARC Center and CROSS hosted the J-PARC Workshop "Deuterium Labeling Study for Neutron Science" on January 15 and 16, 2019. We invited Dr. T. A. Darwith from ANSTO and 20 scientists discussed neutron studies on material and life siences by utlizing deuterium labeling.

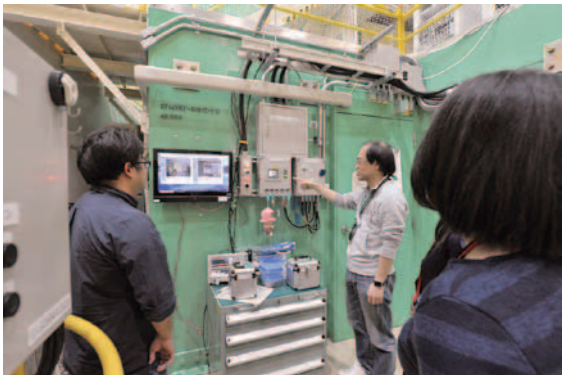

Fig. 4. Dr. Hiroi explaining the operation of the shutter control pannel at TAIKAN at the 3rd Neutron and Muon School hands-on experiment.

4. Resultant outcomes

The research activities in neutron science at the MLF resulted in more than 180 papers and 10 press releases. The number of papers includes articles in influential journals such as Nature Physics (1), Nature Materials (1) and Scientific Reports (6). Press releases include two detector developments, such as a high resolution (~11 nm) emulsion type detector and a high-speed neutron imaging detector via a solid-state superconducting detector.

Dr. Takuro Kawasaki won the 16th Young Researchers Prize of the Japanese Society for Neutron Science for the development of stroboscopic measurements and leading research with the technique on SENJYU (BL18) and TAKUMI (BL19).

RADEN (BL22) group won JAEA President's Award for the development of energy-resolved neutron imaging and leading researches on RADEN.

K. Nakajima[1], Y. Kawakita[1], S. Itoh[1,2] and T. Otomo[1,2]

[1]Neutron Science Section, Materials and Life Science Division, J-PARC Center; [2]Institute of Materials Structure Science, High Energy Accelerator Research Organization, KEK

Neutron Device

As one of the activities at the Neutron Instrumentation Section of the MLF Division, research and development of a neutron polarizing supermirror with high-performance capabilities, such as wide bandwidth, high polarization, and availability at low external fields, has been conducted to meet a variety of research demands in the MLF. Fundamental study, including interactions between sputtering gas particles and growing layer, thin film magnetism, and characterization of the in-plane magnetic structure of multilayers for polarizing supermirrors using polarized neutron scattering, is required to develop the high-performance polarizing supermirror.

For ion beam sputtering (IBS), an Fe/Ge multilayer shows higher polarization than Fe/Si and is suitable for a polarizing supermirror. However, the reason for that phenomenon had not been fully understood. In the present study, the multilayer structure of the Fe/Ge and Fe/Si multilayers fabricated by IBS was investigated using the polarized neutron reflectivity measurement and scanning transmission electron microscopy with energy-dispersive X-ray analysis (STEM-EDX). Figure 5 shows the polarized neutron reflectivity profiles of the Fe/Si and Fe/Ge multilayers. One can see that the Fe/Ge multilayer shows higher polarization than the Fe/Si, as expected. The scattering length density (SLD) profiles, obtained by the fit to the reflectivity data, revealed that the SLD reduction in the Ge layer by 13% contribute to the SLD contrast between Fe and Ge layers almost vanishing for spin-down neutrons, as shown in Fig. 6. This accounts for higher polarization of the Fe/Ge multilayer. In addition, the STEM-EDX measurement showed that the incorporation of Ar sputtering gas particles, backscattered at the target, is responsible for a marked reduction in the SLD in the Ge layer.

The above investigations motivated us to fabricate an Fe/Ge neutron polarizing supermirror with 4994 layers ($m = 5$). The result of the polarized neutron reflectivity measurement is shown in Fig. 7. The reflectivity for spin-up neutrons was higher than 0.70 for the range $q_z \leq 1.085$ nm^{-1} ($m = 5$), as designed. The polarization was higher than 0.972 for $0.217 \leq q_z \leq 1.085$ ($1 \leq m \leq 5$). These results open a possibility for fine-tuning of the SLD for the IBS, which is required to realize a high polarization efficiency of a neutron polarizing supermirror. The mirror is planned to be tested at BL22 and BL17 of the MLF.

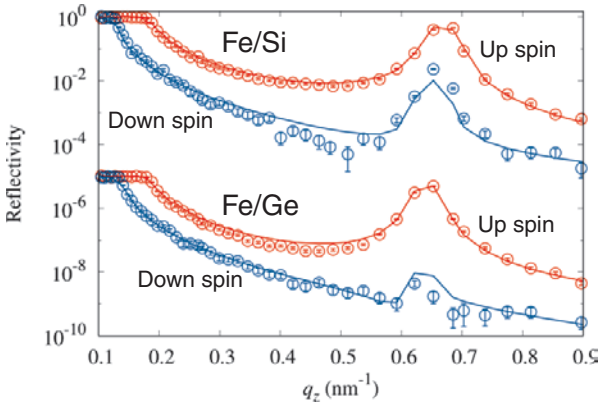

Fig. 5. Polarized neutron reflectivity profiles of Fe/Si and Fe/Ge multilayers.

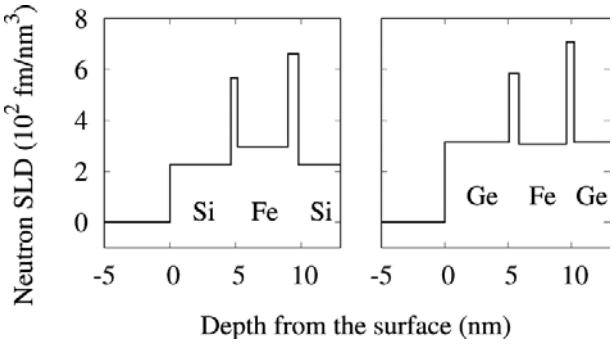

Fig. 6. Estimated scattering length density profiles of the Fe/Si and Fe/Ge multilayers for spin-down neutrons.

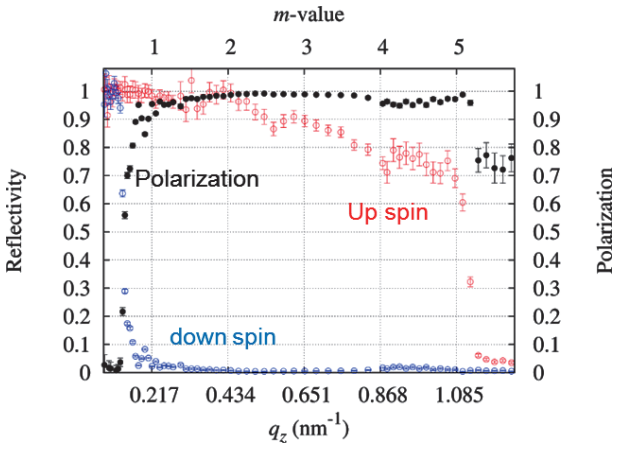

Fig. 7. Polarized neutron reflectivity profiles of Fe/Ge polarizing supermirror with 4994 layers.

Reference

[1] R. Maruyama et al., Nuclear Inst. and Meth. Phys. Res., A**888**, 70 (2018).

Muon Section

Rotating target system: concern after delight

The muon rotating target system is at the heart of the MUSE facility, located on the primary proton beam line of MLF. It consists of a large disk made of graphite, where the radiation damage due to the 3 GeV proton hitting at off-center position is relieved by spraying it along the circumference upon rotation. Since its installation in 2014, the target system has been enjoying stable operation, delivering muon beam to users with ever increasing flux according to the proton beam power that reached 500 kW this year. While the system was designed to allow a 1-MW operation, the day came to test the actual performance when the beam power was temporally ramped up to 1 MW for one hour towards the end of the accelerator operation in early July. The target team was delighted to confirm that the parameters monitoring the status such as target temperature and motor torque met exactly the expectations.

Meanwhile, later, during the summer maintenance, the team identified a potential damage of a flexible coupler for transferring motor rotation to the graphite disk. This cast a serious concern about the possibility of unexpected suspension of the target rotation due to breakdown of the coupler. The option of replacing the whole target system with a brand-new spare one was excluded to avoid the risk of delays in the beam delivery schedule. Based on the numerical simulations of the temperature and stress of still graphite disk exposed to a 500-kW proton beam, some measures were taken to minimize potential hazards expected in case of suspended target rotation. In particular, buffer tanks for exhaust gas (potentially contaminated by tritium emitted from the target) were installed behind the vacuum pump system connected to the proton beamline to prevent its direct emission to the environment (see Fig. 8). Upon ensuring that these measures were in effect, the muon user program was resumed in the beginning of November after two weeks delay from the original schedule.

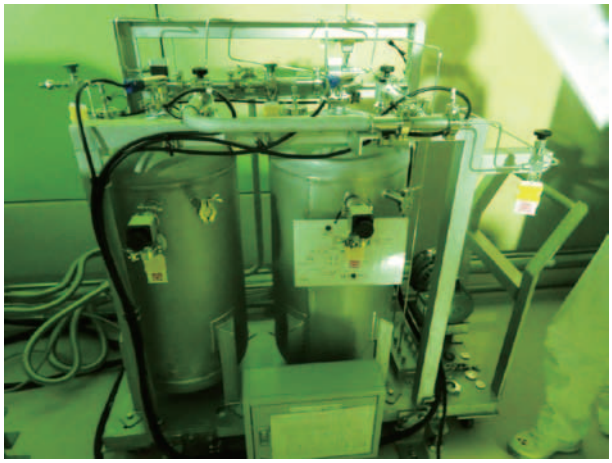

Fig. 8. Exhaust-gas handling system installed on the back of vacuum pump for proton beamline evacuation. It consists of two branches with buffer tanks to accumulate the tritium-contaminated exhausts for controlled emission.

Feasibility of negative muon spin rotation demonstrated on D-line

Positive muons have a great advantage over negative muons for probing magnetic field in matter, as the spin polarization for the former remains much higher than the latter. However, it has been demonstrated that negative muons could be useful in studying hydrogen diffusion in magnesium hydride (MgH_2).

The rotational motion of muon spins (the Lamour precession) monitored by muon decay into positrons/electrons tells the magnitude and distribution/fluctuation of internal fields that carries information on nearby atoms exerting magnetic fields to muons. In MgH_2, while the diffusion of hydrogen ions (exerting magnetic fields to muons) within the material should cause such fluctuation, the possibility of self-diffusion of positive muons as pseudo-hydrogen (that also leads to the fluctuation of the internal field) makes it difficult to discern the cause of fluctuation. By using negative muons, deeply bound to magnesium nuclei as "heavy electrons", researchers succeeded in observing the field fluctuations that might be uniquely attributed to hydrogen diffusion (see Fig. 9). The result also proved that the disadvantage of low spin polarization for negative muons could be overcome by their unprecedented high flux achieved at the D-line under the 500-kW operation.

Construction of electric power substation for H-line in progress

Among the muon beamlines envisaged in the original plan of the MLF, the H-line in experimental hall No. 1 has been in the stage of waiting for funding from MEXT for years. Because of this situation, the J-PARC head quarters decided to provide partial support for putting the plan forward. It will finance primarily the construction of a new electric power substation to cover the huge demand for electricity expected after the H-line becomes fully operational. Following the installation

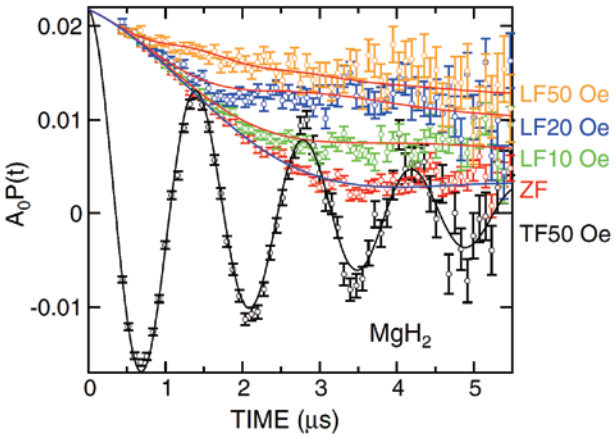

Fig. 9. Time-dependent decay electron asymmetry observed under various external fields upon negative muon implantation in MgH_2. (after J. Sugiyama *et al.*, PRL **121**, 087202: ©APS)

Fig. 10. A snapshot of the construction site for the electric power substation at the east side of the MLF building (October 2018).

of cable racks, pitting of the MLF building wall, and outdoor structures in FY2017, the civil engineering work for the substation site near the MLF building continued (see Fig. 10). By the end of this fiscal year, the installation for the access to electricity also made some progress on the substation site.

Struggle for ultra-slow muons continued

Since the successful generation of ultra-slow muons (USMs) at MUSE in FY2015, experimenters had been working with untiring perseverance to improve the USM yields to the level needed for practical applications. However, they seemed still in the midst of a long crucial stretch throughout this year to gain enough vacuum-ultraviolet (VUV) laser power for the Mu ionization. The promise of a crystal vendor to deliver a high-quality ceramic crystal for the final laser amplifier has not been fulfilled yet, although we still hope that the vendor would manufacture a suitable crystal as soon as possible.

Technology Development Section

1. Routine operation of the deuteration laboratory

A deuteration laboratory, which has been set up on the first floor in the J-PARC research building, started its routine operation in this fiscal year. The laboratory consists of a biological deuteration room and a chemical deuteration room. Special wastewater treatment equipment for draining from biological and chemical deuteration rooms are belonging to the deuteration room. There is also emergency power supply for two days in full operation, which will be used in the case of power failure in the biological deuteration room, because the cultivation equipment usually operates for extended periods of time.

Firstly, we tested the individual equipment for deuteration work and below themes successfully performed by the J-PARC staffs and their collaborators in the biology deuteration laboratory.

1) Cultivation of green algae, which is the source of medium components used in culturing Escherichia coli (Photograph 1).
2) Cultivation of Escherichia coli (non-recombinant) using a deuterated medium.
3) Preparation of deuterated DNA samples.

Also, below themes successfully performed by the J-PARC staffs and their collaborators in the chemical deuteration laboratory.

1) Deuteration of ionic liquids and acrylic monomers (Photograph 2).
2) Chemical structure evaluation by LC-MS.
3) Preparation of deuterated polymer samples for neutron reflectivity measurement.

Statistics of the deuteration laboratory usage is shown in Table 1. It will be soon available for user.

Photograph 1

Photograph 2

Table 1. Statistics of the deuteration laboratory usage.

Laboratory	Equipment	Days	Laboratory	Equipment	Days
Biological deuteration laboratory	Lab bench	17	Chemical deuteration laboratory	Lab bench	4
	Fume hood	12		Vacuum oven	17
	Ultrapure water equipment	13		LC-MS	1
	Shaker	232			
	Clean bench	7			
	Evaporator	1			
	Autoclave	2			
	Spin coater	9			
	HPLC	1			
	FT-IR	2			

2. Development of a high-durability chopper

The development of a high-durability T0 chopper was completed this fiscal year (Fig. 11). We defined it as a second generation T0 chopper of which our operation experience is reflected in the design. It has achieved a stable operation at 100 Hz and is expected to function maintenance free for 10 years. During the 2019 summer maintenance, this chopper will be installed at BL01, which is Fermi-chopper type inelastic neutron-scattering instrument and uses up to epithermal neutron.

As for the second generation of the high-speed disk chopper, we started a trial fabrication of a new disk, which should achieve sufficiently high mechanical strength and reliability for a 350-Hz operation, and will be made of laminated CFRP, mainly consideration of shape and adhesive of CFRP.

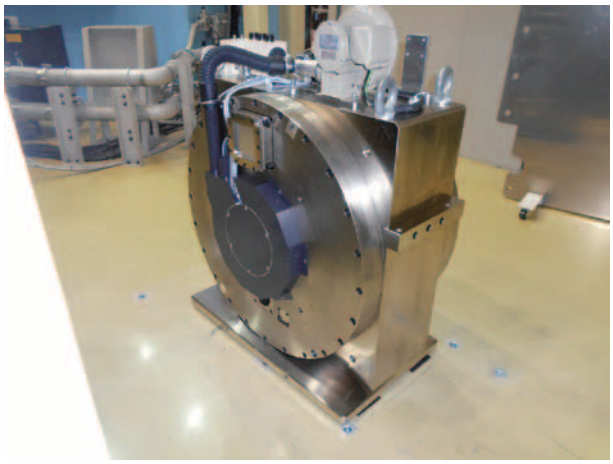

Fig. 11. High-durability T0 chopper

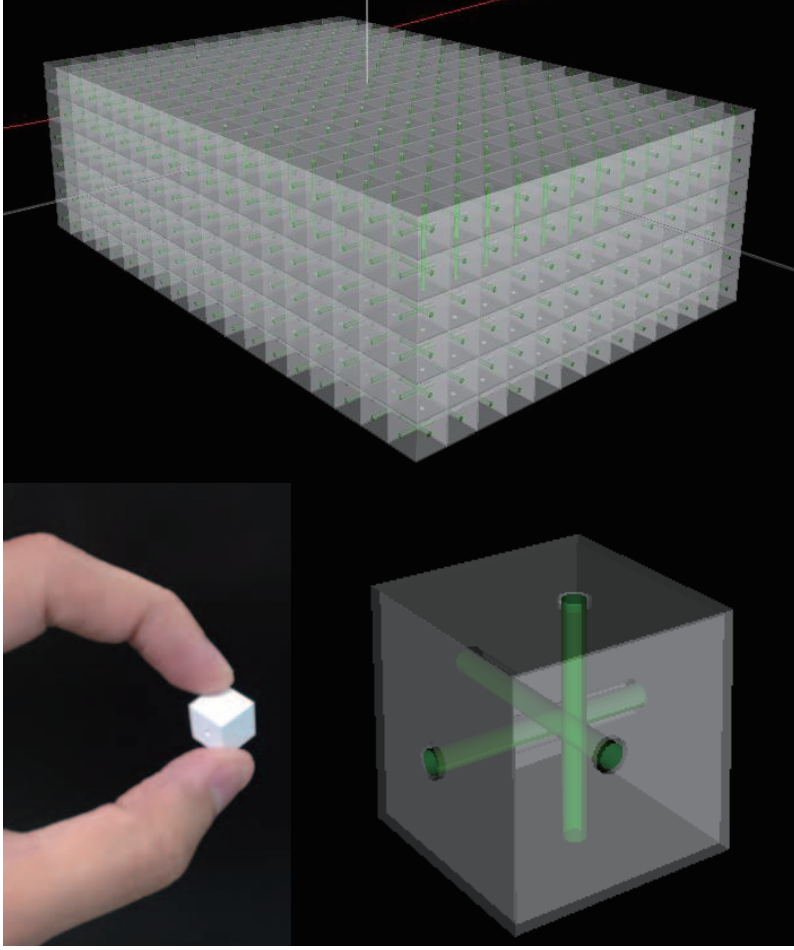

Particle and Nuclear Physics

Neutrino Experiment

T2K run in the fiscal year 2018 continued seamlessly from the 2017 runs in the anti-neutrino mode, and ended on May 31, and entered to a long shut down for the water tank repair of the SuperKamiokande detector. History of the accumulated protons on target (POT) and the beam power are plotted in Fig. 1. Stable operation of 480-kW beam power was successfully achieved. Since the beginning of the experiment, T2K accumulated 16.5×10^{20} POT in the anti-neutrino mode, in addition to so-far accumulated 15.1×10^{20} POT in the neutrino mode.

In January 2019, T2K updated the neutrino oscillation results using all the data taken. With improved

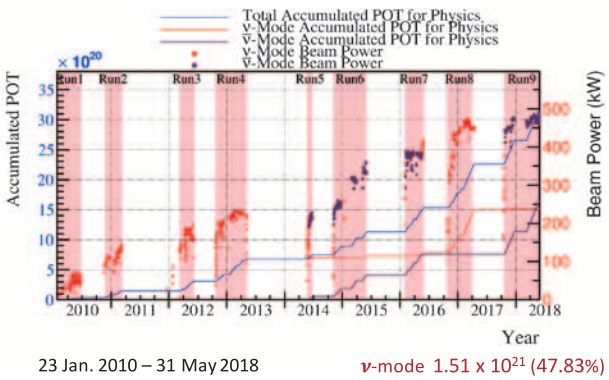

Fig. 1. History of accumulated POT and beam power since the beginning of T2K.

statistics the tension between the neutrino and anti-neutrino remains with a two-sigma indication of the CP violation. θ_{23} analysis result is still consistent to the maximal mixing as shown in Fig. 2. More statistics is eagerly awaited for more conclusive results.

In order to improve the performance of on-site neutrino detector ND280 and to increase the capability of the neutrino beam line to handle beam power beyond 1 MW, extensive works are in progress. The technical design report for each project was reviewed by each dedicated ad hoc committee and by the J-PARC Program Advisory Committee (PAC). The projects are essentially ready to proceed.

Two new neutrino experiments were approved in 2018. The E56 experiment armed with a liquid scintillator detector, searches for sterile neutrinos coming from the MLF target and is planned to start taking data in 2019. The E71 Ninja Experiment, aiming at precision study of neutrino-nucleus interaction with hybrid emulsion detector at the near detector hall, started detector installation and commissioning and is planned to have a physics run in 2019.

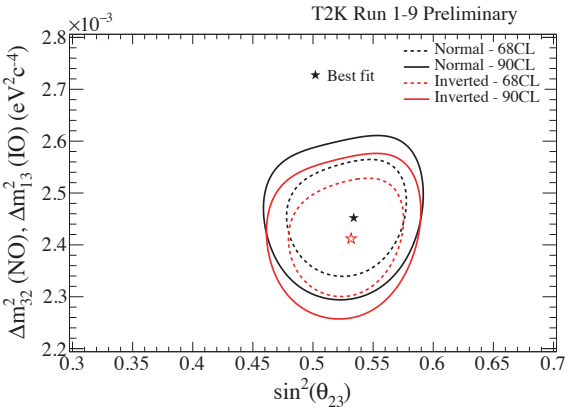

Fig. 2. Contours for ν_μ disappearance parameters $\sin^2\theta_{23}$ and Δm^2_{32} (or Δm^2_{13}) with reactor constraint on $\sin^2\theta_{13}$.

Hadron Experimental Facility

The Hadron Experimental Facility (HEF) of J-PARC is for fixed target particle and nuclear physics experiments with secondary hadron beams produced by the slowly extracted (SX) 30-GeV proton beam from the Main Ring (MR) accelerator. In FY2018, the SX beam operation for users was conducted with a beam power of 51 kW and a repetition cycle of 5.2 s in two periods; from June 1 to 30 for 517 hours and from February 9 to March 18 for 581 hours. The 51 kW is the maximum beam power allowed by the present hadron production target. The total integrated beam power delivered during the FY2018 operation was 2321 kW·days, which corresponds to the operation for full five years with the old KEK 12-GeV Proton Synchrotron stopped in 2005.

Construction of a new primary beam line for the high-momentum (high-p) beam and COMET (a μ-e conversion experiment) was in progress. A Lambertson magnet to separate a fraction of the main proton beam for the high-p beam has been installed in the switch-yard tunnel together with other beam line elements (Fig. 3). In the Hadron Hall, a high-p beam line and an area for the experiment for vector meson production in Nuclei were being prepared.

A new hadron production target with gold was fabricated (Fig. 4) and is ready to install in FY2019. It is indirectly water-cooled from the both sides of the top and bottom and can accept proton beams of about 90 kW.

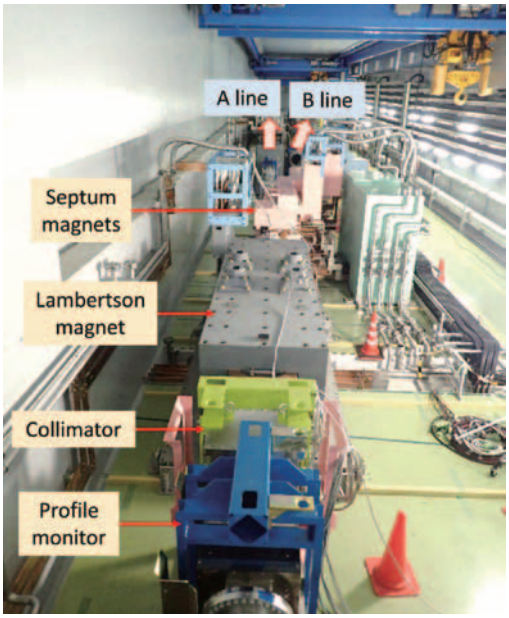

Fig. 3. Photograph of the existing beam line (A-line) and a new beam line (B-line) in the Switch-yard tunnel from MR to Hadron Hall.

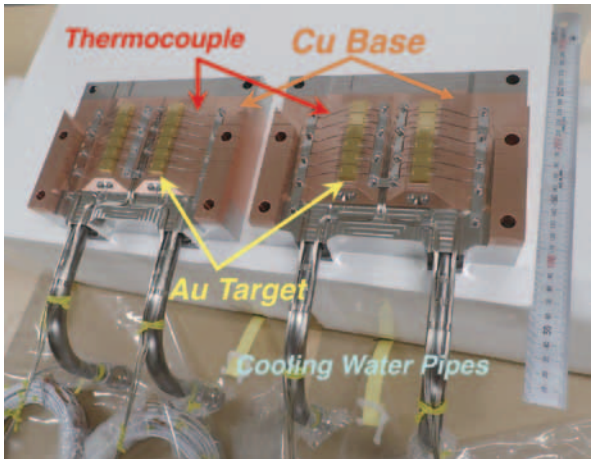

Fig. 4. A new production target for SX beam line under fabrication.

Strangeness/Hadron Physics Experiments

Several strangeness/hadron physics experiments were conducted.

At the K1.8BR beam line, an experiment for X-ray spectroscopy of $^{3/4}$He kaonic atoms (E62) took data in June. It measures isotope-shift of *3d-2p* X-rays using an ultra-high resolution transition edge sensor (TES) detector of ~5eV (FWHM) resolution to study whether the kaon potential at the nuclei is deep or shallow. Another pilot measurement (E57) of X-rays from a kaonic hydrogen atom was in preparation for taking data in April 2019. By a comparison between the kaonic hydrogen and deuterium atoms, the experiment is aiming for disentangle the isospin 0 and 1 components of the $\bar{K}$N interaction.

At K1.8, the Σ hyperon-proton scattering experiment (E40), which gives a key data to understand the origin of the repulsive core in nuclear force, started data-taking in June. Data on Σ^-p scattering were taken by March and data on Σ^+p scattering will be taken in FY2019.

Several results have been published in FY2018. A simplest kaonic nucleus system, the K^-pp, was studied by the E15 experiment. The group showed a possible bound state in the system from the data taken in 2015 at K1.8BR.

A new double-Λ nucleus of a Be isotope was observed by the analysis of the emulsion experiment, E07, which was carried out in 2016 and 2017 at K1.8. The binding energy of the two Λ particles was determined for three possible scenarios that the nucleus is $^{10}_{\Lambda\Lambda}$Be, $^{11}_{\Lambda\Lambda}$Be, or $^{12}_{\Lambda\Lambda}$Be.

Kaon Decay Experiment

The KOTO experiment is designed to study the decay of a long-lived neutral kaon into a neutral π meson (π^0) and a pair of neutrinos. The detection of this decay is challenging, because only two photons from π^0 are observable. The decay mode has not been observed. This decay breaks the CP symmetry directly, and the branching fraction is theoretically well predicted in the SM as $(3.0 \pm 0.3) \times 10^{-11}$. By examining this ultra-rare decay, a new source of CP symmetry breaking that can explain the matter–antimatter asymmetry in the universe may be revealed.

In FY2018, KOTO continued the data acquisition as well as conducted the upgrade of the calorimeter readout. New results from the data collected in FY2015, improving the world's best sensitivity by an order of magnitude, were published. In parallel, the analysis of the data collected in FY2016-2018 is ongoing intensively. These activities are described in details in the Research Highlights of this report.

Muon Experiments

The COMET, J-PARC E21 experiment, aims at searching for muon-to-electron conversion with a sensitivity of better than 10^{-14} in the first phase of the experiment. Intensive R&D has been continued in 2018 toward the start of the experiment. The performance test of the cylindrical drift chamber was successfully conducted using cosmic-ray muons. The construction of the Straw-tube tracker and the mass production of lutetium yttrium ortho-silicate (LYSO) used for the electron calorimeter continued.

Construction of the Capture Solenoid (CS), used to collect and transport pions/muons produced at the COMET primary proton target, continued on schedule together with preparation of the cryogenic system. Design of the radiation shield to be inserted inside CS for the purpose of protecting the super-conducting wires from radiation progressed significantly.

The E34 collaboration prepares for precision measurements of muon anomalous magnetic moment and its electric dipole moment. The revised technical design report was submitted and the experiment was approved after reviews by the J-PARC PAC. The collaboration has carried out development of experimental technology and components. A test experiment was performed at the MLF D2 area for the measurement of longitudinal distribution of a RF accelerated negative muonium beam.

Highlight: First Major Result from KOTO: Breaking the World's Best Sensitivity for a CP-Violating Rare Kaon Decay by an Order of Magnitude

The matter–antimatter asymmetry in the universe is one of the most mysterious puzzles in physics. The long history of the studies on charge and parity (CP) symmetry breaking in the quark sector, which started from the observation of the CP violation phenomena in neutral K mesons (kaon) in 1964, had established in the Standard Model (SM) how particles and antiparticles behave differently. However, it is known that CP violation in the SM alone cannot explain quantitatively the situation of the current universe, and other sources of CP violation must exist. One of the best probes to search for such new mechanisms is $K_L^0 \to \pi^0\nu\bar{\nu}$, a CP-violating ultra-rare kaon decay. Its branching ratio is predicted precisely in the SM to be $(3.0 \pm 0.3) \times 10^{-11}$, and deviation from the prediction is directly related to the existence of a new contributor. Because of the extremely small branching ratio, the decay has not been observed.

KOTO (standing for "K0 at Tokai") is a dedicated experiment to search for the $K_L^0 \to \pi^0\nu\bar{\nu}$ decay at the Hadron Experimental Facility (HEF) of J-PARC. The international collaboration consists of 69 members from Japan, Korea, Russia, Taiwan, and USA. KOTO took the first physics data in 2013 for 100 hours and achieved a comparable sensitivity level to the world record [1]. KOTO resumed data taking in 2015 and continues accumulating physics data since then. In 2018, KOTO completed the analysis of the data recorded in 2015 and published the new result, as described in this article, which improved the world's best sensitivity by an order of magnitude [2].

How to identify the $K_L^0 \to \pi^0\nu\bar{\nu}$ decay signal? The signal is characterized as an event that consists of two photons from the π^0 decay in the final state and nothing else. Figure 5 shows a schematic view of the KOTO detector in 2015. A 30-GeV proton beam, extracted from the J-PARC Main Ring accelerator, hits a gold target at HEF and produces secondary particles. Neutral kaons (and other long- lived neutral particles such as photons and neutrons) are transported through beam collimators to the KOTO experimental apparatus, located 21 m downstream of the target. The KOTO detector in a large cylindrical vacuum tank surrounds the beam path and captures the daughter particles from kaon decays. An electromagnetic calorimeter, which is an array of 2716 undoped cesium iodide (CsI) crystals (labeled CSI in Fig. 5), measures the energies and positions of the photons. Other components of the detector are veto counters to detect any extra particles besides the two photons if they exist.

A key for the rare decay search is to suppress and control the background events that mimic the signal. For example, a $K_L^0 \to 2\pi^0$ decay, whose branching ratio is

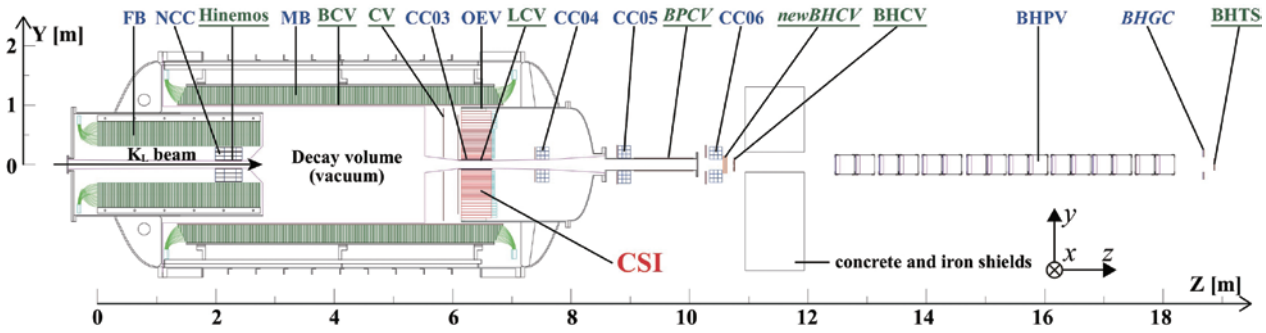

Fig. 5. Cross-sectional view of the KOTO detector.

8 orders of magnitude larger than $K_L^0 \to \pi^0\nu\bar{\nu}$, can be recognized as a single π^0 event if two photons escape from being detected. It is essential to operate veto counters with extremely high efficiency. A neutron hitting the calorimeter and producing two photon-like activities can also fake a signal. Development of photon and neutron discrimination using the calorimeter information is indispensable to reduce this type of background.

Figure 6 shows the scatter plot of the events in the plane of the reconstructed π^0 transverse momentum (P_t) and π^0 decay vertex position (Z_{vtx}) with all the event selections imposed. The region inside the red polygon is the signal region. The black dots represent the observed events, and the color contour indicates the expected distribution of the $K_L^0 \to \pi^0\nu\bar{\nu}$ signal obtained by the Monte Carlo simulation. The black and red numbers indicate the numbers of observed and expected background events for each region surrounded by the lines, respectively. Consistency between these two numbers demonstrates that the background events are well understood. No candidate is observed inside the signal region, and KOTO set the upper limit on the branching ratio of the $K_L^0 \to \pi^0\nu\bar{\nu}$ decay as 3.0×10^{-9} at 90% confidence level. This improved the world's best sensitivity for the search by an order of magnitude. KOTO also updated the limit for $K_L^0 \to \pi^0 X^0$ as 2.4×10^{-9}, where X^0 is an invisible boson with a mass of 135 MeV/c^2.

After the runs in 2015, KOTO conducted a major detector upgrade in early 2016. An additional barrel-shaped photon detector 3 m long in the beam direction and 1.9 m in the outer diameter, was installed inside the existing cylindrical photon veto counter. From 2016 to 2018, about 40% larger amount of data was collected than that in 2015 with the new detector configuration, i.e. more than twice better sensitivity is expected with the accumulated data in total. Intensive analysis of the data is ongoing, and the new result will come in 2019.

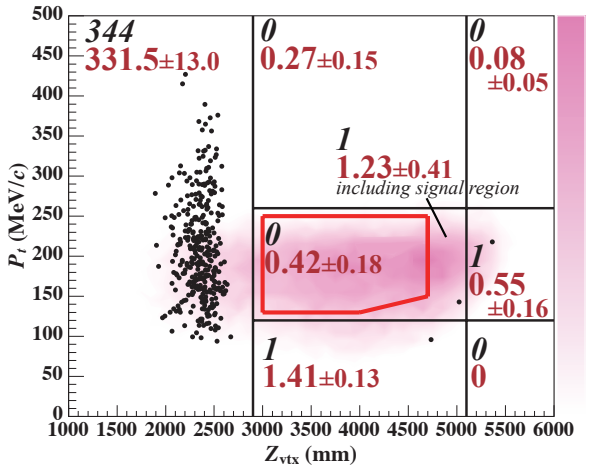

Fig. 6. Two-dimensional plot summarizing the results from the analysis of the data recorded in 2015 [2].

Following the runs in the spring season of 2018, KOTO performed a second major upgrade. To further suppress the neutron-induced background, the both-end readout scheme has been devised and implemented for the electromagnetic calorimeter. In addition to the existing photomultiplier attached at the rear end of each CsI crystal, thin photon sensors MPPCs (Multi-Pixel Photon Counter) have been newly installed at the front end. The idea is that the timing difference between two readouts can provide the depth information of shower development in the calorimeter, which is different in the electromagnetic case for photons and hadronic case for neutrons. KOTO completed the upgrade and resumed data collection in February 2019.

References

[1] J. K. Ahn *et al.* (KOTO collaboration), Prog. Theor. Exp. Phys. **2017**, no. 2, 021C01 (2017).

[2] J. K. Ahn, *et al.* (KOTO collaboration), Phys. Rev. Lett. **122**, 021802 (2019).

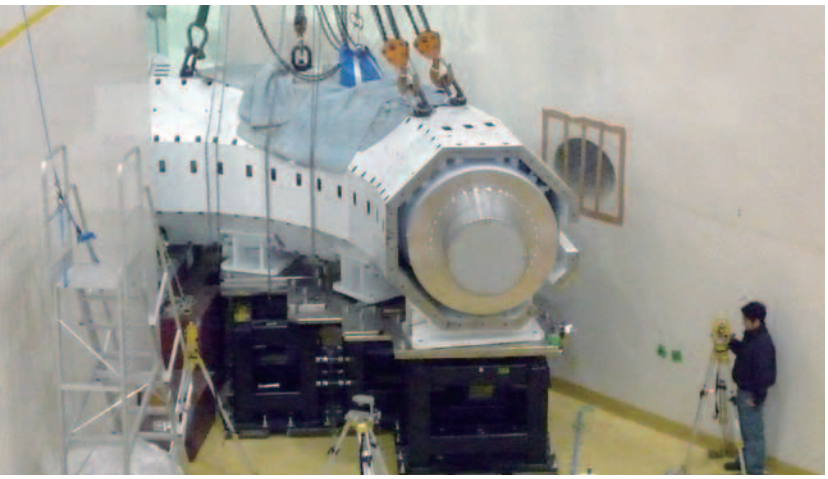

Cryogenics Section

Overview

The Cryogenics Section supports scientific activities in applied superconductivity and cryogenic engineering, carried out at J-PARC. It also supplies cryogen of liquid helium and liquid nitrogen. The support work includes maintainance and operation of the superconducting magnet systems for the neutrino beamline, for the muon beamline at the Materials and Life Science Experimental Facility (MLF) and construction of the magnet systems at the Hadron Experimental Facility (HEF). It also actively conducts R&D works for future projects at J-PARC.

Cryogen Supply and Technical Support

The Cryogenics Section provides liquid helium cryogen for physics experiments at J-PARC. The used helium is recycled by the helium gas recovery facility at the Cryogenics Section. Figure 1 summarizes the liquid helium supply in FY2018.

Liquid nitrogen was also supplied to the users for their convenience. Its amount in FY2018 is summarized in Fig. 2. Liquid nitrogen has been regularly provided to the Radiation Safety Section for operation of a gas chromatograph. It was also supplied to the users in the MLF and the HEF.

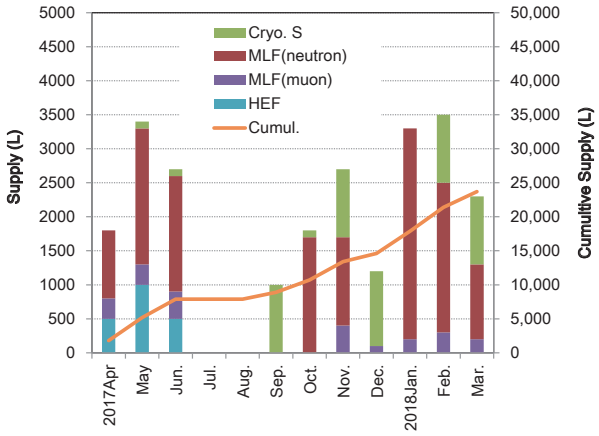

Fig. 1. Liquid helium supply at J-PARC from April 2018, to March 2019.

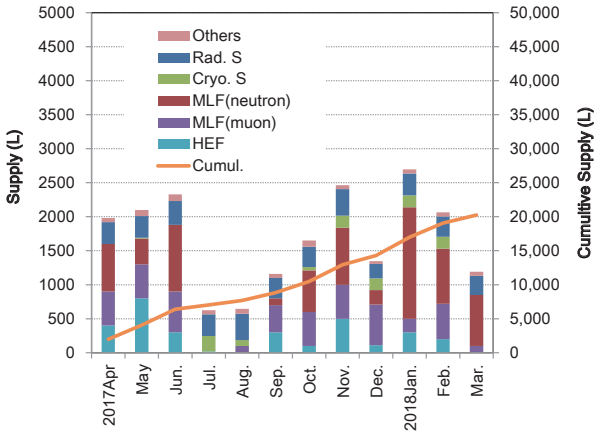

Fig. 2. Liquid nitrogen supply at J-PARC from April 2018, to March 2019.

Superconducting Magnet System for T2K

The superconducting magnet system for the T2K experiment operated during the periods shown in Table 1. The system worked well without disturbing the beam time. The operation time was short and regular maintenances were carried out in the summer. Figure 3 summarizes the incidents in the refrigeration system from FY2009. The system was suspended only in its early period due to problems in the hardware and control parameters. After FY2012, no refrigerator suspension occurred, except for accidental power outage. Recently, the system has been very stable. Although a few problems with hardware parts occur every year, the troubles have been resolved without interrupting the operation.

Table 1. Operation history of the T2K superconducting magnet system.

	2018 Apr.	May	June	Jul.	Aug.	Sep.	Oct.	Nov.	Dec.	2019 Jan.	Feb.	Mar.
Operation	2/28-6/1											3/13-3/29
Maintenance												

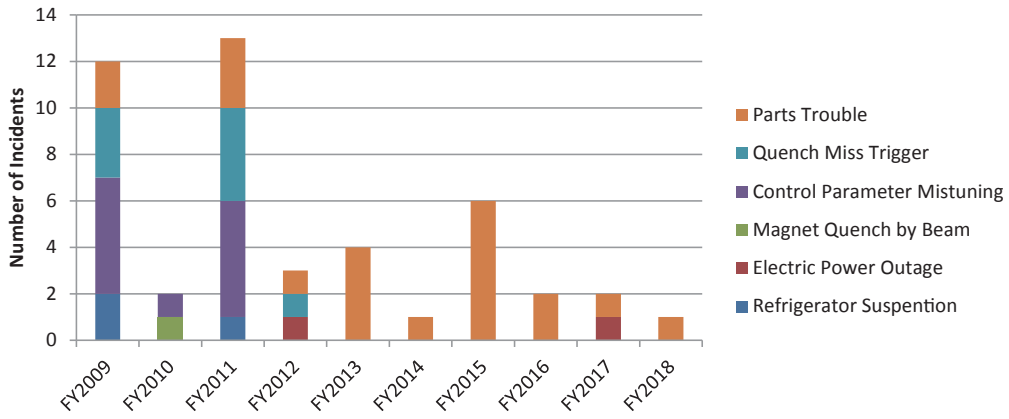

Fig. 3. Summary of incidents in the Refrigerator System for T2K.

Superconducting Magnet Systems at the MLF

The Cryogenic Section contributes to the operation and maintenance of the superconducting magnet systems at the Muon Science Facility (MUSE) in the MLF. The superconducting solenoid in the Decay Muon Line (D-line) was operated from January to the end of June 2018. After the annual maintenance in the summer shutdown from July to September, it was restarted on October 15. It was stopped on December 21 for the New Year holidays and resumed on January 15. No serious problem was found in the cryogenic system for D-line magnets in FY2018. In July and September 2018, two superconducting solenoid magnets were cooled down and tested. It took about two weeks for both magnets to cool down to 4 K, and they were successfully ramped up to a current of 187 A, corresponding to 105% of the nominal current of 178.5 A. These magnets will be installed in the High Momentum Muon Line (H-line) soon.

Superconducting Magnet Systems at the HEF

The COMET experiment is under construction in the Hadron South Experimental Hall (HDS) of the Hadron Experimental Facility (HEF). The Cryogenics Section was involved in the construction of the cryogenic system and superconducting magnets. Production of the superconducting solenoid magnet using radiation-resistant materials is in progress for the muon source. The detailed design of the cryostat of the Pion Capture Solenoid was improved.

The magnets are designed to be cooled by a two-phase flow of liquid helium which is supplied by a helium refrigeration system built in HDS. The cooling capacity of the helium refrigerator has been measured to be 140 W at 4.5 K in the case of 500 W heat load on shield gas. Currently, a lead system which includes helium distribution is under development.

The transfer line from the current lead system to the Muon Transport Solenoid (MTS) was fabricated and installed in the HDS in FY2018. It has four cooling pipes and four bundles of superconducting wires which are cooled down by thermal conduction from a 4-K pipe. Before the fabrication, we performed cooldown tests with a short cut model of the transfer line to optimize the thermal contacts to bundles of superconducting wires. It was found that each bundle of 3 wires had to be surrounded by a thin Indium sheet and the thermal anchor blocks needed additional pure aluminum at the contacts to cool down properly all superconducting wires. It was clarified from the tests that all 12 wires reached a temperature less than 4.6 K. Figure 4 shows a thermal anchor blocks for 4 bundles fabricated in the factory. At the end of the installation, the superconducting wires were soldered with the lead wires to the protection diodes of the MTS, as shown in Fig. 5.

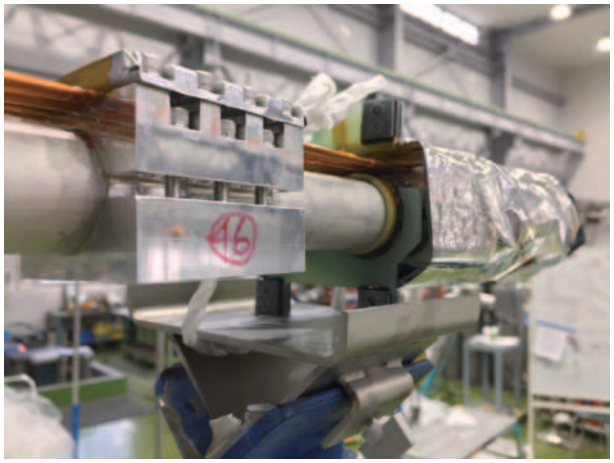

Fig. 4. Thermal anchor block with 12 superconducting wires in the transfer line.

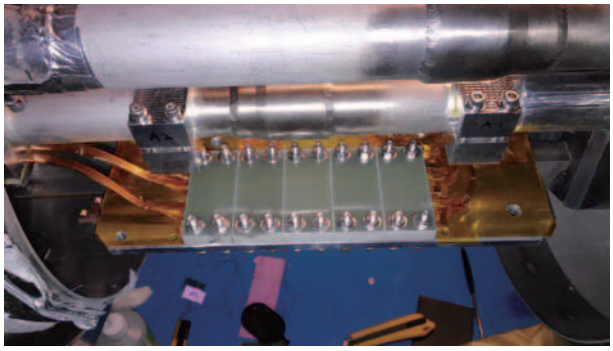

Fig. 5. Soldered splices at the interface to the protection diodes of the Muon Transport Solenoid.

R&D for the Future Projects at J-PARC

The g-2/EDM project aims for the precise measurement of the anomalous magnetic moment and the electric dipole moment of muons. This experiment was proposed at the MUSE H-Line. A superconducting solenoid with a high field homogeneity, better than 1 ppm locally, plays a very important role as a muon storage ring. In 2018, the design study focused on the kicker coil. The shielding effect of transient field of the kicker coil due to SUS chamber was calculated in detail and the chamber size was increased to reduce the shielding effect.

A muonium hyperfine structure measurement, called MuSEUM experiment, has been proposed for the same beam line as the g-2/EDM project. In the experiment, the energy state transition in muonium will be observed under a static magnetic field with local homogeneity of 1 ppm. A standard NMR probe to determine the absolute magnetic field is being developed to calibrate other probes. Cross calibration tests in the collaborative framework between the USA and Japan have been in progress since 2017. The comparison between the US probe and the newly developed KEK probe was carried out at the Argonne National Laboratory (ANL) in January and February 2019, as shown in Fig. 6. The data analysis is in progress, and the discussion will take place in J-PARC in September 2019.

Fig. 6. Cross calibration test between KEK and US probes in the MRI magnet at the ANL.

HTS Maglev Coaster for Demonstration

Cryogenics Section conducted constructing superconducting magnetic levitation coasters for public relations and for educational lessons to demonstrate cryogenics with the ReBCO high-temperature superconductor. For easy treatment and safety, a long track rail made of rubber magnet ribbon has been utilized recently, instead of Neodymium magnets. The light weight superconducting coaster is fabricated with a ReBCO tape coated conductor to achieve enough levitation and pinning on the weak magnet track.

Information System

Overview

The Information System Section plans, designs, manages and operates the network infrastructure of J-PARC and also provides support to ensure its information security. In terms of computing, until now, J-PARC has owed its major computer resource for analyzing and storing data from neutrinos, nuclear physics and MLF experiments to the KEK central computer system. The section connects the J-PARC network to the KEK central computing system directory and helps the users to utilize the system effectively.

Status of Networking

Since 2002, the J-PARC network infrastructure, called JLAN, has been operated independently from KEK LAN and JAEA LAN in terms of logical structure and operational policy. In 2018, the total number of hosts (servers and PCs) on JLAN exceeded 5,000 and the number has increased by 106% from the last year. The growth curve of edge switches, wireless LAN access points and hosts connected to JLAN are shown in Figure 1.

In April 2016, the National Institute of Informatics (NII) upgraded SINET (Japan Science Information Network https://www.sinet.ad.jp) from version 4 to 5. SINET is not only a gateway from JLAN to the internet but also an important connection between Tokai and KEK Tsukuba site in J-PARC.

Figures 2 and 3 show the network utilization of the internet from/to JLAN. Since the bandwidth capacity for the internet through the SINET is 10 Gigabits per second (Gbps), it is clear that there is enough space for additional activity. Figures 4 and 5 show the statistics of data transfer between the Tokai site and the Tsukuba site. The network bandwidth capacity between the two sites is 10 Gbps. This shows the usage level has been approaching a half of it, especially during the period when the Hadron facility was running. In addition to the current bandwidth, the upgrade offers a future option of 20 Gbps for both of internet and Tokai-Tsukuba connections, if J-PARC network can be adapted.

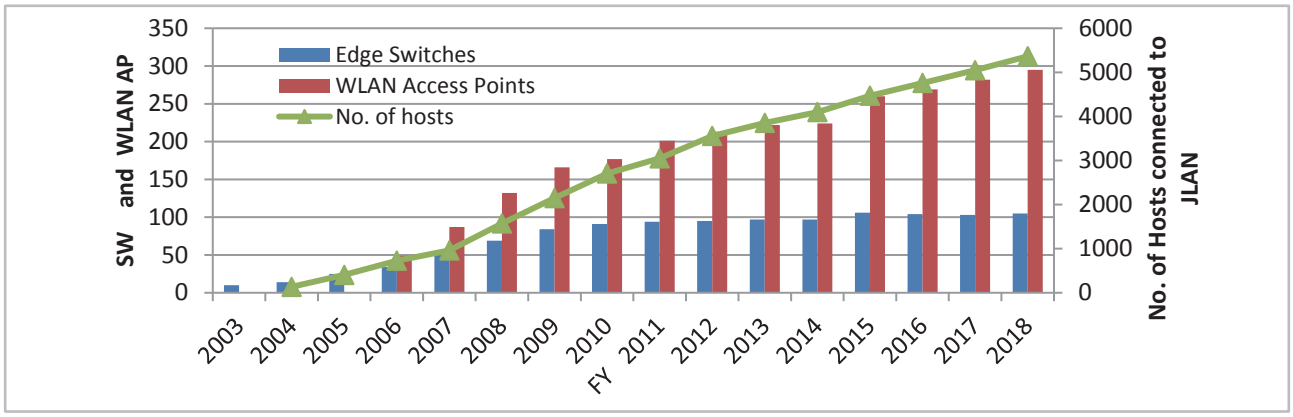

Fig. 1. Number of hosts, edge SW and wireless AP on JLAN

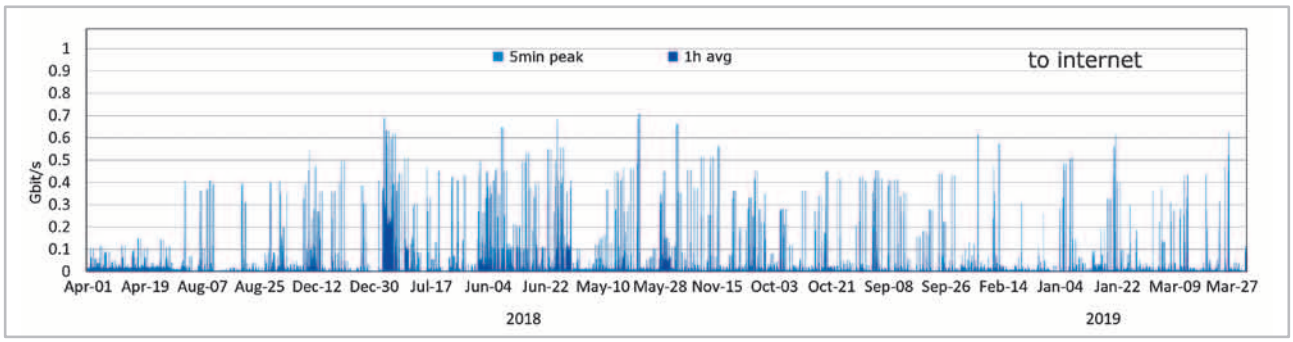

Fig. 2. Network traffic from JLAN to the internet
(1 hour average and 5 minutes peak value).

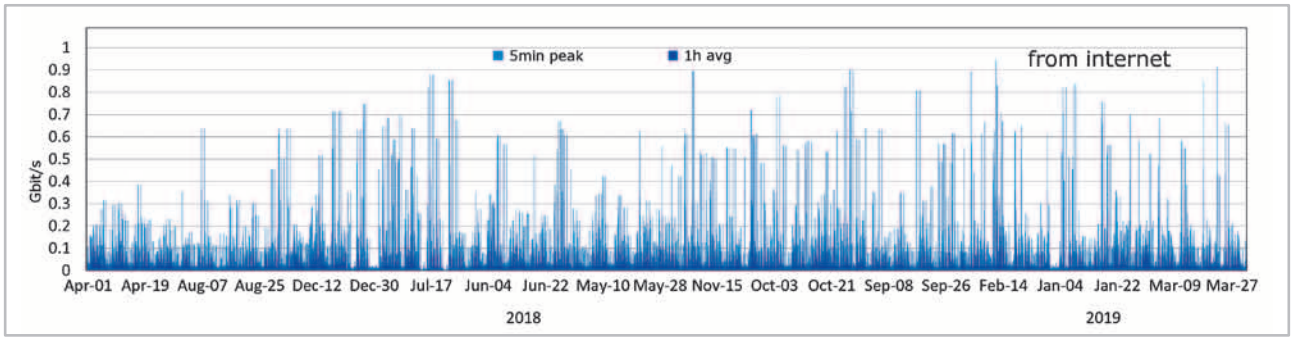

Fig. 3. Network traffic from the internet to JLAN

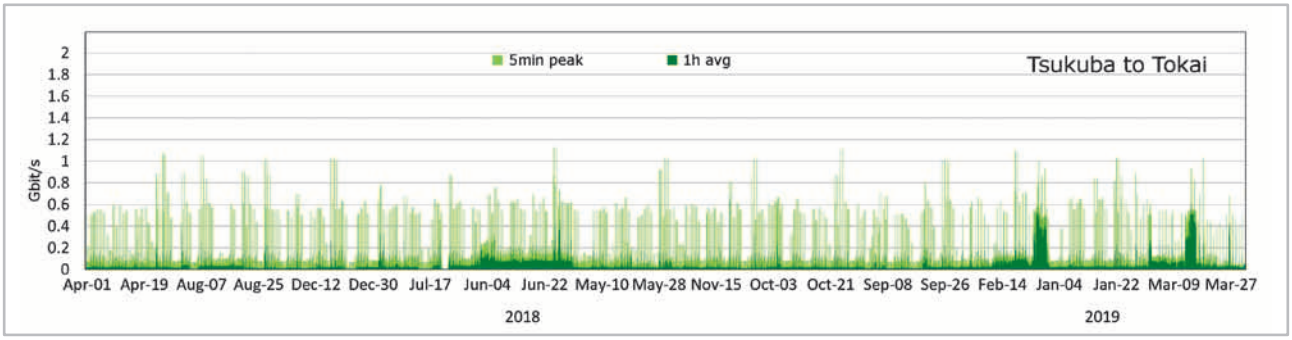

Fig. 4. Network traffic from Tsukuba site to Tokai site.

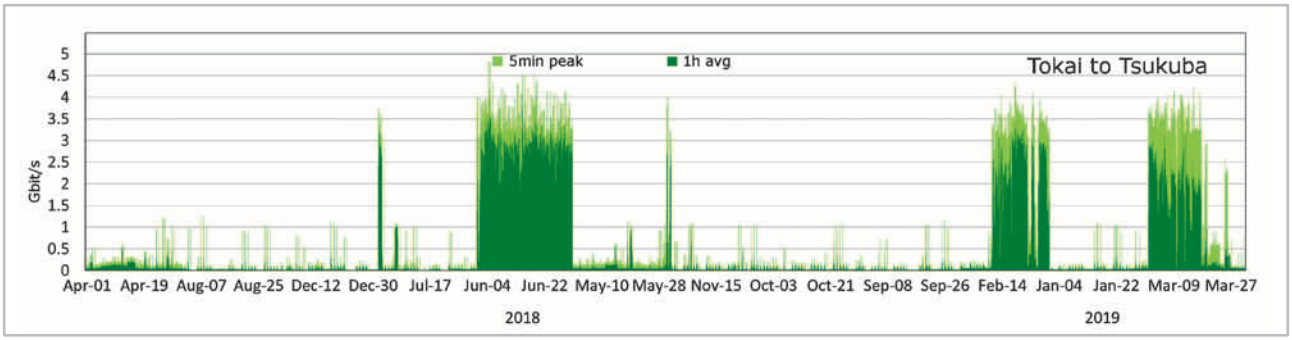

Fig. 5. Network traffic from Tokai site to Tsukuba site.

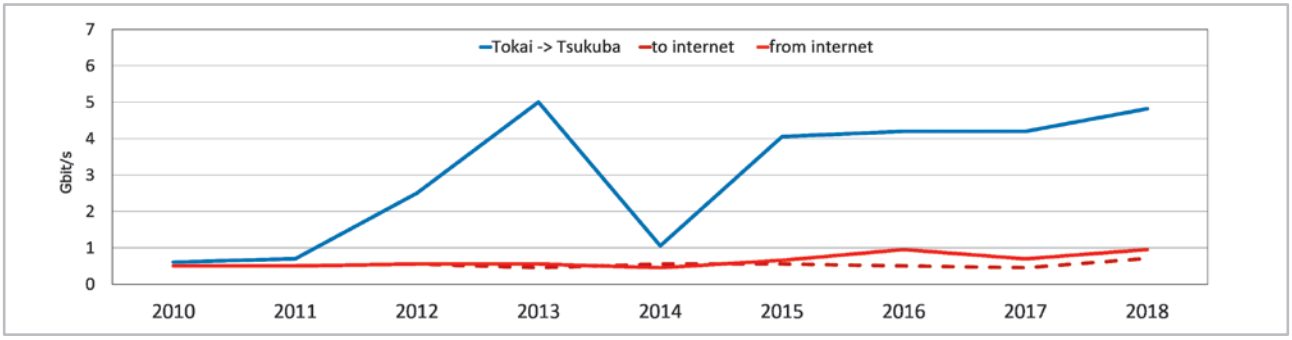

Fig. 6. Peak network traffic for recent years.

Internet Connection Services for Visitors and Public Users of J-PARC

Since 2009, J-PARC has offered a Guest network (GWLAN) service, which is a wireless internet connection service for short-term visitors, available in almost all J-PARC buildings. In the end of 2014, additional network service called User LAN has started. In using the GWLAN, users are required to receive a password at the J-PARC Users Office beforehand, while in the User LAN users are authenticated by the same ID and password for the User Support System, which is also used for dormitory reservation or so on. From March 2016, a new service called "eduroam" has been started. The eduroam (https://www.eduroam.org/) is a secure roaming access service developed for the international research and education community and mutually used among a huge number of research institutes, universities and other institutions around the world. The eduroam service will be a convenient third option of internet connection service for J-PARC visitors. Figure 7 shows this FY usage statistics of GWLAN, User LAN and the newly introduced eduroam service.

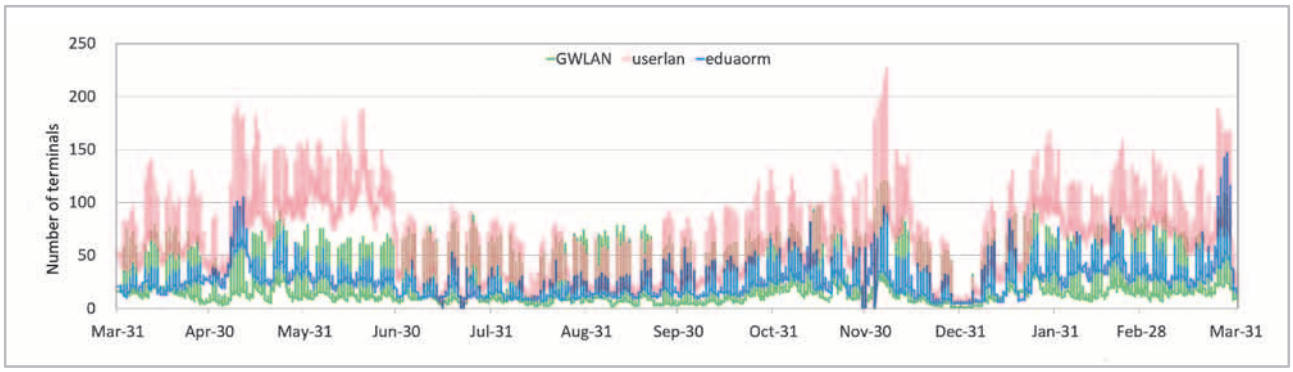

Fig. 7. Usage trends of GWLAN, User LAN and eduroam.

Status of Computing

J-PARC does not have computing resources for physics analysis, so since 2009, the KEK central computing system (KEKCC) at the KEK Tsukuba campus has been mainly used. At the Neutrino (T2K), Hadron and Neutron (MLF) experiments, the data taken in J-PARC are temporarily saved at their facilities and then promptly transferred, stored and analyzed at the system in Tsukuba. The storage of the system is also be utilized as a permanent data archive for their data.

The second upgrade of the system was completed in 2016, and the computing resources assigned to J-PARC are shown in Table 1. Figures 8-10 show the utilization statistics of the computing resources in 2018. The main users who used the CPU and storage constantly were from the Hadron experiment (KOTO) and Neutrino groups. The MLF group also started to store data to tapes on the system.

Table 1. Assigned computing resources to J-PARC activities in the KEKCC

CPU (Intel Xeon E5-2697v3)	4700 cores
RAID Disk (GPFS)	4.5 Peta Bytes
Tape (HSM)	27 Peta Bytes

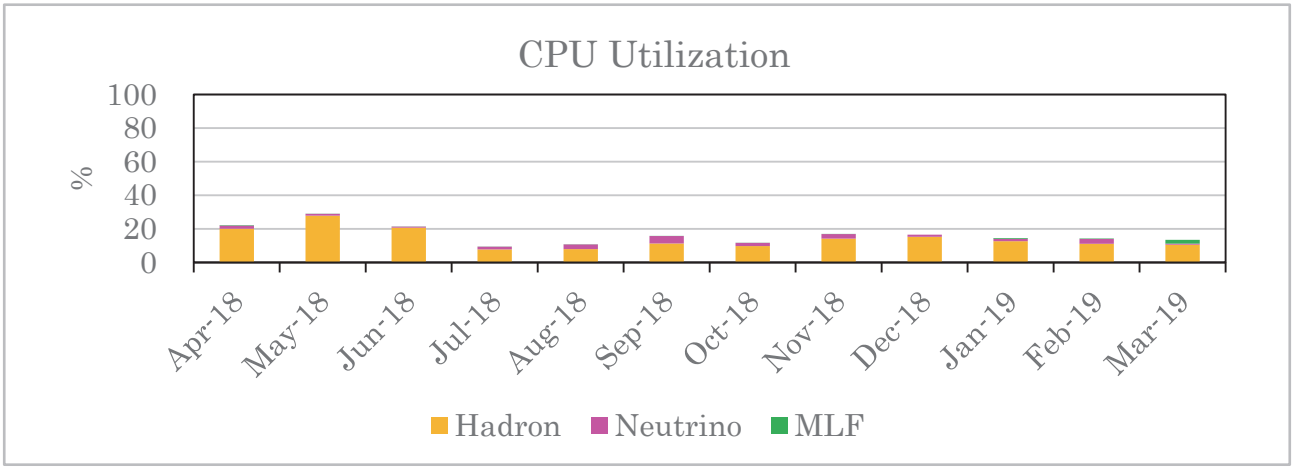

Fig. 8. CPU usage statistics (the yellow line shows resource assignment for J-PARC)

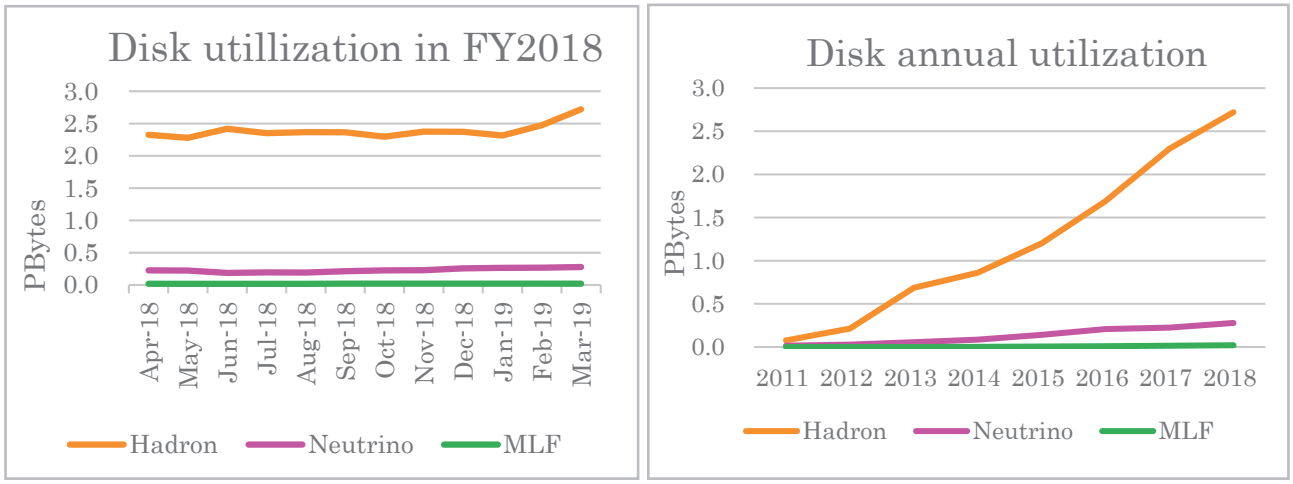

Fig. 9. Disk usage statistics (Left: trend of this FY year; Right: annual trend)

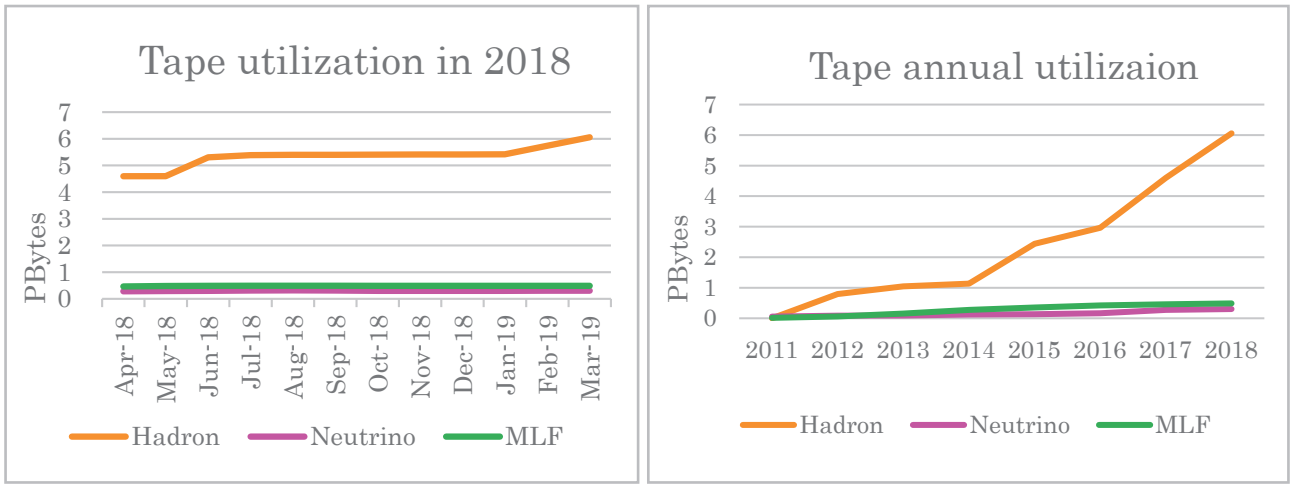

Fig. 10. Tape library usage statistics (Left: trend of this FY year; Right: annual trend)

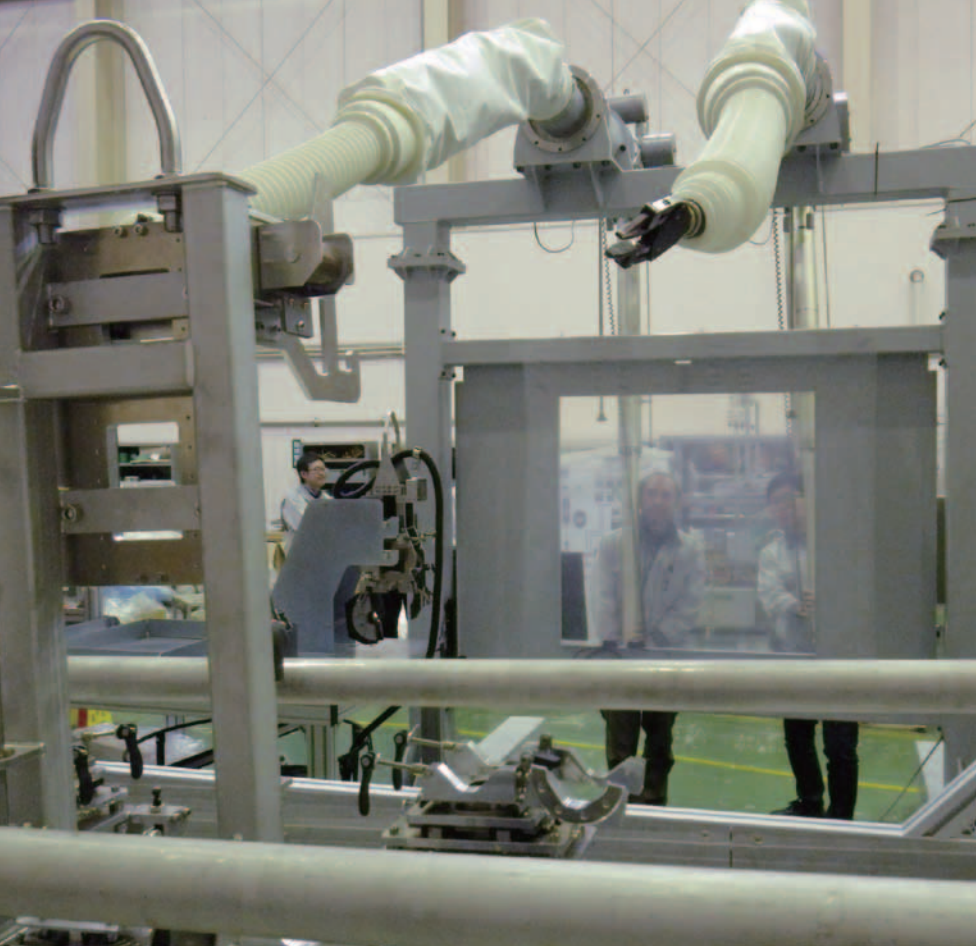

Transmutation Studies

Overview

We have been working on R&D for developing nuclear transmutation technology with accelerator-driven systems (ADS) using the J-PARC's research resources and expertise on high-power accelerator and target technologies. The ADS is an effective nuclear system for volume reduction and mitigation of harmfulness of high-level radioactive waste.

Nearly 20 years ago, we proposed the concept of an experimental facility, Transmutation Experimental Facility (TEF), for development of ADS. TEF consists of two individual facilities; the ADS Target Test Facility (TEF-T) for irradiation of beam window materials, which is required for development of high-power lead-bismuth eutectic (LBE) targets, and the Transmutation Physics Experimental Facility (TEF-P) for reactor physics study for proton beam driven subcritical cores with bearing minor actinide fuels. A technical design report for TEF-T (JAEA-Technology 2017-003, 539 pages) and a safety design report for TEF-P (JAEA-Technology 2017-033, 383 pages) have been published. In 2018, the design report for TEF-T was further reinforced and translated into English. Owing to these efforts, we believe that the basic design of TEF-T and TEF-P has been completed.

In 2018, we have started reorienting the concept of the experimental facility to make it more attractive and effective by introducing leading edge knowledge to its purpose and specifications. The main purpose of the new facility is the same as TEF-T, that is, irradiation

of beam window materials of ADS by impinging the proton beam to the LBE target. In addition, since there is a strong demand to irradiate beam window and target materials at J-PARC's existing experimental facilities, the new facility is equipped with a space in front of the LBE target to irradiate various sample materials by the proton beam. Thus, the new facility is a proton irradiation facility.

The idea of TEF-T is to irradiate sample materials at TEF-T, and once they are irradiated, the materials are transported to JAEA's hot-labo facilities for post-irradiation examination (PIE). However, this method is inefficient because of the problems with transportation of radioactive materials, and the JAEA's hot-labo facilities are rather old. Hence, the new facility is furnished with a hot-labo. The hot-labo can be used for PIE for irradiated materials in both the new facility and the existing J-PARC's experimental facilities. Accordingly, the new facility can contribute not only to the development of ADS but also to upgrading the J-PARC's existing facilities.

We have continued our R&D activities to support the design of the experimental facility and ADS. We are developing the LBE target technologies on the topics of thermal-hydraulics, materials corrosion, instrumentation including oxygen concentration control, acquiring operation experience by mainly using two large LBE circulation loops, etc. We are continuing the measurement of nuclide production and displacement cross sections, and the development of proton beam monitors, which can withstand a high-power proton beam. We are also continuing reactor physics experiments by using critical assemblies. Details of these R&D activities are described in this chapter. In 2018, we launched an R&D activity to develop superconducting linac for ADS with the full cooperation of J-PARC's accelerator team.

On February 14 and 15, 2019, the fourth TEF Technical Advisory Committee (T-TAC), which was one of the technical advisory committees under the J-PARC International Advisory Committee, was held (Fig. 1). The T-TAC encouraged our efforts for the reorientation of the facility as "The proposed approach builds on J-PARC's strong expertise in the field of accelerator and target technologies and addresses a scope that encompasses not only the ADS mission but also other high-power accelerator applications. T-TAC finds that the proposed applications are sound and technically feasible."

Fig. 1. T-TAC members and attendees.

Research and development

Studies for proton irradiation facility

The experimental studies to establish the proton irradiation facility for ADS development have been progressing. In the LBE loop experiment, the operation for steady state and transient experiments has been performed by using IMMORTAL (Integrated Multi-functional MOckup for TEF-T Real-scale TArget loop). Regarding the target materials, conditioning operation and functional tests of OLLOCHI (Oxygen-controlled LBE LOop Corrosion tests in HIgh-temperature) started. In the area of instrument developments, the manufacturing of oxygen sensors and the development of a freeze-seal type valve (FV) are progressing as a key instrumentation technology for the LBE loop system. Development of remote handling technology for target maintenance has been advancing. The results are described in detail below.

IMMORTAL

To acquire verification and validation (V&V) data for the safety analysis code, we performed steady state and transient experiments by using IMMORTAL.

Fig. 2. Exterior of IMMORTAL.

A simulation test for accidental beam over power condition under a constant flowrate operation was performed. To simulate the beam over power condition, the output of the Main Heater (MH) was changed in the range from the initial state (100%, 57 kW) to 118% at the maximum. The flowrate of the primary (LBE) system and the secondary (pressurized water) system were 46 liter/min and 60 liter/min, respectively. As a result, it was confirmed that the temperature of each system rose up simultaneously. There was no significant change in the temperature difference compared with the initial conditions. Further, the heat transfer performance of a primary heat exchanger (HX) was preliminarily verified by the results of several non-isothermal operation tests. However, since the verification was based on a limited amount of experimental data, we will continue the experiments to accumulate more experimental data contributing to the verification and validation of the safety analysis code.

OLLOCHI

Before the corrosion test in OLLOCHI, the conditioning operation and the functional tests of the components were carried out. The electro-magnetic flowmeters (EMFs) were calibrated at 400˚C. As a functional test for the main heaters and the cooler, non-isothermal operations were performed at 450˚C with temperature difference of 100˚C. From the results, we obtained the correlation between the inlet valve lift of the air cooler and the temperature difference.

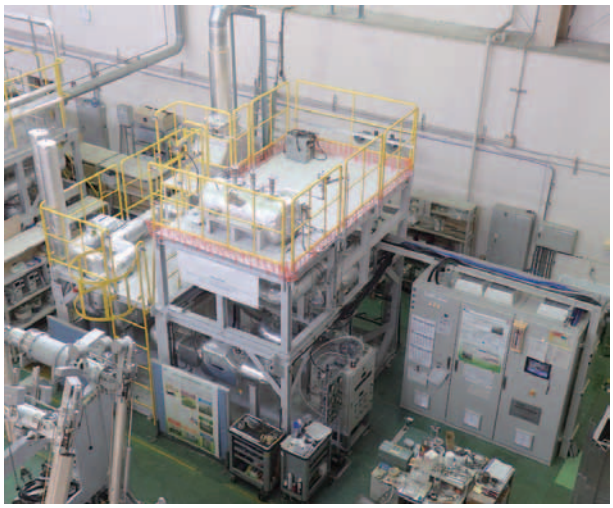

Fig. 3. Outline of OLLOCHI.

The dissolved oxygen concentration (OC) control tests started in January 2019. We managed to maintain manually the oxygen concentration within a certain range by mixing of the inlet gases. The control tests will be continued to obtain loop-specific parameters necessary for the automatic control of OC.

Oxygen concentration (OC) control tests

In order to control OC in LBE automatically, oxidizing gas or reducing gas is temporarily added to the cover gas phase when the oxygen sensor output

crosses the setting thresholds. As a result of demonstration experiment, OC was kept at a target value (0.98 V) constant under stagnant LBE condition using an oxygen sensor calibration system (Fig.4). By applying the same control scheme to the LBE loops, we will start an automatic control test under the LBE flow condition in FY2019.

Fig. 4. Oxygen sensor calibration system under stagnant LBE condition

Freeze-seal valve development

Freeze-seal valve (FV) is under development to add passive safety function to the LBE spallation target loop. By applying FV to the LBE loop, we can minimize the slow leak of LBE due to (1) sticking small chemical compounds into the seal of the mechanical valve, (2) accidents, such as station blackouts. LBE in FV melts by their own latent heat and LBE will be drained out automatically. However, LBE shows re-crystallization with volumetric expansion after solidification and that will generate stress in the FV. To mitigate the generated stress inside the FV piping, the hoop and axial stress for the stainless-steel container with LBE was measured by using apparatuses shown in Fig. 5. As a result, it was found that annealing at 50-80˚C was the most effective to reduce the stress. Cooling rate dependence was not observed in the stress. The stresses were lower than the allowable stress of SS304.

Fig. 5. Apparatuses for strain measurement.

Remote handling technology

Throughout the annual operation, the target vessel will be damaged from the bombardment by the pulsed proton beam and will be highly activated. It is essential, therefore, to develop remote exchanging technology for the target vessel. We have been evaluating the applicability of target exchange technology by remote cutting / welding of the loop piping. A prototypical remote jig to assist works has been improved. The operability of the revised jig was improved by adding new concepts, such as a simultaneous mounting structure of a commercial pipe cutter and a welding machine. Further, we adopted radiation testing as a candidate inspection method after welding. We will perform demonstration tests to establish a series of remote works for the exchanging of the target vessel by using these improved jigs shown in Fig. 6.

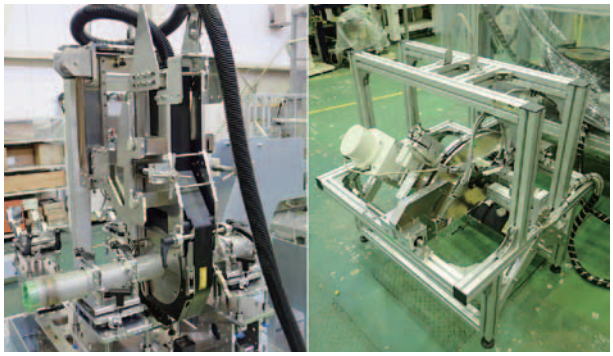

Fig. 6. Improved remote jig (left side) and a mockup of remote RT machine (right side).

Displacement cross section measurement

As an index of radiation damage of materials, displacement per atom (DPA) is widely used in many fields, such as fission and fusion reactors, and accelerator facilities. The DPA can be estimated by integrating a particle flux by the displacement cross section. Since the experimental displacement cross section data were scarce for protons with energy higher than 20 MeV, the experiment was conducted in J-PARC. The displacement cross section could be delivered from an electric resistivity increase of a sample by proton irradiation. To prevent the defect from recovering by the thermal motion of atoms, the sample was cooled to about 4 K by using a cryocooler. In Fig. 7, the present result of the displacement cross section of copper for 3-GeV proton is compared with the experimental data carried out in the

lower energy region and the calculation. The present data showed overestimation of about 4 times the calculation with Norgertt-Robinson-Torrens (NRT) model, which is widely utilized to obtain the displacement cross section. It was also shown that the PHITS with the improved model with athermal recombination correction model based on Nordlund parameter showed remarkably good agreement with the experimental data. By accumulation of experimental data in future work, the accuracy of the radiation damage calculation is expected to be improved.

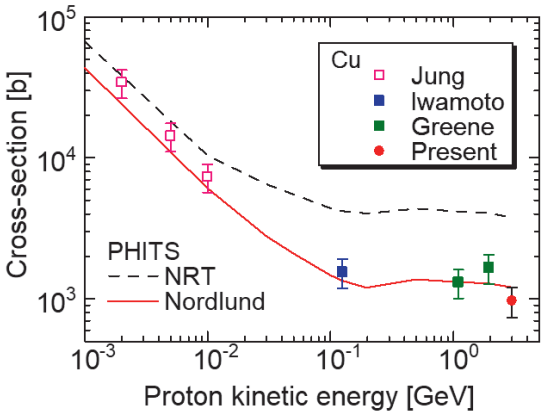

Fig. 7. Displacement cross section obtained with the experiment at J-PARC compared with a previous experiment and the calculations.

Improvement of the spallation model

The particle transport simulation plays an important role in the neutronic and shielding design of high-energy accelerator facilities and accelerator-driven nuclear transmutation systems. In the particle transport simulation at energies above several tens of mega-electron volts, a nuclear reaction model provides information about secondary particles and the spallation products produced from the spallation reactions.

As illustrated in Fig. 8, the spallation reaction is divided into two processes according to their dynamical time scales and mechanisms: the intranuclear cascade process and deexcitation process. In the first process, protons and neutrons that consist of a nucleus repeatedly collide with one another and emit from the target nucleus. Because the residual nucleus just after the first process is in highly excited state, it becomes stable in the subsequent process by emitting energetic particles. For heavy targets such as lead and mercury, a nuclear fission may occur competing with the particle emission.

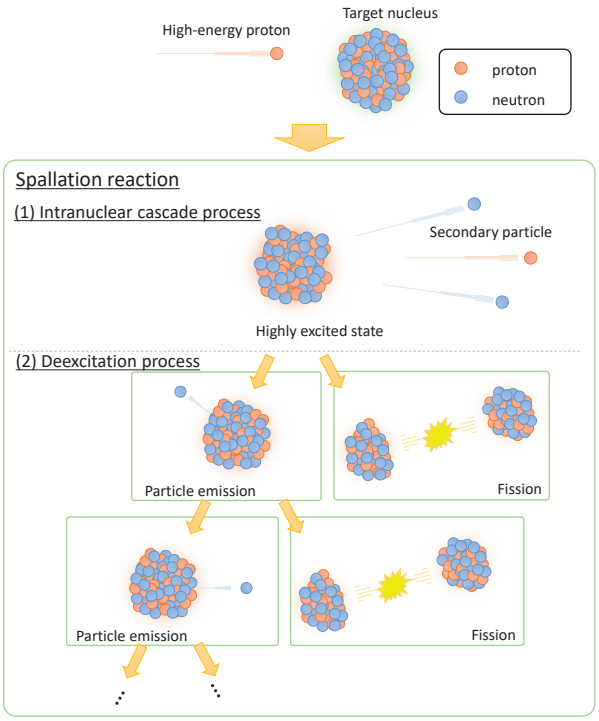

Fig. 8. Schematic of the spallation reaction

In our study, to improve the predictive capability of spallation product yields, particularly produced from the nuclear fission, a description of the fission probability in the spallation model was proposed [1]. Figure 9 shows the fission cross-sections of ^{208}Pb, ^{209}Bi, and ^{181}Ta calculated with the conventional and our proposed models. Comparing with experimental data for heavy nuclei showed that our proposed model can provide a unified prediction of the proton- and neutron-induced fission cross sections with markedly improved accuracy. In future work, the proposed model is expected to be

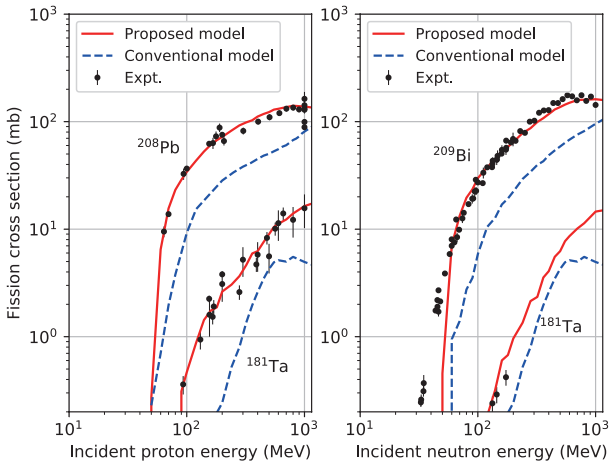

Fig. 9. Proton-induced (left panel) and neutron-induced (right panel) fission cross sections compared with the calculations and experimental values.

utilized in designing the accelerator-driven system for nuclear transmutation and its experimental facility at J-PARC.

MA transmutation experiments

ADS feasibility studies have been conducted at several experimental facilities of reactor physics, including the MASRUCA reactor (France), the YALINA booster (Belarus), the VENUS-F facility (Belgium), and the KUCA at Kyoto University (Japan). The Transmutation Experimental Facility (TEF) and the Multi-purpose hYbrid Research Reactor for High-tech Applications (MYRRHA) have been planned to construct functional experimental facilities for implementation of nuclear transmutation of MA by ADS. ADS incorporates an innovative system of safety whereby a reactor is operated at a subcritical state, with the combined use of a high-energy proton accelerator and a fast spectrum reactor core. Subcritical irradiation of MA by ADS with a critical assembly even at zero power is a very important step, before operating actual ADS facilities.

Using the KUCA facility, as shown in Fig. 10, the first significant attempt was made to demonstrate the principle of nuclear transmutation of MA by ADS through the injection of high-energy neutrons into the uranium fueled core at a subcritical state. The main objective of this experiments is to confirm fission reactions of neptunium-237 (^{237}Np) and americium-241 (^{241}Am), and capture reactions of ^{237}Np. Subcritical irradiation of ^{237}Np and ^{241}Am foils is conducted in a hard spectrum core with the use of the back-to-back fission chamber that obtains simultaneously two signals from specially installed test (^{237}Np or ^{241}Am) and reference (uranium-235) foils. Figure 11 shows an example of experimental results: the pulsed heights as the horizontal axis correspond to the kinetic energy of fission fragments in ^{237}Np and ^{235}U fission events.

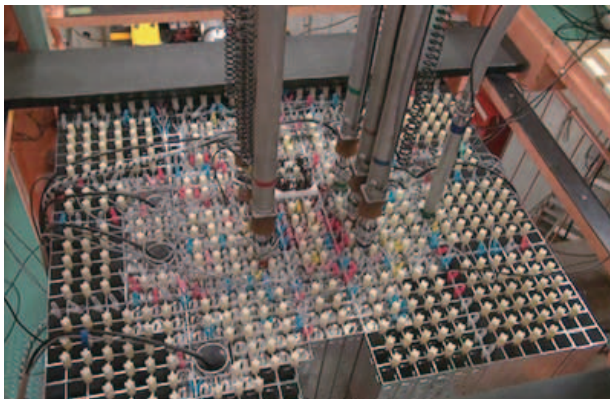

Fig. 10. Photograph of the solid moderated core of the KUCA facility.

The first nuclear transmutation of ^{237}Np and ^{241}Am by ADS soundly implemented by combining the subcritical core and the 100 MeV proton accelerator, and the use of a lead-bismuth target, is conclusively demonstrated through the experimental results of fission and capture reaction events [2].

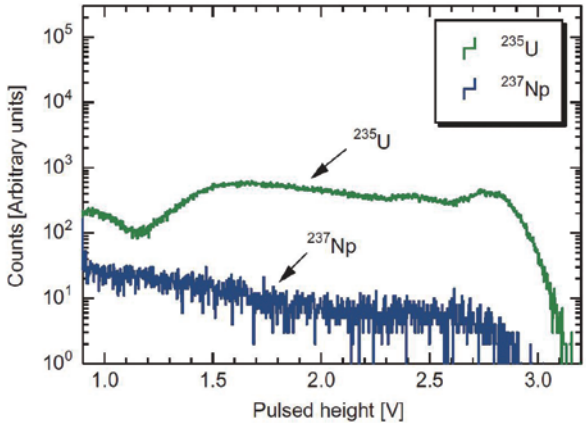

Fig. 11. An example of experimental results (Pulsed heights of ^{237}Np and ^{235}U fission reaction rates at subcritical state) [2].

References

[1] H. Iwamoto and S. Meigo, Journal of Nucl. Sci. and Technol. **56**, 160-171 (2019).

[2] CH. Pyeon *et al*., Journal of Nucl. Sci. and Technol. **56**, 684-689 (2019).

Safety

Safety

1. Major events on safety culture and safety activities at the J-PARC Center

The major events on safety culture and safety activities at the J-PARC Center are listed in Table 1.

Every year since 2014, the J-PARC Center holds workshop 5.23 for fostering safety culture to keep fresh the lessons of the radioactive material leak incident at the Hadron Experimental Facility on May 23, 2013. A "Safety Day" was launched last year, which, in addition to workshop 5.23, also includes a discussion of the safety culture. The safety day took place on May 25. In the morning, we held a meeting between the sections to exchange information on the safety efforts. The number of participants was 106. The director of the J-PARC Center gave away three "Safety Awards for good examples". The hadron section received one because they reported more good examples of safety in their daily works than the other sections. The other two were given to the neutron science section/technology development section/CROSS and accelerator section 1, because they reported excellent good examples.

Dr. Yoshimi Kasugai from the radiation safety section gave a scientific talk with the title "Where will the tritium generated in mercury via the spallation reaction be transferred?". Dr. Hiroshi Takada from the neutron source section introduced the safety work of the MLF facility under the title "Example of tritium emission control at the time of mercury target container exchange work". Also, Dr. Yoshinori Kurimoto from accelerator section 5 introduced the safety work of the accelerator facility under the title "Safety measures for the capacitor bank for main electromagnet power at the main ring – fuse wire melting trial and operation".

In the afternoon part of the Safety Day, workshop 5.23 for fostering safety culture was held at the auditorium of the Nuclear Science Research Institute with 284 attendees. Mr. Haruyasu Hoshino, project manager of the safety and health promotion division of Toyota Motor Corporation was invited this year; he spoke about a safety response and safety culture construction at the time of automation of work at Toyota.

The emergency drill was carried out on September 6. It was assumed that a big fire occurred in the Linac accelerator tunnel during a summer shutdown. The main purpose of the drill this year was to practice the response when an early attempt to extinguish the fire has failed.

The J-PARC Safety Audit in FY2018 was conducted by two external auditors (Prof. Akira Tose from Niigata University and Dr. Katsumi Hayashi from the Institution of Professional Engineers) on November 20-21. They reviewed mainly five points: safety control of work, introduction of "the business improvement pertaining to prevention of radiation hazards", effectiveness and review of the radiation safety education, notification of abnormal and emergency, activities for fostering safety culture. They suggested to put "stop oneself" in the idea of "stop work". They also pointed out that a culture to think and operate by ourselves was important.

Fig. 1. Emergency drill

2. Radiological license update and facility inspection

Applications to update the radiological license were submitted to the Nuclear Regulation Authority on July 9 and November 21. The major application items are listed in Table 2. The permits for the applications were issued on August 22 and on February 4, 2018, respectively. There were no cases requiring a facility inspection in FY2018.

3. Meeting of the committee on the radiation safety matter

The basic policies on radiation safety in the J-PARC are supposed to be discussed by the J-PARC Radiation Safety Committee (RSC). Meanwhile, the J-PARC Radiation Safety Review Committee (RSRC) is expected to discuss specific subjects of radiation safety in the J-PARC. The RSC meetings were held twice and those of the RSRC, three times. The major issues are summarized in Table 3.

4. Radiation exposure of radiation workers

In FY2018, 3342 persons were registered as

radiation workers. In these five years the number of workers fluctuated between 3000 and 3500, except for FY2014 when many contractors took part in the construction work of the hadron south experimental-hall, located in the radiation-controlled area of the Hadron Experimental facility.

The distribution of annual exposed doses is summarized in Table 4 for each category of workers: in-house staff, users and contractors. The exposed doses of gamma-rays and of neutrons were measured with an optically stimulated luminescence (OSL) dosimeter and with a plastic solid-state track detector, respectively. All users and almost in-house staff and contractors were exposed less than detection limit (Not Detected, expressed as "ND" in the table). The maximum exposed dose was 0.9 mSv. Though it was less than the administrative dose limit at the J-PARC (7 mSv/year), we should continue to make an effort to reduce the exposed doses of all workers.

Table 1. List of major events on safety in FY2018

Year	Date	Events
2018	May 25	Safety Day (Meeting to exchange safety information between all sections, Workshop for fostering safety culture)
	July 29	Liaison committee on safety and health for contractors
	Sep. 27, Oct. 3, 31 Nov. 2, 29	Refresher course on radiation safety for in-house staff
	Sep. 6	Emergency drill assuming a big fire in the Linac accelerator tunnel during a summer shutdown.
	Nov. 20 - 21	FY2018 J-PARC Safety Audit
2019	Jan. 24 - 25	6th Symposium on Safety in Accelerator Facilities

Table 2. Major application items of the radiological license

Facility	Items of an application
RCS	• Addition of samples for the proton beam irradiation experiment
MLF	• Change of material of the radiation shielding in the M2 beam line • Addition of description concerning maintenance work in the U-line • Addition of sealed radioisotopes • Reduction of a storage facility for induced radioactive materials
HD	• Beam intensity: $4.0 \times 10^{16} \rightarrow 4.3 \times 10^{16}$ protons/hour
NU	• Addition of disposal method of radioactive liquid waste in the second utility building • Change in the concentration assessment in the exhaust of radioactive gaseous waste generated inside a helium vessel
All	• Optimization of the application document

Table 3. Radiation Safety Committee (RSC) and Radiation Safety Review Committee (RSRC) in FY2018

No.	Date	Major Issues
The Radiation Safety Committee		
30th	28th May 2018	• Report of radiation exposure status in FY2017 • Policy on the radiological license update for the MLF, the HD and the Neutrino facilities • Report of deliberation status of revision proposal of the Local Radiation Protection Rule for J-PARC
31st	2nd Oct. 2018	• Policy on the revision of organizational structure for radiation safety management
32nd	27th Dec. 2018	• Report about the RSC • Report of revision of the Local Radiation Protection Rule for J-PARC
33rd	28th Mar. 2019	• Deliberation about the role of the RSC • Policy on the radiological license update in FY2019 • Report about the deliberation in RSRC
The Radiation Safety Review Committee		
19th	11th May 2018	• Update of the radiological license for the MLF, the HD and the Neutrino facilities
20th	3rd Jul. 2018	• Report of radiation exposure status in FY2017 • Revision proposal of the Local Radiation Protection Rule for J-PARC
21st	10th Sep. 2018	• Revision of the radiological license update for the RCS and the MLF facilities • Report of a hearing by the secretariat of the Nuclear Regulation Authority about a revision proposal of the Local Radiation Protection Rule for J-PARC
22nd	17th Dec. 2018	• Revision of the Local Radiation Protection Rule for J-PARC • Revision of the Detailed Rule of Local Radiation Protection Rule for J-PARC • Revision of the Transportation Rule for Radioactive Materials in J-PARC Site
23rd	20th Mar. 2019	• Update of the radiological license for the Linac, the RCS, the MR and the MLF facilities • Use of the X-ray generator at the JRB and the MLF facilities

Table 4. Annual exposed doses in FY2018

	# of workers	Dose range x (mSv)				Collective dose (person mSv)	Maximum dose (mSv)
		ND	0.1≤ x ≤1.0	1.0< x ≤5.0	5.0< x		
In-house staff	696	661	35	0	0	11.5	0.9
Users	1,296	1,296	0	0	0	0	0
Contractors	1,365	1,303	62	0	0	16.2	0.9
Total	3,342	3,245	97	0	0	27.7	0.9

User Service

Users Office (UO)

Outline

The J-PARC Users Office (UO) was established in 2007. It opened an office on the first floor of the IBARAKI Quantum Beam Research Center in Tokai-mura, in December 2008. UO maintains the Tokai Dormitory for the J-PARC users. UO provides on-site and WEB support with one-stop service for the utilization of the J-PARC. As of March 31, 2018, UO had 14 staffs and 4 WEB Support SE staffs in the Users Affairs Section. The J-PARC Users, after the approval of their experiment, follow the administrative procedures outlined on the Users Office (UO) WEB Portal Site, related to the registration as a J-PARC User, radiation worker registration, safety education, accommodation, invitation letter for visa and other requirements. Then, the UO staffs provide them with support by e-mail. After their arrival in the J-PARC, UO gives on-site assistance to the J-PARC Users, like receiving the J-PARC ID, glass badge, and safety education. Since 2015, UO had been doing its part to improve the J-PARC on-line experiment system and make it more user-friendly.

Map to J-PARC Users Office

Members of Users Affairs Section including UO staffs

1st row , left to right KIMURA Rie, KOYA Michiyo, ISHIKAWA Tomoko, KATOGI Aki, HOSHINO Junko, OIKAWA Kota, SOMEYA Mie.
2nd, left to right ENDO Maya, SANAO Ai, WAKU Satoshi, HASEGAWA Shigeo, NAMIKI Shinji.
3rd, ISOZAKI Mari, ISHIKAWA Taeko, OKUKI Rika, HANAWA Masahiro, MAEDA Kenji, HAGIWARA Tomonori, AIZAWA Yusuke.

Activities of UO

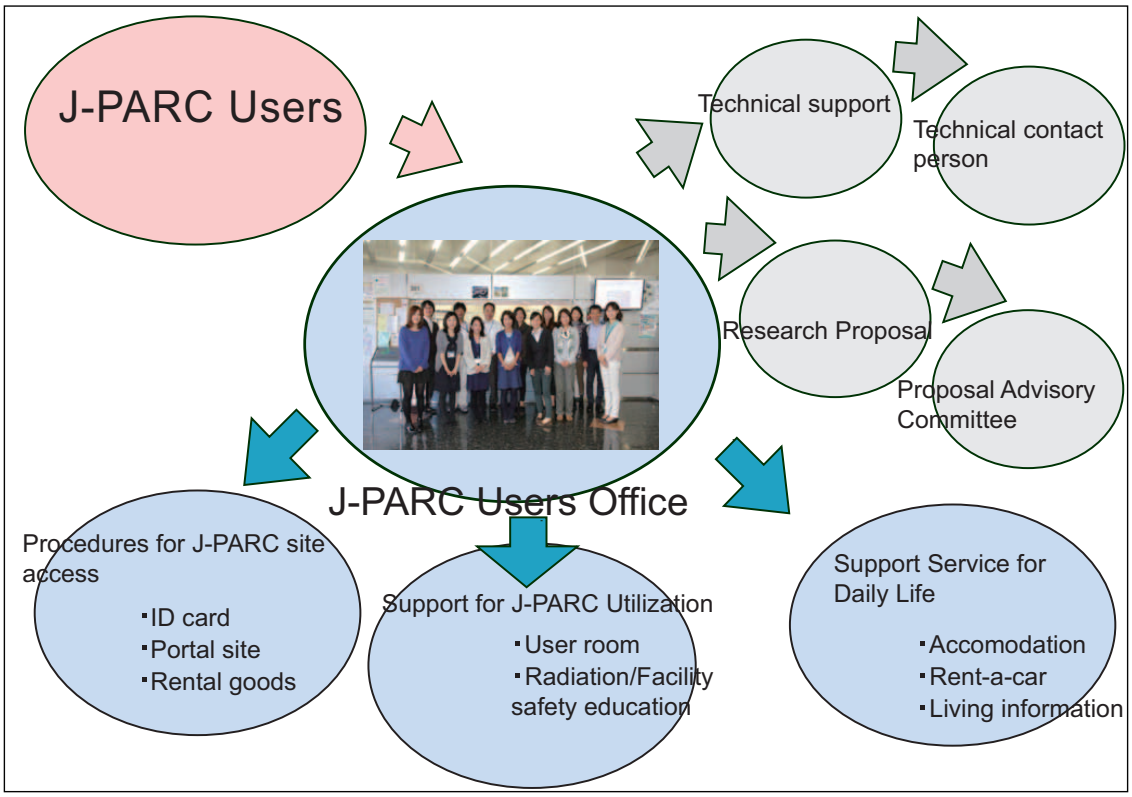

One stop service for J-PARC users

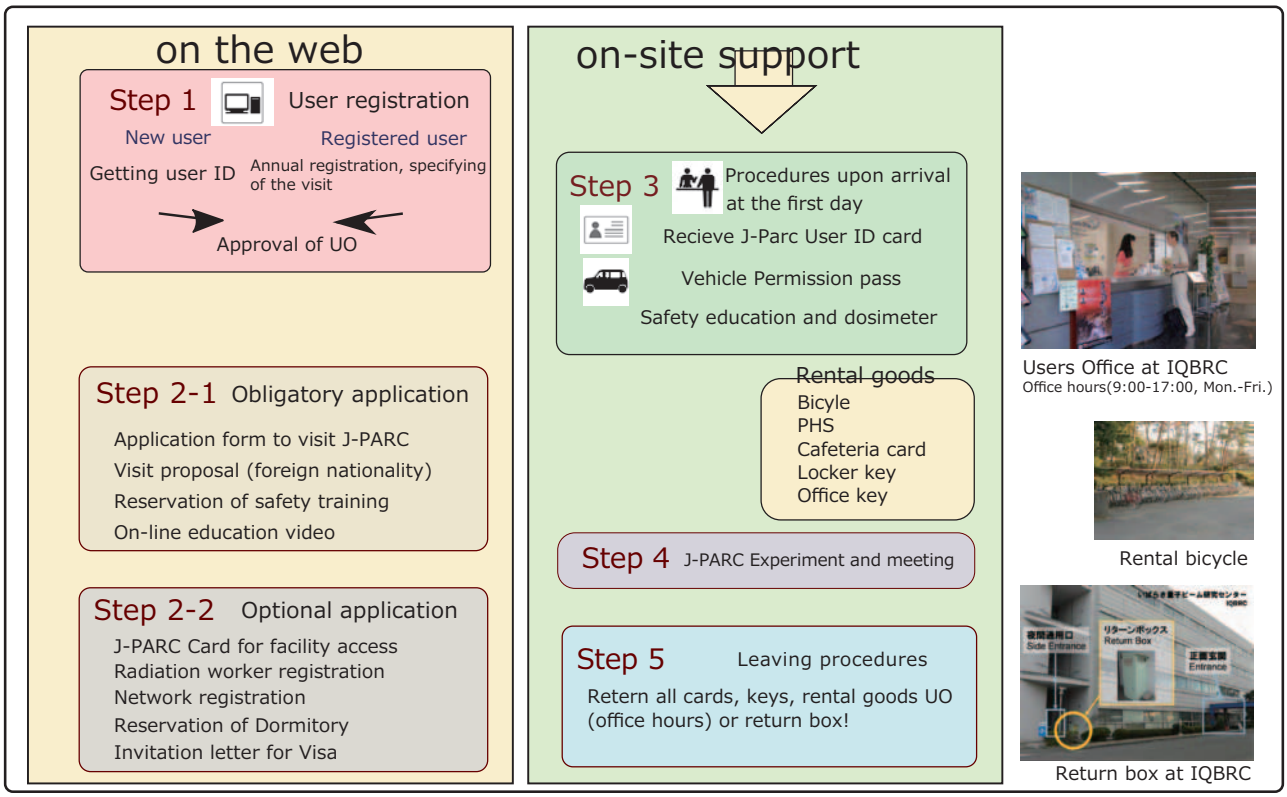

User Statistics

Users in 2018 (Japanese/Foreigners, person-days)

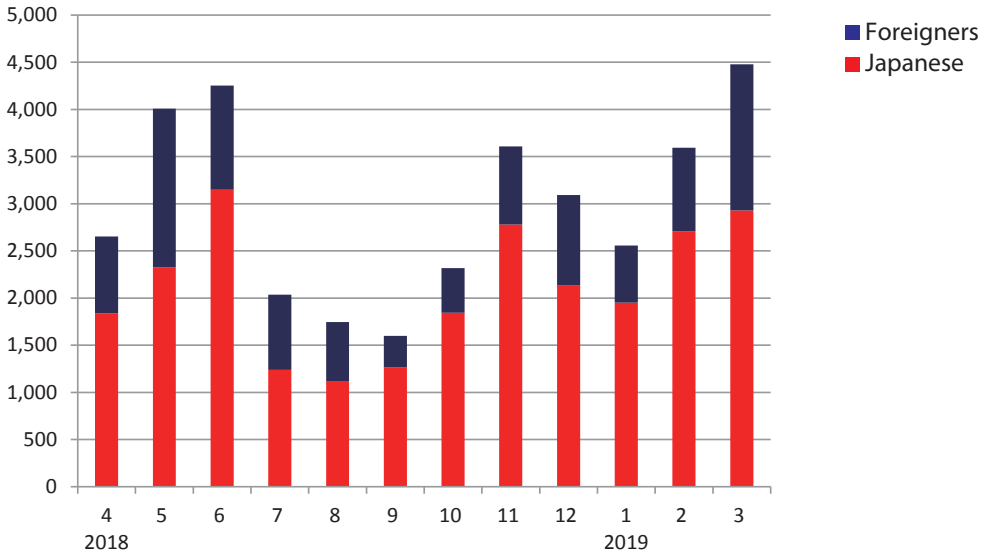

Users in 2018 (according to facilities, person-days)

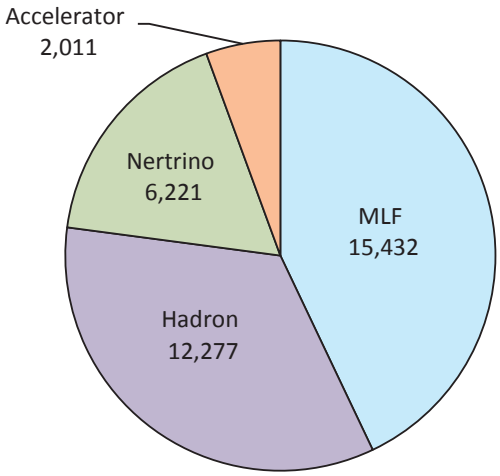

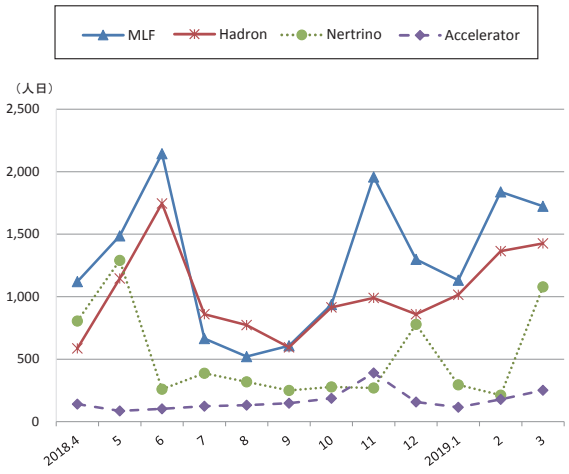

Users in 2018 (according to organizations, person-days)

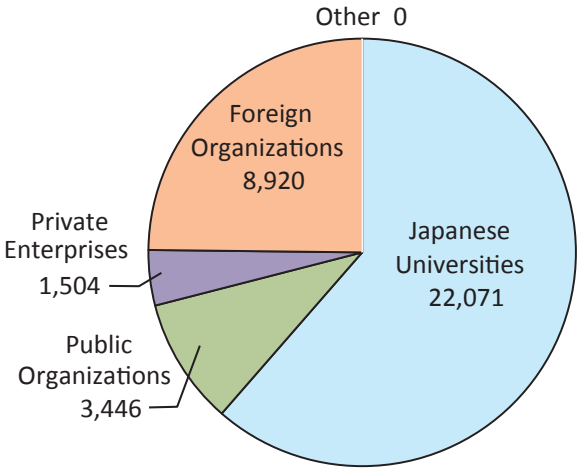

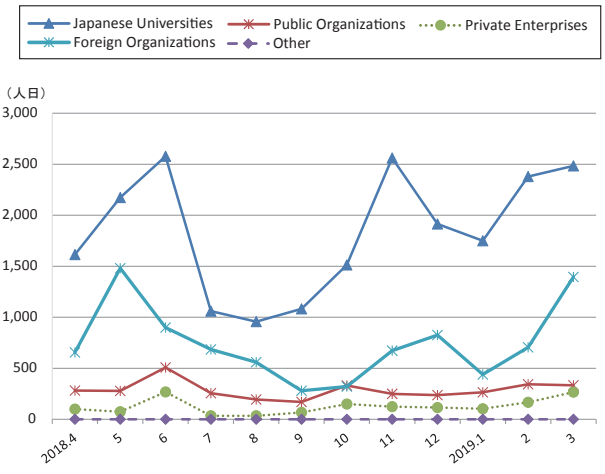

MLF Proposals Summary - FY2018

Table 1. Breakdown of Proposals Numbers for the 2018 Rounds

Beam-line	Instrument		2018A		2018B		Full Year			
			Submitted	Approved	Submitted	Approved	Submitted		Approved	
			GU	GU	GU	GU	PU/S	IU	PU/S	IU
BL01	4D-Space Access Neutron Spectrometer - ***4SEASONS***		18(0)	10(0)	18(0)	13(0)	1	1	1	1
BL02	Biomolecular Dynamics Spectrometer - ***DNA***		14(1)	12(1)	25(2)	13(2)	2	1	2	1
BL03	Ibaraki Biological Crystal Diffractometer - ***iBIX***	(100-β)‡	4	2	2	1	0	0	0	0
		(β)†	0	0	0	0	33	0	33	0
BL04	Accurate Neutron-Nucleus Reaction Measurement Instrument - ***ANNRI***		6	4	10	4	1	1	1	1
BL05	Neutron Optics and Physics - ***NOP***		3	3	5	5	0	0	0	0
BL06	Neutron Resonance Spin Echo Spectrometers - ***VIN ROSE***		2	2	7	4	0	0	0	0
BL08	Super High Resolution Powder Diffractometer - ***S-HRPD***		8	7	9	8(0)	0	0	0	0
BL09	Special Environment Neutron Power Diffractometer - ***SPICA***		4	1	2	2	0	0	0	0
BL10	Neutron Beamline for Observation and Research Use - ***NOBORU***		4	4	10	7	2	1	2	1
BL11	High-Pressure Neutron Diffractometer - ***PLANET***		9(0)	7(0)	7(0)	7	0	1	0	1
BL12	High Resolution Chopper Spectrometer - ***HRC***		8	6	7	7	1	0	1	0
BL14	Cold-neutron Disk-chopper Spectrometer - ***AMATERAS***		34	17	24	13	3	1	3	1
BL15	Small and Wide Angle Neutron Scattering Instrument - ***TAIKAN***		34(3)	17(3)	36(3)	22(3)	3	3	3	3
BL16	High-Performance Neutron Reflectometer with a horizontal Sample Geometry - ***SOFIA***		20	18	20	19	0	1	0	1
BL17	Polarized Neutron Reflectometer - ***SHARAKU***		16(0)	11(0)	20(1)	14(1)	2	3	2	3
BL18	Extreme Environment Single Crystal Neutron Diffractometer - ***SENJU***		24(0)	12(0)	18(0)	5(0)	1	2	1	2
BL19	Engineering Diffractometer - ***TAKUMI***		20	18	22		1	1	1	1
BL20	Ibaraki Materials Design Diffractometer - ***iMATERIA***	(100-β)‡	8	7	7	7	0	0	0	0
		(β)†	31	31	31	31	25	0	25	0
BL21	High Intensity Total Diffractometer - ***NOVA***		15	13	25	19	0	0	0	0
BL22	Energy Resolved Neutron Imaging System - ***RADEN***		13(1)	12(1)	20(2)	15(2)	0	3	0	3
BL23	Polarization Analysis Neutron Spectrometer - ***POLANO***		0	0	0	0	0	0	0	0
D1	Muon Spectrometer for Materials and Life Science Experiments - ***D1***		9(1)	6(1)	15(1)	4(1)	0	1	0	1
D2	Muon Spectrometer for Basic Science Experiments - ***D2***		8(0)	6(0)	9(0)	6(0)	0	1	0	1
S1	General purpose μSR spectrometer - ***ARTEMIS***		13(0)	12(0)	25(2)	18(2)	0	1	0	1
UA	Muon U		0	0	0	0	0	1	0	1
Total			***325***	***238***	***374***	***266***	***75***	***23***	***75***	***23***

GU : General Use **PU :** Project Use or Ibaraki Pref. Project Use **S :** S-type Proposals
IU : Instrument Group Use
† : Ibaraki Pref. Exclusive Use Beamtime (β = 80% in FY2018
‡ : J-PARC Center General Use Beamtime (100-β = 20% in FY2018)
( ) : Proposal Numbers under New User Promotion or P-type proposals (D1,D2) in GU

Table 2. Proposals Numbers of Long Term Proposal for the 2018 Rounds

Application	Submitted	Approved
2018	9	5

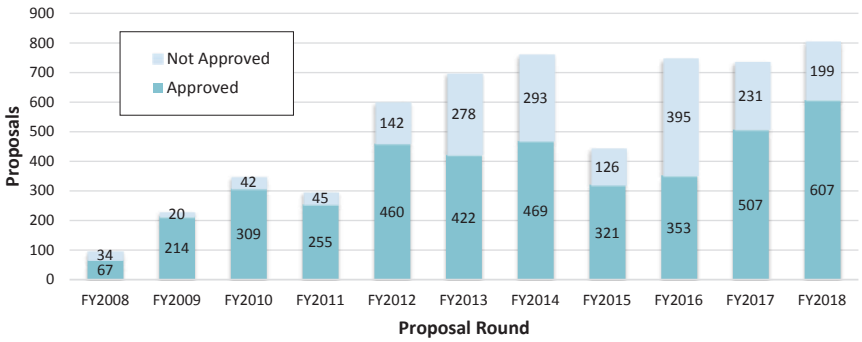

Fig. 1. MLF Proposal Numbers over Time

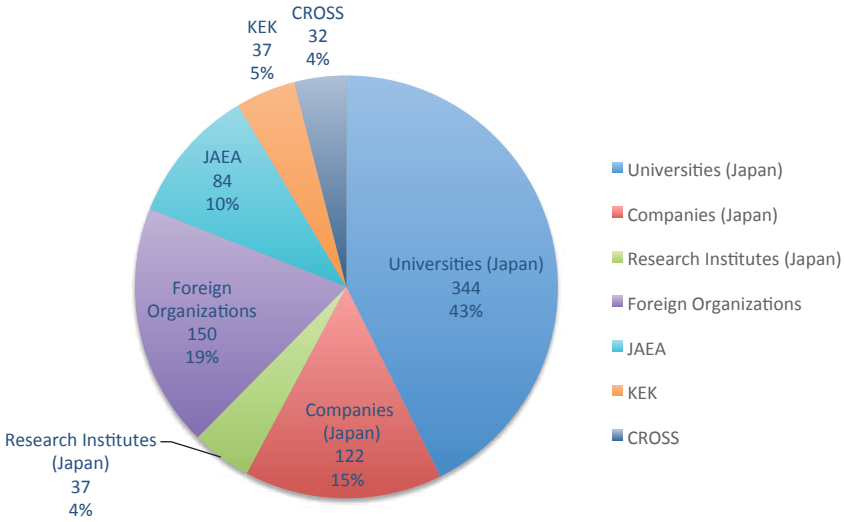

Fig. 2. Origin of Submitted Proposals by affiliation - FY2018

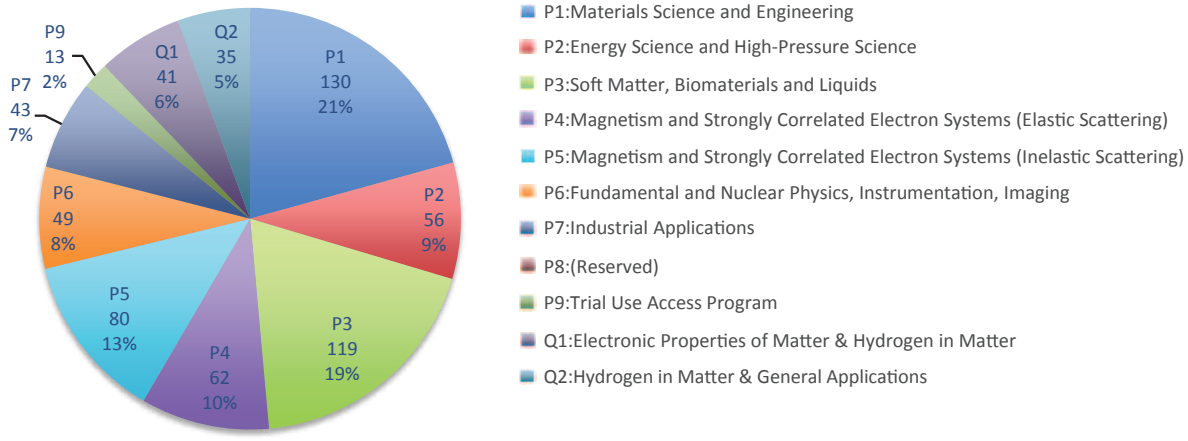

Fig. 3. Submitted Proposals by Sub-committee/Expert Panel – FY2018

J-PARC PAC Approval Summary for the 2018 Rounds

	(Co-) Spokespersons	Affiliation	Title of the experiment	Approval status (PAC recommendation)	Beamline	Status
E03	K.Tanida	JAEA	Measurement of X rays from Ξ^- Atom	Stage 2	K1.8	In preparation
P04	J.C.Peng; S.Sawada	U of Illinois at Urbana-Champaign; KEK	Measurement of High-Mass Dimuon Production at the 50-GeV Proton Synchrotron	Deferred	Primary	
E05	T.Nagae	Kyoto U	Spectroscopic Study of Ξ-Hypernucleus, $^{12}_{\Xi}$Be, via the ^{12}C(K^-, K^+) Reaction	Stage 2 New experiment E70 based on the S-2S spectrometer	K1.8	Finished
E06	J.Imazato	KEK	Measurement of T-violating Transverse Muon Polarization in $K^+ \to \pi^0 \mu^+ \nu$ Decays	E36 as the first step	K1.1BR	
E07	K.Imai, K.Nakazawa, H.Tamura	JAEA, Gifu U, Tohoku U	Systematic Study of Double Strangeness System with an Emulsion-counter Hybrid Method	Stage 2	K1.8	Finished Data analysis
E08	A.Krutenkova	ITEP	Pion double charge exchange on oxygen at J-PARC	Stage 1	K1.8	
E10	A.Sakaguchi, T.Fukuda	Osaka U, Osaka EC U	Production of Neutron-Rich Lambda-Hypernuclei with the Double Charge-Exchange Reaction (Revised from Initial P10)	Stage 2	K1.8	Li run finished, Be target run with S-2S
E11	T. Nakaya, M. Wascho	KEK	Tokai-to-Kamioka (T2K) Long Baseline Neutrino Oscillation Experimental Proposal	Stage 2	neutrino	Data taking
E13	H.Tamura	Tohoku U	Gamma-ray spectroscopy of light hypernuclei	Stage 2	K1.8	Finished
E14	T.Yamanaka	Osaka U	Proposal for $K_L \to \pi^0 \nu \bar{\nu}$ Experiment at J-PARC	Stage 2	KL	Data taking
E15	M.Iwasaki, T.Nagae	RIKEN, Kyoto U	A Search for deeply-bound kaonic nuclear states by in-flight 3He(K-, n) reaction	Stage 2	K1.8BR	Finished
E16	S.Yokkaichi	RIKEN	Measurements of spectral change of vector mesons in nuclei (previously "Electron pair spectrometer at the J-PARC 50-GeV PS to explore the chiral symmetry in QCD")	Stage 2 for Run 0	High p	
E17	R.Hayano, H.Outa	U Tokyo, RIKEN	Precision spectroscopy of Kaonic ^{3}He 3d->2p X-rays	Registered as E62 with an updated proposal	K1.8BR	
E18	H.Bhang, H.Outa, H.Park	SNU, RIKEN, KRISS	Coincidence Measurement of the Weak Decay of $^{12}_{\Lambda}$C and the three-body weak interaction process	Stage 2	K1.8	
E19	M.Naruki	KEK	High-resolution Search for Θ^+ Pentaquark in $\pi^- p \to K^- X$ Reactions	Stage 2	K1.8	Finished
E21	Y.Kuno	Osaka U	An Experimental Search for $\mu - e$ Conversion at a Sensitivity of 10^{-16} with a Slow-Extracted Bunched Beam	Phase-I Stage 2 Engineering desing and operation plan to be presented.	COMET	
E22	S.Ajimura, A.Sakaguchi	Osaka U	Exclusive Study on the Lambda-N Weak Interaction in A=4 Lambda-Hypernuclei	Stage 1	K1.8	
T25	S.Mihara	KEK	Extinction Measurement of J-PARC Proton Beam at K1.8BR	Test Experiment (coord'ed by JPNC)	K1.8BR	Finished
E26	K.Ozawa	KEK	Search for ω-meson nuclear bound states in the $\pi^- + {}^A Z \to n + {}^{(A-1)}_{\omega}(Z-1)$ reaction, and for ω mass modification in the in-medium $\omega \to \pi^0 \gamma$ decay	Stage 1	K1.8	
E27	T.Nagae	Kyoto U	Search for a nuclear Kbar bound state K-pp in the d(π^+, K^+) reaction	Stage 2	K1.8	Fisnished
E29	H.Ohnishi	RIKEN	Search for ϕ-meson nuclear bound states in the pbar + ${}^A Z \to \phi + {}^{(A-1)}_{\phi}(Z-1)$ reaction	Stage 1	K1.1	
E31	H.Noumi	Osaka U	Spectroscopic study of hyperon resonances below KN threshold via the (K^-,n) reaction on Deuteron	Stage 2	K1.8BR	Finished Data analysis
T32	A.Rubbia	ETH, Zurich	Towards a Long Baseline Neutrino and Nucleon Decay Experiment with a next-generation 100 kton Liquid Argon TPC	Test Experiment	K1.1BR	Finished
P33	H.M.Shimizu	Nagoya U	Measurement of Neutron Electric Dipole Moment	Deferred	Linac	
E34	T. Mibe	KEK, RIKEN	An Experimental Proposal on a New Measurement of the Muon Anomalous Magnetic Moment g-2 and Electric Dipole Moment at J-PARC	Stage 2	MLF	
E36	M.Kohl, S.Shimizu	Hampton U, Osaka U	Measurement of $\Gamma(K^+ \to e^+ \nu)/\Gamma(K^+ \to \mu^+ \nu)$ and Search for heavy sterile neutrinos using the TREK detector system	Stage 2	K1.1BR	Finished Data analysis
E40	K.Miwa	Tohoku U	Measurement of the cross sections of Σp scatterings	Stage 2	K1.8	Data taking
P41	M.Aoki	Osaka U	An Experimental Search for $\mu - e$ Conversion in Nuclear Field at a Sensitivity of 10^{-14} with Pulsed Proton Beam from RCS	Deferred	MLF	Reviewed in MLF/IMSS
E42	J.K.Ahn	Pusan National U	Search for H-Dibaryon with a Large Acceptance Hyperon Spectrometer	Stage 2 Commissioning and physics run plan to be submitted	K1.8	
E45	K.H.Hicks, H.Sako	Ohio U, JAEA	3-Body Hadronic Reactions for New Aspects of Baryon Spectroscopy	Stage 2 PAC requests that the group further examine ways to reduce the total beam time requested and to find an efficient running scheme, including quick but careful beam tuning.	K1.8	
T46	K.Ozawa	KEK	EDIT2013 beam test program	Test Experiment	K1.1BR	Abandonded

	(Co-) Spokespersons	Affiliation	Title of the experiment	Approval status (PAC recommendation)	Beamline	Status
T49	T.Maruyama	KEK	Test for 250L Liquid Argon TPC	Test Experiment	K1.1BR	Withdrawn
E50	H.Noumi	Osaka U	Charmed Baryon Spectroscopy via the (π,D^{*-}) reaction	Stage 1 The FIFC, IPNS, and E50 should investigate the beam-line feasibility	High p	
T51	S.Mihara	KEK	Research Proposal for COMET(E21) Calorimeter Prototype Beam Test	Test Experiment	K1.1BR	had to be stopped
T52	Y.Sugimoto	KEK	Test of fine pixel CCDs for ILC vertex detector	Test Experiment	K1.1BR	not performed yet
T53	D.Kawama	RIKEN	Test of GEM Tracker, Hadron Blind Detector and Lead-glass EMC for the J-PARC E16 experiment	Test Experiment	K1.1BR	not performed yet
T54	K.Miwa	Tohoku U	Test experiment for a performance evaluation of a scattered proton detector system for the Σp scattering experiment E40	Test Experiment	K1.1BR	not performed yet
T55	A.Toyoda	KEK	Second Test of Aerogel Cherenkov counter for the J-PARC E36 experiment	Test Experiment	K1.1BR	had to be stopped
E56	T.Maruyama	KEK	A Search for Sterile Neutrino at J-PARC Materials and Life Science Experimental Facility	Stage 2	MLF	
E57	J. Zmeskal	Stefan Meyer Institute for Subatomic Physics	Measurement of the strong interaction induced shift and width of the 1s state of kaonic deuterium at J-PARC	Stage 1 Beam time for the pilot run to be allocated.	K1.8BR	in preparation
P58	M. Yokoyama	U. Tokyo	A Long Baseline Neutrino Oscillation Experiment Using J-PARC Neutrino Beam and Hyper-Kamiokande	Deferred	neutrino	
T59	A. Minamino	Kyoto U	A test experiment to measure neutrino cross sections using a 3D grid-like neutrino detector with a water target at the near detector hall of J-PARC neutrino beam-line	To be arranged by IPNS and KEK-T2K	neutrino monitor bld	Finished
T60	T. Fukuda	Toho U	Proposal of an emulsion-based test experiment at J-PARC	Arranged by IPNS and KEK-T2K	neutrino monitor bld	Finished
E61	M. Wilking	Stony Brook U	NuPRISM/TITUS	Stage 1 committee encourages Lab management to develop a plan for reviewing the coordinated E61 and Hyper-Kamiokande effort	neutrino	
E62	R. Hayano, S. Okada, H. Outa	U. Tokyo, RIKEN	Precision Spectroscopy of kaonic atom X-rays with TES	Stage 2	K1.8BR	Finished
E63	H. Tamura	Tohoku U	Gamma-ray spectroscopy of light hypernuclei II	Stage 2	K1.1	BL not ready yet. Exp. in
T64	Y. Koshio	Okayama U	Measurement of the gamma-ray and neutron background from the T2k neutrino/anti-neutrino at J-PARC B2 Hall	Arranged by IPNS and KEK-T2K	neutrino	
E65	T. Nakaya	Kyoto U	Proposal for T2K Extended Run	Stage 1	neutrino	
T66	T. Fukuda	Nagoya U	Proposal of an emulsion-based test experiment at J-PARC	Test Experiment	neutrino	
P67	I. Meigo	JAEA	Measurement of displacement cross section of proton in energy region between 3 and 30 GeV for high-intensity proton accelerator facility	Carry out the experiment within the framework of facility development	MR	
T68	T. Fukuda	Nagoya U	Extension of T60/T66 Experiment: Proposal for the Run from 2017 Autumn	Test Experiment	neutrino	
E69	A. Minamino	Yokohama National U	Study of neutrino-nucleus ineraction at around 1GeV using cuboid lattice neutrino detector, WAGASHI, muon range detectors and magnetized spectrometer, Baby MIND, at J- PARC neutrino monitor hall	Stage 2	neutrino	
E70	T. Nagae	Kyoto U	Proposal for the next E05 run with the S-2S spectrometer	Stage 1 Encourage to submit a TDR	K1.8	
E71	T. Fukuda	Nagoya U	Proposal for precise measurement of neutrinop-water cross- section in NINJA physics run	Stage-2	neutrino	
E72	K. Tanida	JAEA	Search for a Narrow Λ* Resonance using the p(K-, Λ)η Reaction with the hypTPC Detector	Stage-1 PAC expects the E72 to submit a run plan in the next meeting, where the PAC considers recommendation of a stage-2 approval	K1.8BR	
P73	Yue Ma	RIKEN	$^{3}_{\Lambda}$H and $^{4}_{\Lambda}$H mesonic weak decay lifetime measurement with ^{3,4}He(K$^-$, π^0)$^{3,4}_{\Lambda}$H reaction	Deferred PAC will anticipate the recommendation for stage-1 approval of one hypertriton lifetime measurement in the next PAC meeting.	K1.8BR	
P74	A.Feliciello	INFN, Torino	Direct measurement of the 3ΛH and 4ΛH lifetimes using the 3,4He(π-, K0)3,4ΛH reactions	Deferred PAC will anticipate the recommendation for stage-1 approval of one hypertriton lifetime measurement in the next PAC meeting.	K1.1	
P75	H.Fujioka	Tokyo Inst. Tech,	Decay Pion Spectroscopy of 5$\Lambda\Lambda$H Produced by Ξ-hypernuclear Decay	Deferred PAC encourages the proponent to update the proposal for a stage-1 approval. The requested beam time should be finally revised, taking into account the data taken by E70.	K1.8	

Organization and Committees

Organization Structure

J-PARC Center Management System Chart

as of April 1, 2018

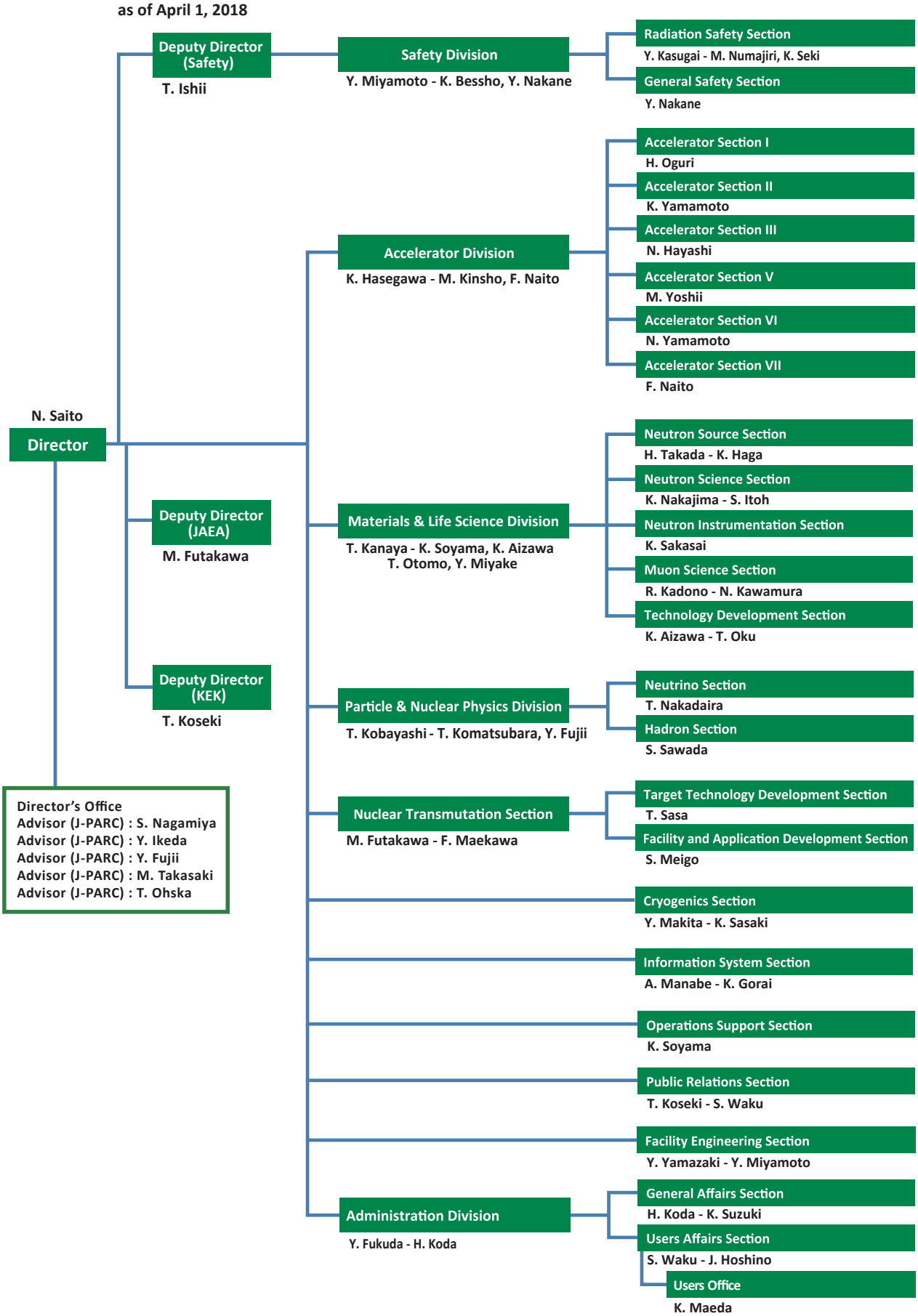

Members of the Committees Organized for J-PARC

(as of March, 2019)

1) Steering Committee

Junji Haba	High Energy Accelerator Research Organization (KEK), Japan
Toshikazu Ishii	High Energy Accelerator Research Organization (KEK), Japan
Katsuo Tokusyuku	High Energy Accelerator Research Organization (KEK), Japan
Nobuhiro Kosugi	High Energy Accelerator Research Organization (KEK), Japan
Seiya Yamaguchi	High Energy Accelerator Research Organization (KEK), Japan
Yukitoshi Miura	Japan Atomic Energy Agency (JAEA), Japan
Yutaka Maeda	Japan Atomic Energy Agency (JAEA), Japan
Masayasu Takeda	Japan Atomic Energy Agency (JAEA), Japan
Hiroyuki Oigawa	Japan Atomic Energy Agency (JAEA), Japan
Kazuo Minato	Japan Atomic Energy Agency (JAEA), Japan
Naohito Saito	J-PARC Center, Japan

2) International Advisory Committee

Jean-Michel Poutissou	TRIUMF, Canada
Thomas Prokscha	The Paul Scherrer Institute (PSI), Switzerland
Jun Sugiyama	Toyota Central R & D Labs., Inc., Japan
Jie Wei	Michigan State University, USA
Roland Garoby	European Spallation Source, Sweden
Eckhard Elsen	European Organization for Nuclear Research (CERN), Switzerland
Patricia McBride	Fermi National Accelerator Laboratory (FNAL), USA
Robert Tribble	Brookhaven National Laboratory (BNL), USA
Donald F. Geesaman	Argonne National Laboratory, USA
Paolo Giubellino	GSI Helmholzzentrum für Schwerionenforschung, Germany
Hamid Aït Abderrahim	SCK • CEN, Belgium
Akira Hasegawa	Tohoku University, Japan
Paul Langan	Oak Ridge National Laboratory (ORNL), USA
Hidetoshi Fukuyama	Tokyo University of Science, Japan
Dan Alan Neumann	National Institute of Standards and Technology (NIST), USA
Andrew Dawson Taylor	Science and Technology Facilities Council (STFC), UK
Helmut Schober	Institut Laue–Langevin, France

3) User Consultative Committee for J-PARC

Tsuyoshi Nakaya	Kyoto University, Japan
Taku Yamanaka	Osaka University, Japan
Hiroaki Aihara	University of Tokyo, Japan
Takashi Kobayashi	High Energy Accelerator Research Organization (KEK), Japan
Hirokazu Tamura	Tohoku University, Japan
Tomofumi Nagae	Kyoto University, Japan
Hiroyuki Noumi	Osaka University, Japan

Shinya Sawada	High Energy Accelerator Research Organization (KEK), Japan
Toshiyuki Takahashi	High Energy Accelerator Research Organization (KEK), Japan
Masaki Fujita	Tohoku University, Japan
Naoya Torikai	Mie University, Japan
Osamu Yamamuro	University of Tokyo, Japan
Yasushi Idemoto	Tokyo University of Science, Japan
Yoshiaki Kiyanagi	Nagoya University, Japan
Tosiji Kanaya	High Energy Accelerator Research Organization (KEK), Japan
Jun Akimitsu	Okayama University/Hiroshima University, Japan
Tadashi Adachi	Sophia University, Japan
Yasuhiro Miyake	High Energy Accelerator Research Organization (KEK), Japan
Jun Sugiyama	Toyota Central R&D Labs., Inc.
Hiroyuki Kishimoto	Sumitomo Rubber Industries, Ltd.
Masaaki Hibi	Nippon Steel & Sumitomo Metal Corp.
Kenya Kubo	International Christian University, Japan
Toshiro Tomida	Ibaraki Prefecture
Satoru Yamashita	University of Tokyo, Japan
Cheol-Ho Pyeon	Kyoto University, Japan
Yoshiyuki Kaji	Japan Atomic Energy Agency (JAEA), Japan

4) Accelerator Technical Advisory Committee

Wolfram Fischer	Brookhaven National Laboratory (BNL), USA
Mats Lindroos	European Spallation Source, Sweden
John Thomason	Science and Technology Facilities Council (STFC), UK
Sheng Wang	Institute of High Energy Physics (IHEP), China
Toshiyuki Shirai	National Institutes for Quantum and Radiological Science and Technology (QST),Japan
Michael Plum	Oak Ridge National Laboratory (ORNL), USA
Jie Wei	Michigan State Univ., USA
Robert Zwaska	Fermi National Accelerator Laboratory (FNAL), USA
Simone Gilardoni	European Organization for Nuclear Research (CERN), Switzerland

5) Neutron Advisory Committee

Robert McGreevy	Science and Technology Facilities Council (STFC), UK
Bertrand Blau	Paul Scherrer Institut (PSI), Switzerland
Mark Wendel	Oak Ridge National Laboratory (ORNL), USA
Yoshiaki Kiyanagi	Nagoya University, Japan
Christiane Alba-Simionesco	The Laboratoire Leon Brilloin (LLB), France
Jamie Schulz	Australian Nuclear Science and Technology Organization(ANSTO), Australia
Andreas Schreyer	European Spallation Source, Sweden
Sung-Min Choi	Korea Advanced Institute of Science and Technology, Korea
Yoshie Otake	RIKEN, Japan
Masaaki Sugiyama	Kyoto University, Japan
Christian Rüegg	The Paul Scherrer Institute (PSI), Switzerland

6) Muon Advisory Committee

Martin Månsson	KTH Royal Institute of Technology, Sweden
Thomas Prokscha	Paul Scherrer Institut (PSI), Switzerland
Andrew MacFarlane	University of British Columbia, Canada
Klaus Kirch	Paul Scherrer Institut (PSI), Switzerland
Kenya Kubo	International Chiristian University, Japan
Tadayuki Takahashi	University of Tokyo, Japan
Takashi Nakano	Osaka University, Japan
Hiroshi Amitsuka	Hokkaido University, Japan

7) Radiation Safety Committee

Yoshimoto Uwamino	RIKEN, Japan
Yoshihiro Asano	University of Hyogo, Japan
Hiroshi Watabe	Tohoku University, Japan
Takeshi Iimoto	University of Tokyo, Japan
Takeshi Murakami	National Institute of Radiological Science, Japan
Hitoshi Kobayashi	High Energy Accelerator Research Organization (KEK), Japan
Yoshihito Namito	High Energy Accelerator Research Organization (KEK), Japan
Shinichi Sasaki	High Energy Accelerator Research Organization (KEK), Japan
Kazuo Minato	Japan Atomic Energy Agency (JAEA), Japan
Michio Yoshizawa	Japan Atomic Energy Agency (JAEA), Japan
Nobuyuki Kinouchi	Japan Atomic Energy Agency (JAEA), Japan

8) Radiation Safety Review Committee

Tetsuro Ishii	Japan Atomic Energy Agency (JAEA), Japan
Yukihiro Miyamoto	Japan Atomic Energy Agency (JAEA), Japan
Masaharu Numajiri	High Energy Accelerator Researchi Organization (KEK), Japan
Hidetoshi Kikunaga	Tohoku University, Japan
Hiroshi Yashima	Kyoto Univaersity, Japan
Kanenobu Tanaka	Institute of Physical and Chemical Research (RIKEN), Japan
Shunsuke Yonai	National Institute for Quantum and Radiological Science and Technoloty (QST), Japan
Yasuhiro Yamaguchi	Comprehensive Reserch Organization for Science and Society (CROSS), Japan
Akira Hirose	Japan Atomic Energy Agency (JAEA), Japan
Akihiko Osa	Japan Atomic Energy Agency (JAEA), Japan
Makoto Kobayashi	Japan Atomic Energy Agency (JAEA), Japan
Nobukazu Toge	High Energy Accelerator Researchi Organization (KEK), Japan
Kazuyoshi Masumoto	High Energy Accelerator Researchi Organization (KEK), Japan
Hiroshi Matsumura	High Energy Accelerator Researchi Organization (KEK), Japan
Kazuo Hasegawa	Japan Atomic Energy Agency (JAEA), Japan
Yoshiaki Fujii	High Energy Accelerator Researchi Organization (KEK), Japan
Takeshi Komatsubara	High Energy Accelerator Researchi Organization (KEK), Japan
Kazuhiko Soyama	Japan Atomic Energy Agency (JAEA), Japan
Kotaro Bessho	High Energy Accelerator Researchi Organization (KEK), Japan
Yoshimi Kasugai	Japan Atomic Energy Agency (JAEA), Japan

9) MLF Advisory Board

Jun Akimitsu	Okayama University/Hiroshima University, Japan
Masaaki Sugiyama	Kyoto University, Japan
Yoshiaki Kiyanagi	Nagoya University, Japan
Mitsuhiro Shibayama	The University of Tokyo, Japan
Jun Sugiyama	Toyota Central R&D Labs., Inc., Japan
Jun Takahara	Kyusyu University, Japan
Takahisa Arima	The University of Tokyo, Japan
Michihiro Furusaka	National Institute of Advanced Industrial Science and Technology (AIST), Japan
Masaki Takada	Tohoku University, Japan
Toshio Yamaguchi	Fukuoka University, Japan
Hiroshi Amitsuka	Hokkaido University, Japan
Kenya Kubo	International Christian University, Japan
Toshiji Kanaya	High Energy Accelerator Research Organization (KEK), Japan
Hideki Seto	High Energy Accelerator Research Organization (KEK), Japan
Takashi Kamiyama	High Energy Accelerator Research Organization (KEK), Japan
Toshiya Otomo	High Energy Accelerator Research Organization (KEK), Japan
Yasuhiro Miyake	High Energy Accelerator Research Organization (KEK), Japan
Ryosuke Kadono	High Energy Accelerator Research Organization (KEK), Japan
Masatoshi Futakawa	Japan Atomic Energy Agency (JAEA), Japan
Kazuya Aizawa	Japan Atomic Energy Agency (JAEA), Japan
Masayasu Takeda	Japan Atomic Energy Agency (JAEA), Japan
Kazuhiko Soyama	Japan Atomic Energy Agency (JAEA), Japan
Kenji Nakajima	Japan Atomic Energy Agency (JAEA), Japan
Yukinobu Kawakita	Japan Atomic Energy Agency (JAEA), Japan
Jun-ichi Suzuki	Comprehensive Research Organization for Science and Society (CROSS), Japan

10) Program Advisory Committee (PAC) for Nuclear and Particle Physics Experiments at the J-PARC 50Gev Proton Synchrotron

Nori Aoi	Osaka University, Japan
Ryuichiro Kitano	High Energy Accelerator Research Organization (KEK), Japan
Masahiro Kuze	Tokyo Institute of Technology, Japan
Hirokazu Tamura	Tohoku University, Japan
Ichiro Adachi	High Energy Accelerator Research Organization (KEK), Japan
Yoshitaka Itow	High Energy Accelerator Research Organization (KEK), Japan
Akira Ohnishi	Kyoto University, Japan
Deborah Harris	Fermi National Accelerator Laboratory (FNAL), USA
Steven Kettell	Brookhaven National Laboratory (BNL), USA
Josef Pochodzalla	University of Mainz, Germany
Monika Blanke	Karlsruhe Institute of Technology, Germany
Francois Le Diberder	The French National Institute of Nuclear and Particle Physics (IN2P3), France
Anthony William Thomas	University of Adelaide, Australia
Nu Xu	Lawrence Berkeley National Laboratory, USA
Rikutaro Yoshida	Thomas Jefferson National Accelerator Facility, USA

11) TEF Technical Advisory Committee

Marc Schyns	SCK • CEN, Belgium
Michael Butzek	Forschungszentrum Jülich, Germany
Michael Wohlmuther	Paul Scherrer Institut (PSI), Switzerland
Yoshiaki Kiyanagi	Nagoya University, Japan
Keishi Sakamoto	National Institutes for Quantum and Radiological Science and Technology (QST), Japan
Georg Müller	Karlsruhe Institute of Technology, Germany
Masatoshi Kondo	Tokyo Institute of Technology, Japan

Main Parameters

Present main parameters of Accelerator

Linac	
Accelerated Particles	Negative hydrogen
Energy	400 MeV
Peak Current	50 mA
Pulse Width	0.27 ms for MLF 0.50 ms for MR-FX 0.10 ms for MR-SX
Repetition Rate	25 Hz
Freq. of RFQ, DTL, and SDTL	324 MHz
Freq. of ACS	972 MHz
RCS	
Circumference	348.333 m
Injection Energy	400 MeV
Extraction Energy	3 GeV
Repetition Rate	25 Hz
RF Frequency	0.938 MHz → 1.67 MHz
Harmonic Number	2
Number of RF cavities	12
Number of Bending Magnet	24
Main Ring	
Circumference	1567.5 m
Injection Energy	3 GeV
Extraction Energy	30 GeV
Repetition Rate	~0.4 Hz
RF Frequency	1.67 MHz → 1.72 MHz
Harmonic Number	9
Number of RF cavities	9
Number of Bending Magnet	96

Key parameters of Materials and Life Science Experimental Facility

Injection energy	3 GeV
Repetition rate	25 Hz
Neutron Source	
Target material	Mercury
Number of moderators	3
Moderator material	Liquid hydrogen
Moderator temperature/pressure	20 K/1.5 MPa
Number of neutron beam extraction ports	23
Muon production target	
Target material	Graphite
Number of muon beam extraction ports	4
Neutron instruments *	
Open for user program (general use)	20
Under commissioning/construction	1/0
Muon Instruments *	
Open for user program (general use)	3
Under commissioning/construction	1/0

(* As of March, 2018)

Events

Events

Safety Day at J-PARC (May 25)

To improve safety awareness of the staff and ensure that the lessons of the radioactive material leak accident at the Hadron Experimental Facility on May 23, 2013, are not forgotten, the J-PARC Center holds a Safety Day on the fourth Friday of May every year. The 2018 Safety Day was May 25, and the event included two sessions, a "Meeting to exchange information on safety" in the morning, and a "5/23 workshop for fostering safety culture" in the afternoon.

J-PARC "Hello Science" - Reducing waste in nuclear power generation in hybrid nuclear reactor- nuclear reactor driven by accelerators, and the accelerator-driven system- (June 29)

The J-PARC Center holds a science café named "Hello Science" every month at the Tokai Village Industry and Information Plaza "Ivill" in Ibaraki Prefecture. In June, Dr. Toshinobu Sasa, the leader of the Target Technology Development Section, Nuclear Transmutation Division, delivered a lecture on nuclear transmutation technology. That technology uses an accelerator to

reduce the harm from the waste in the nuclear power generation. He explained that J-PARC has been conducting research to build a new nuclear reactor called "Accelerator-Driven System" (ADS), which transmutes nuclear waste efficiently and safely by combining an accelerator and a nuclear reactor.

J-PARC Exhibited at the GSA (GEO SPACE ADVENTURE) 2018 (July 14-15)

The GSA is an underground exploration event held every summer, which is performed in Kamioka-cho, Gifu Prefecture, using the actual tunnel of the Kamioka mine and the cutting-edge research facilities of astrophysics, such as Super Kamiokande (SK). The event is organized by the "GSA Executive Committee", which is put on by Hida citizens and volunteer staff. Since 2017, we have been contributing to it as an exhibitor.

At the Kamioka-cho Community Center, we performed briefings about the experiment of the Gauss exhibit, and the experiments in J-PARC, including the T2K Experiment.

The Gauss Accelerator

Debriefing on the industrial use of J-PARC MLF in fiscal year 2018 (July 23-24)

We held a debriefing on the industrial use of the Material and Life Science Experimental Facility (MLF) in Tokyo, and over 300 people from the government, various industries and the academia visited the venue. At the debriefing, we also held a commemorative session celebrating the 10th anniversary of the inauguration of the Industrial Users Society for Neutron Application. It launched at the same time when MLF user operation started. Vice-president Etsuhiko Shoyama, who is among the promoters, expressed his thoughts. Naohito Saito, Director of the J-PARC Center, reported the present state of the adoption of more than 500 proposals so far on the industrial use and the successful stable operation of MLF for approximately one hour at a beam power of 1MW in early July.

J-PARC runs a booth "Eco Accelerated with J-PARC" at Eco Festival Hitachi 2018 (July 21)

J-PARC ran a booth at Eco Festival Hitachi 2018 at the Hitachi Civic Center. We introduced our research activities and explained the functions of our facilities, and exhibited Sumitomo Rubber Industries, Ltd.'s high-performance tire. It was an anti-wear tire product improved by using MLF's neutron beam. In addition, at a superconductive coaster experiment corner, many children excitedly worked on the experiment.

J-PARC Center's outreach activities (August 1-2, 4, 22, 24, 28)

The J-PARC Center conducts scientific experiment classes at schools, libraries and other facilities during the school summer vacation, with the aim to encourage children's interest in science. The center held the events on the topics of light, accelerators, and energy.

At Tokai Library

2018 opening of J-PARC's facilities to the public (August 19)

We conducted the 2018 opening of the J-PARC facilities to the public. Approximately 1,500 people visited the usually inaccessible facilities, such as accelerators in a tunnel and experimental facilities. There were also some seminars on J-PARC's cutting-edge research activities, science café on elementary particle and material and life science.

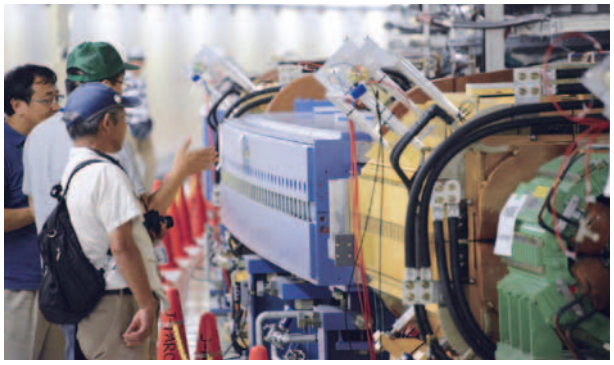

Visitors looking at electromagnets in the MR tunnel

People observing different light sources

Participation in the 6th Ozora Marche 2018 event with a booth, J-PARC Science Experience Corner (October 21)

The 6th Ozora Marche event took place at Daijingu and Muramatsusan Kokuzodo in Tokai Village. This year, J-PARC had a joint booth with the Nuclear Science Research Institute, a research division of the Japan Atomic Energy Agency (JAEA), to introduce J-PARC's experimental facilities and the generated results that found industrial use. Visitors also enjoyed the experiment of a superconductive rollercoaster.

Experiment of superconductive roller coaster

Nagoya University branch office established in J-PARC (October 26)

There was a signing ceremony at the J-PARC Research Building between the High Energy Accelerator Research Organization (KEK) and Nagoya University on the memorandum to establish a research base. The establishment of a branch office of that university follows the ones by Osaka University in March 2016, Kyoto University in February 2017, and Kyushu University in March 2018.

Masahide Takahashi, Trustee and Vice President of Nagoya University (left), Yasuhiro Okada, Executive Director of KEK (right)

J-PARC Science Café, "Hello Science" Workshop, featuring "Let's Create an Optical Kaleidoscope" held during the Nuclear Fusion Facility Visiting Tour (October 21)

The Naka Fusion Institute, a division of the National Institute for Quantum and Radiological Science and Technology (QST), received visitors for a facility study tour. The J-PARC Center offered a craft/experiment class of the "Hello Science" Workshop,

"Let's Create an Optical Kaleidoscope".

Special request event of "Hello Science" (October 26)

Our science communicator Dr. Shinichi Sakamoto explained three topics previously requested by participants: a review of the standard model of the elementary particles, the CP symmetry breaking of neutrinos, and the observation of gravitational waves.

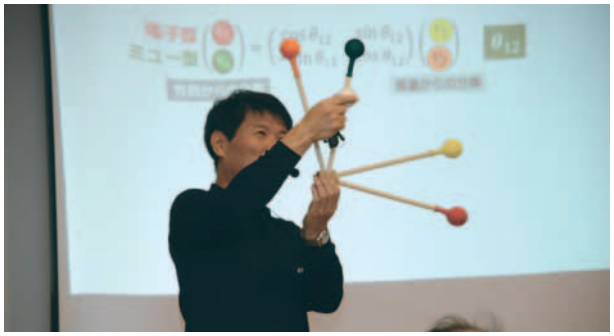

Dr. Shinichi Sakamoto explaining neutrino oscillation with handmade coordinate axis models

g-2/EDM collaboration meeting (May 14-17, November 20-23)

There were two collaboration meetings on the E34 experiment in 2018 at J-PARC. The experiment's topic is the muon anomalous magnetic dipole movement (g-2)/electric dipole moment (EDM). About 60 and 50 researchers attended them, respectively.

Participants of the workshop

Third Neutron and Muon School (November 20-24)

The J-PARC Center and the Comprehensive Research Organization for Science and Society (CROSS) held the third Neutron and Muon School jointly with 11 organizations in Japan. The school drew some 35 students and young researchers from Japan, China, South Korea, India, Thailand, Russia and Great Britain. It also functioned as an international forum for human resource training by J-PARC.

Three public lectures held by the Japan Society for Neutron Science (December 8)

A series of public lectures organized by the Japan Society for Neutron Science was held at the Ibaraki Quantum Beam Research Center (IQBRC). The titles of the three lectures were: "Are neutron beams useful? Living, industry, medicine and space", "Utilization of neutron beams that open up future applications in living, industry and medicine" and "What you should know about particle therapy for cancer treatment".

KOTO Experiment collaboration meeting (June 13-15, December 14-16)

The KOTO Experiment on the rare decay of the neutral kaon has been running at the Hadron Experimental Facility as an international collaborative research project. To promote this research, the group holds meetings twice a year.

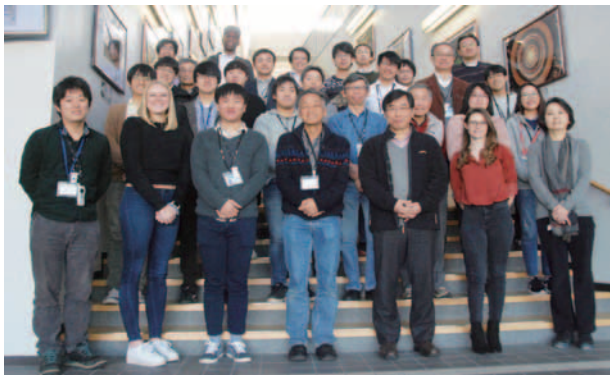

A group photo of the participants

Reimei Workshop "J-PARC-HI opens up the Physics of High-Density Materials and Strangeness" (December 15)

J-PARC held a workshop to study the strangeness of the highest density matter in the universe. Around 60 researchers in the field of nuclear physics discussed the significance of the J-PARC Heavy Ion Project (J-PARC-HI).

6th Accelerator Facility Safety Symposium (January 24-25)

The 6th Accelerator Facility Safety Symposium was held at the Ibaraki Quantum Beam Research Center (IQBRC). Various initiatives were introduced under the theme of personal dose management and fire emer-

gency response at accelerator facilities. Mr. Fabian Saretzki, in charge of safety at accelerator facilities in Germany, gave a talk on the fire emergency response measures at European XFEL, which operates a 3-km long accelerator tunnel.

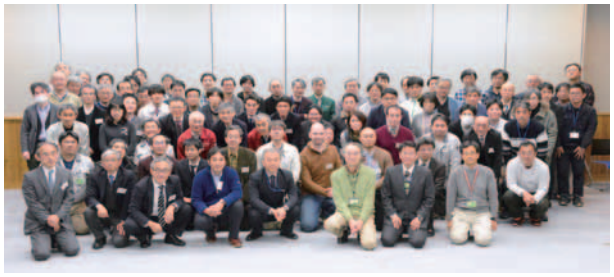

A group photo of the participants

J-PARC "Hello Science" - "Investigating the matter inside neutron stars based on "strange" nuclei (January 25)

Neutron stars are thought to be the densest objects in the universe, and a research on the hyper-nuclei containing strange quarks is currently underway to understand the matter, which forms the neutron stars. Dr. Toshiyuki Takahashi of the Hadron Section presented an introductory overview of the research.

J-PARC "Hello Science" Exhibition at the 26th Hitachi Science Show Festival (February 3)

The J-PARC "Hello Science" Exhibition at the 26th Hitachi Science Show Festival was held on February 3.

What color is light?

J-PARC "Hello Science" - Visualization of secondary lithium-ion batteries using neutron beams (February 22)

Dr. Masao Yonemura delivered a lecture on the forefront of research and development of batteries that utilize neutron beams created at MLF's Special Environment Neutron Diffractometer (BL09 SPICA). He explained what reaction would take place inside a lithium-ion secondary battery and what to do to improve its performance.

Okayama University signed the MOU towards establishing a J-PARC branch office (March 14)

The signing ceremony of "Memorandum of Understanding on Establishing an Education and Research Hub between KEK and Okayama University" was held in Tokyo.

Masanori Yamauchi, KEK Director General (left) and Hirofumi Makino, President of Okayama University (right)

The Quantum Beam Science Festa 2018, 10th Symposium/36th PF Symposium (March 12-13)

The Quantum Beam Science Festa was held under the joint auspices of KEK IMSS and J-PARC Center MLF. It attracted approximately 580 participants.

At the Tsukuba International Congress Center

T2K collaboration meeting (May 8-12, August 20-25, December 3-7, March 25-29)

In fiscal year 2018, T2K collaboration meetings were held four times. Three of them were in the Ibaraki Quantum Beam Research Center (IQBRC) in Tokai Village, the August meeting was held in Toyama Prefecture.

The lecture at IQBRC

J-PARC Workshop "Collaborative Research Conference of Small to Large Facilities" (March 28)

The Japanese Society for Neutron Science, the J-PARC Center, and Japan Collaboration Accelerator-driven Neutron Sources (JCANS) jointly held a "Collaborative Research Conference of Small to Large Neutron Source Facilities" as a J-PARC Workshop. There were about 90 participants and 11 facilities presented their reports.

Visitors

In fiscal year 2018, J-PARC was visited by the following distinguished guests:

Taylor Wilson, nuclear physicist (April 12, November 15)

His Excellency Magnus Robach, Swedish Ambassador to Japan (November 13)

Yoshimasa Uno, Vice Governor of Ibaraki Prefecture (December 3)

Liu Weiping, Vice President of the China Institute of Atomic Energy (CIAE) (December 5)

Mary Alice Hayward, the Deputy Director General and Head of the Department of Management of the International Atomic Energy Agency (IAEA) (January 23)

Keiko Nagaoka, Vice Minister of the Ministry of Education, Culture, Sports, Science and Technology (MEXT) (January 24).

In total, there were 2,957 visitors to J-PARC for the period from April 2018 to the end of March 2019.

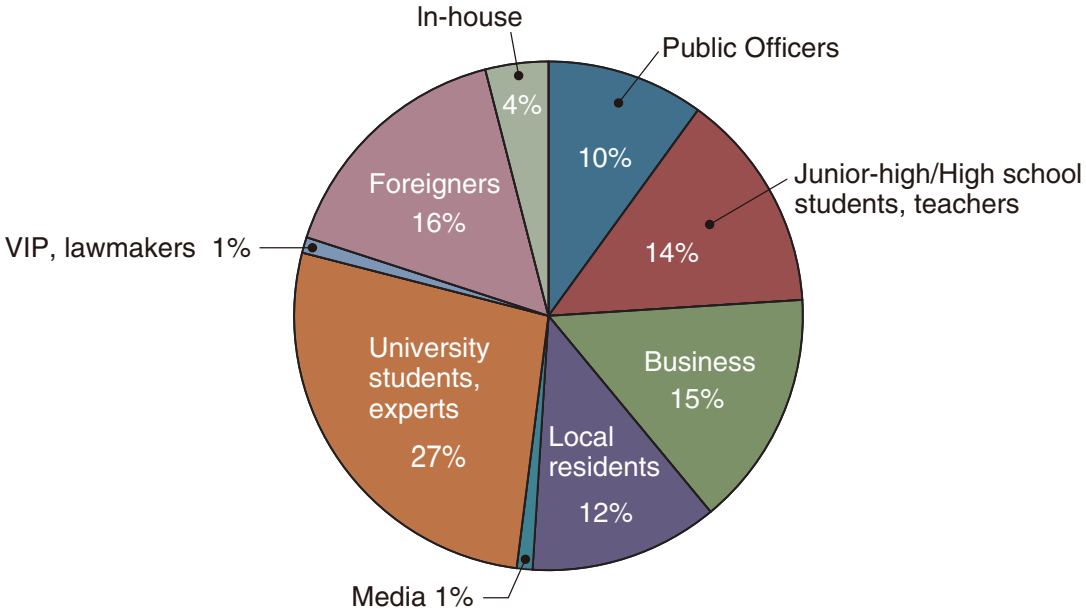

Publications

Publications in Periodical Journals

A-001
S. Lee, *et al*.
Crystal and Magnetic Structures of La2CoPtO6 Double Perovskite
ACS Omega, Vol. 3, 11624

A-002
T. Takami, *et al*.
Appearance of Lithium-Ion Conduction in a La–Li–Co–O Band Insulator: Possible Route to Oxide Electrolyte
ACS Appl. Energy Mater., Vol. 1, 2546

A-003
N. Yano, *et al*.
Status of the neutron time-of-flight single-crystal diffraction data-processing software STARGazer
Acta Crystallogr. D STRUCTURAL BIOLOGY, Vol. D74, 1041-1052

A-004
J. W. Bae, *et al*.
Exceptional phase-transformation strengthening of ferrous medium-entropy alloys at cryogenic temperatures
ACTA MATER., Vol. 161, 388-399

A-005
K. Suekuni, *et al*.
Retreat from stress: rattling in a planar coordination
Adv. Mater., Vol. 30, 1706230

A-006
K. Tomiyasu, *et al*.
Quantum paramagnet near spin-state transition
Advanced Quantum Technologies, 2018, 1800057

A-007
K. Ikeuchi, *et al*.
Al-impurity-induced magnetic excitations in heavily over-doped La1.7Sr0.3Cu0.95Al0.05O4
AIP Adv., Vol. 8, 101318

A-008
Y. Fukushima, *et al*.
Dynamic of organic species in organo-clay / polypropyrene composite by quesi-elastic neutron scattering
Appl. Clay Sci., Vol. 155, 15-19

A-009
H. Iwase, *et al*.
Structural investigation of hectorite aqueous suspensions by dielectric microscopy and small-angle neutron scattering coupling with rheological measurement
Appl. Clay Sci., Vol. 157, 24-30

A-010
C. H. Lee, *et al*.
Effect of rattling motion without cage structure on lattice thermal conductivity in LaOBiS2–xSex
Appl. Phys. Lett., Vol. 112, 023903

A-011
K. Abe, *et al*.
Search for Neutrinos in Super-Kamiokande Associated with the GW170817 Neutron-star Merger
Astrophys. J. Lett., Vol. 857, L4

A-012
Z. Tan, *et al*.
Synthesis, Structural and Magnetic Properties of La0.5Ba0.5CoO2.75+x
Atom Indonesia, Vol. 44, 49

A-013
M. Hirai, *et al*.
Direct evidence for the effect of glycerol on protein hydration and thermal structural transition
Biophys. J., Vol. 115, 313-327

A-014
Y. Kameda, *et al*.
Neutron Diffraction Study on Partial Pair Correlation Functions of Water at Ambient Temperature
Bull. Chem. Soc. Jpn., Vol. 91, 1586-1595

A-015
H. Nishihara, *et al*.
Graphene-based ordered framework with a diverse range of carbon polygons formed in zeolite nanochannels
Carbon, Vol. 129, 854-862

A-016
M. Yoshimoto, *et al*.
Mesoscopic investigation of an "immiscible" cyclohexane and water micro-mixture in carbon micropores by contrast variation small-angle neutron scattering
Chem. Lett., Vol. 47, 336-339

A-017
K. Kataoka, *et al*.
High ionic conductor member of garnet-type oxide Li6.5La3Zr1.5Ta0.5O12
ChemElectroChem, Vol. 5, 2551-2557

A-018
S. Takada, *et al*.
Visualization of He II boiling process under the microgravity condition for 4.7 s by using a drop tower experiment
Cryogenics, Vol. 89, 157

A-019
T. Yagai, *et al*.
Development of design for large scale conductors and coils using MgB2 for superconducting magnetic energy storage device
Cryogenics, Vol. 96, 75

A-020
A. Chanyshev, *et al*.
High-Pressure - High-Temperature Study of Benzene: Refined Crystal Structure and New Phase Diagram up to 8 GPa and 923K
Cryst. Growth Des., Vol. 18, 3016-3026

A-021
Y. Muraba, *et al*.
Phase transition in CaFeAsH: bridging 1111 and 122 iron-based superconductors
Dalton Transactions, Vol. 47, 12964-12971

A-022
A. M. Baldini, *et al*.
The design of the MEG II experiment
EPJ C, Vol. 78, 380

A-023
N. Naganawa, *et al*.
A Cold/Ultracold Neutron Detector using Fine-grained Nuclear Emulsion with Spatial Resolution less than 100 nm
EPJ C, Vol. 78, 959

A-024
H. Iwamoto, *et al*.
Sensitivity and uncertainty analysis of beff for MYRRHA using a Monte Carlo technique
EPJ Nucl. Sci. Technol., Vol. 4, 42

A-025
Y. Seki, *et al*.
Efficient phase imaging using wavelength-resolved neutron Talbot-Lau interferometry with TOF method
EPL, Vol. 123, 12002

A-026
S. Kumano, *et al*.
Hadron Tomography and Its Application to Gravitational Radii of Hadrons
Few-Body Syst., Vol. 59, 102

A-027
K. Mishima, *et al*.
Accurate determination of the absolute 3He/4He ratio of a synthesized helium standard gas (Helium Standard of Japan, HESJ): Towards revision of the atmospheric 3He/4He ratio
Geochemistry, Geophysics, Geosystems, Vol. 19, 3995-4005

A-028
T. Suwa, et al.
Evaluation of Thermal Strain Induced in Components of Nb3Sn Strand During

Cooling
IEEE Trans. Appl. Supercond., Vol. 28, 1-4

A-029
M. Sugano, *et al*.
Training Performance With Increased Coil Prestress of the 2 m Model Magnet of Beam Separation Dipole for the HL-LHC Upgrade
IEEE Trans. Appl. Supercond., Vol. 28, 4000805

A-030
Y. Yang, *et al*.
Study of Irradiation Effects on Thermal Characteristics for COMET Pion Capture Solenoid
IEEE Trans. Appl. Supercond., Vol. 28, 4001405

A-031
K. Suzuki, *et al*.
Quench Protection Heater Study With the 2-m Model Magnet of Beam Separation Dipole for the HL-LHC Upgrade
IEEE Trans. Appl. Supercond., Vol. 28, 4002505

A-032
E. Nilsson, *et al*.
Influence of 3-D Effects on Field Quality in the Straight Part of Accelerator Magnets for the High-Luminosity Large Hadron Collider
IEEE Trans. Appl. Supercond., Vol. 28, 4003005

A-033
S. Enomoto, *et al*.
Field Measurement to Evaluate Iron Saturation and Coil End Effects in a Modified Model Magnet of Beam Separation Dipole for the HL-LHC Upgrade
IEEE Trans. Appl. Supercond., Vol. 28, 4004505

A-034
T. Takayanagi,*et al*.
A New Pulse Magnet for the RCS Injection Shift Bump Magnet at J-PARC
IEEE Trans. Appl. Supercond., Vol. 28, 4100505

A-035
M. Aoki, *et al*.
Evaluation of Strain Dependence of Superconducting Magnet Quenches by Using a Three-Point Bending Test Stand
IEEE Trans. Appl. Supercond., Vol. 28, 4702904

A-036
M. Tomita, *et al*.
Superconducting Properties of a Prototype Pancake Coil Using a MgB2 Rutherford-Type Stranded Conductor
IEEE Trans. Appl. Supercond., Vol. 28, 5700604

A-037
Wang L., *et al*.
Measurement and Mechanism Investigation of Negative and Positive Muon-Induced Upsets in 65nm Bulk SRAMs
IEEE Trans. Nucl. Sci., Vol. 65, 1734

A-038
S. Manabe, *et al*.
Negative and Positive Muon-Induced Single Event Upsets in 65-nm UTBB SOI SRAMs
IEEE Trans. Nucl. Sci., Vol. 65, 1742

A-039
N. M. Truong, *et al*.
Real-Time Lossless Compression of Waveforms Using an FPGA
IEEE Trans. Nucl. Sci., Vol. 65, 2650

A-040
Y. Higaki, *et al*.
Counteranion-Specific Hydration States of Cationic Polyelectrolyte Brushes
Ind. Eng. Chem. Res., Vol. 57, 5268–5275

A-041
K. Asano, *et al*.
Structural Variation of Self-Organized Mg Hydride Nanoclusters in Immiscible Ti Matrix by Hydrogenation
Inorg. Chem., Vol. 57, 11831–11838

A-042
F. Takeiri, *et al*.
A Fluorine-rich Perovskite Oxyfluoride AgFeOF2
Inorg. Chem., Vol. 57, 6686-6691

A-043
W. Gong, *et al*.
Deformation behavior of as-cast and as-extruded Mg97Zn1Y2 alloys during compression, as tracked by in situ neutron diffraction
Int. J. Plast., Vol. 111, 288-306

A-044
K. Itoh, *et al*.
Inhomogeneity of local packing density and atomic bonding of Ni67Zr33 amorphous alloy
J. ALLOYS COMPD., Vol. 732, 585-592

A-045
T. Ohkubo
Insights from ab initio molecular dynamics simulations for a multicomponent oxide glass
J. Am. Ceram. Soc., Vol. 101, 1122-1134

A-046
N. Matsui, *et al*.
Ambient pressure synthesis of La2LiHO3 as a solid electrolyte for a hydrogen electrochemical cell
J. Am. Ceram. Soc., Vol. 102, 3228–3235

A-047
H. Yamashita, et al.
Chemical Pressure-induced Anion Order-disorder Transition in LnHO Enabled by Hydride Size Flexibility
J. Am. Chem. Soc., Vol. 140, 11170-11173

A-048
Y. Nagata, *et al*.
Elucidating the solvent effect on the switch of the helicity of poly(quinoxaline-2,3-diyl) s: A conformational analysis by small-angle neutron scattering
J. Am. Chem. Soc., Vol. 140, 2722-2726

A-049
T. Okuchi, *et al*.
Quasielastic neutron scattering of brucite to analyse hydrogen transport on the atomic scale
J. Appl. Crystallog., Vol. 51, 1564-1570

A-050
T. Kawasaki, *et al*.
Stroboscopic time-of-flight neutron diffraction during cyclic testing using the event data recording system at J-PARC
J. Appl. Crystallog., Vol. 51, 630-634

A-051
P. G. Xu, *et al*.
High stereographic resolution texture and residual stress evaluation using time-of-flight neutron diffraction
J. Appl. Crystallogr., Vol. 51, 746-760

A-052
A. Shinozaki, *et al*.
Behavior of intermolecular interactions in a-glycine under high pressure
J. Chem. Phys., Vol. 148, 044507

A-053
F. Nemoto, *et al*.
Neutron scattering studies on short- and long-range layer structures and related dynamics in imidazolium-based ionic liquids
J. Chem. Phys., Vol. 149, 054502/1-11

A-054
K. Yoshida, *et al*.
Thermal behavior, structure, dynamic properties of aqueous glycine solutions confined in mesoporous silica MCM-41 investigated by x-ray diffraction and quasi-elastic neutron scattering
J. Chem. Phys., Vol. 149, 124502

A-055
S. Takada, *et al*.
Characterization of germanium detectors for the measurement of the angular distribution of prompt γ-rays at the ANNRI in the MLF of the J-PARC
J. Instrum., Vol. 13, P02018

A-056
V. Bayliss, *et al*.
The liquid-hydrogen absorber for MICE
J. Instrum., Vol. 13, T09008

A-057
A. Suzuki, *et al*.
The LiteBIRD Satellite Mission: Sub-Kelvin

Instrument
J. Low Temp. Phyis., Vol. 193, 1048

A-058
T. Hasebe, *et al*.
Concept Study of Optical Configurations for High-Frequency Telescope for LiteBIRD
J. Low Temp. Phys., Vol. 193, 841

A-059
K. Fujii, *et al*.
High oxide-ion conductivity by the overbonded channel oxygens in Si-deficient La9.565(Si5.826□0.174)O26 apatite without interstitial oxygens
J. Mater. Chem. A, Vol. 6, 10835-10846

A-060
Y. Iwasaki, *et al*.
Synthesis, crystal structure, and ionic conductivity of hydride ion-conducting Ln2LiHO3 (Ln = La, Pr, Nd) oxyhydrides
J. Mater. Chem. A, Vol. 6, 23457-23463

A-061
H. Abe, *et al*.
Dynamic properties of nano-confined water in an ionic liquid
J. Mol. Liq., Vol. 264, 54-57

A-062
H. Muta, *et al*.
Effect of hydrogenation conditions on the microstructure and mechanical properties of zirconium hydride
J. Nucl. Mater., Vol. 500, 145-152

A-063
A. Mori, *et al*.
Manufacturing and characterization of Ni-free N-containing ODS austenitic alloy
J. Nucl. Mater., Vol. 501, 72-81

A-064
T. Wakui, *et al*.
Recent studies for structural integrity evaluation and defect inspection of J-PARC spallation neutron source target vessel
J. Nucl. Mater., Vol. 506, 3-11

A-065
Y. Iwamoto, *et al*.
Measurement of displacement cross sections of aluminum and copper at 5 K by using 200 MeV protons
J. Nucl. Mater., Vol. 508, 195

A-066
H. Katagiri, *et al*.
Development of an all-sky gamma-ray Compton camera based on scintillators for high-dose environments
J. Nucl. Sci. and Technol., Vol. 55, 1172

A-067
K. Terada, *et al*.
Measurements of neutron total and capture cross sections of 241Am with ANNRI at J-PARC
J. Nucl. Sci. and Technol., Vol. 55, 1198-1211

A-068
H. Takei, *et al*.
Evaluation of mean time between accidental interruptions for accelerator klystron systems based on the reliability engineering and method
J. Nucl. Sci. and Technol., Vol. 55, 996-1008

A-069
H. Iwamoto, *et al*.
Monte Carlo uncertainty quantification of the effective delayed neutron fraction
J. Nucl. Sci. Technol., Vol. 55, 539-547

A-070
H. Matsuda, S. Meigo, H. Iwamoto
Proton-induced activation cross section measurement for aluminum with proton energy range from 0.4 to 3 GeV at J-PARC
J. Nucl. Sci. Technol., Vol. 55, 955-961

A-071
M. Hirai, *et al*.
Restoration of myoglobin native fold from its initial state of amyloid formation by trehalose
J. Phys. Chem. B, Vol. 122, 11962-11968

A-072
Y. Kameda, *et al*.
Neutron Diffraction Study on the Structure of Hydrated Li(+) in Dilute Aqueous Solutions
J. Phys. Chem. B, Vol. 122, 1695-1701

A-073
S. Ajito, *et al*.
Sugar-mediated stabilization of protein against chemical or thermal denaturation
J. Phys. Chem. B, Vol. 122, 8685-8697

A-074
J. Kijima, *et al*.
Structural characterization of myoglobin molecules adsorbed within mesoporous silicas
J. Phys. Chem. C, Vol. 122, 15567-15574

A-075
S. Taminato, *et al*.
Reversible Structural Changes and High-Rate Capability of Li3PO4-Modified Li2RuO3 for Lithium-Rich Layered Rocksalt Oxide Cathodes
J. Phys. Chem. C, Vol. 122, 16607

A-076
F. Tamura, *et al*.
Baseband simulation model of the vector rf voltage control system for the J-PARC RCS
J. Phys. Conf. Ser., Vol. 1067, 072030_1 - 072030_6

A-077
T. Tsuchiya, *et al*.
Mn2VAl Heusler alloy thin films: Appearance of antiferromagnetism and exchange bias in a layered structure with Fe
J. Phys. D: Appl. Phys., Vol. 51, 065001

A-078
K. Iwasa, *et al*.
Magnetic-Ordering Propagation Vectors of Terbium Hexaboride Revisited
J. Phys. Soc. Jpn., Vol. 87, 64705

A-079
T. Nakajima, *et al*.
Uniaxial-stress effects on helimagnetic orders and skyrmion lattice in Cu2OSeO3
J. Phys. Soc. Jpn., Vol. 87, 094709

A-080
T. Matsushita, *et al*.
Principle and Reconstruction Algorithm for Atomic-Resolution Holography
J. Phys. Soc. Jpn., Vol. 87, 061002

A-081
H. Kadowaki, *et al*.
Continuum excitation and pseudospin wave in quantum spin-liquid and quadrupole ordered states of Tb2+xTi2-xO7+y
J. Phys. Soc. Jpn., Vol. 87, 064704

A-082
N. Metoki, *et al*.
Neutron Inelastic Scattering Study of the f-Electron States in NdPd5Al2
J. Phys. Soc. Jpn., Vol. 87, 084708

A-083
Y. Oba, *et al*.
Imaging Measurement of Neutron Attenuation by Small-Angle Neutron Scattering Using Soller Collimator
J. Phys. Soc. Jpn., Vol. 87, 094004

A-084
K. Oyama, *et al*.
Neutron Diffraction Studies on Valence Ordering Compound YbPd
J. Phys. Soc. Jpn., Vol. 87, 114705

A-085
Y. Idemoto, *et al*.
Effect of operating temperature on local structure during first discharge of 0.4Li2MnO3-0.6LiMn1/3Ni1/3Co1/3O2 electrodes
J. POWER SOURCES, Vol. 378, 198-208

A-086
K. Ninomiya, *et al*.
Muonic X-ray measurements on mixtures of CaO/MgO and Fe3O4/MnO
J. Radioanal. Nucl. Chem., Vol. 316, 1107-1111

A-087
N.V. Mdlovu, *et al*.

Multifunctional nanocarrier as a potential micro-RNA delivery vehicle for neuroblastoma treatment
J. Taiwan Inst. Chem. Eng., Vol. 96, 526-537

A-088
W. Uno, *et al*.
Experimental visualization of oxide-ion diffusion paths in pyrochlore-type Yb2Ti2O7
JCS-Japan, Vol. 126, 341-345

A-089
K. Fujii, *et al*.
Discovery and development of BaNdInO4 - A brief review -
JCS-Japan, Vol. 126, 852-859

A-090
Y. Kitanaka, *et al*.
Crystal Structure and ferroelectric polarization of tetragonal (Bi1/2Na1/2) TiO3–12 %BaTiO3
Jpn. J. Appl. Phys., Vol. 57, 11UD05

A-091
Y. Ogata, *et al*.
Impact of the Solid Interface on Proton Conductivity in Nafion Thin Films
Langmuir, Vol. 34, 15483-15489

A-092
K. Shimokita, *et al*.
Effect of Preferential Orientation of Lamellae in Interfacial Region between Block Copolymer-based Pressure-Sensitive Adhesive and Solid Substrate on the Peel Strength
Langmuir, Vol. 34, 2856-2864

A-093
K. Yanagi, *et al*.
Polyrotaxane brushes dynamically formed at a water/elastomer interface
Langmuir, Vol. 34, 5297-5302

A-094
F. Endo, *et al*.
Mechanically tough syndiotactic polypropylene (sPP) gels realized by fast quenching using liquid nitrogen
Macromolecules, Vol. 51, 2321-2327

A-095
Y. Shudo, *et al*.
Diffusion Behavior of Methanol Molecules Confined in Cross-linked Phenolic Resins Studied using Neutron Scattering and Molecular Dynamics Simulations
Macromolecules, Vol. 51, 6334-6343

A-096
T. Iwamoto, *et al*.
Conformations of ring polystyrenes in semidilute solutions and in linear polymer matrices studied by SANS
Macromolecules, Vol. 51, 6836–6847

A-097
T. Sun, *et al*.
Investigation of residual stress distribution and texture evolution in AA7050 stationary shoulder friction stir welded joints
Mater. Sci. Eng. A,, Vol. 712, 531-538

A-098
K. Murasawa, *et al*.
Determination Approach of Dislocation Density and Crystallite Size Using a Convolutional Multiple Whole Profile Software
Mater. Trans., Vol. 59, 1135-1141

A-099
A. Taketani, *et al*.
Quantification of localized water image in under-film corroded steel with high spatial resolution, high time resolution, and wide view by neutron radiography
Mater. Trans., Vol. 59, 976-983

A-100
T. Wan, S. Saito
Flow-Accelerated Corrosion of Type 316L Stainless Steel Caused by Turbulent Lead?Bismuth Eutectic Flow
Metals, Vol. 8, 627, pp. 1-22 https://doi.org/10.3390/met8080627

A-101
B. Li, *et al*.
Liquid-like thermal conduction in intercalated layered crystalline solids
Nat. Mater., Vol. 17, 226-230

A-102
W. Yao, *et al*.
Topological spin excitations in a three dimensional antiferromagnet
Nat. Phys., Vol. 14, 1011-1015

A-103
T. Matsumura, *et al*.
A neutral-beam profile monitor with a phosphor screen and a high-sensitivity camera for the J-PARC KOTO experiment
Nucl. Instrum. Methods Phys. Res. Sect. A, Vol. 885, 91

A-104
K. Satou, *et al*.
New data acquisition system for beam loss monitor used in J-PARC main ring
Nucl. Instrum. Methods Phys. Res. Sect. A, Vol. 887, 174

A-105
R. Maruyama, *et al*.
Development of high-polarization Fe/Ge neutron polarizing supermirror: Possibility of fine-tuning of scattering length density in ion beam sputtering
Nucl. Instrum. Methods Phys. Res. Sect. A, Vol. 888, 70-78

A-106
M. Abe, *et al*.
Magnetic design and method of a superconducting magnet for muon g - 2/EDM precise measurements in a cylindrical volume with homogeneous magnetic field
Nucl. Instrum. Methods Phys. Res. Sect. A, Vol. 890, 51

A-107
B. Kim, *et al*.
Development of a microchannel plate based beam profile monitor for a re-accelerated muon beam
Nucl. Instrum. Methods Phys. Res. Sect. A, Vol. 899, 22-27

A-108
H. Ito, *et al*.
Performance check of the CsI(Tl) calorimeter for the J-PARC E36 experiment by observing e+ from muon decay
Nucl. Instrum. Methods Phys. Res. Sect. A, Vol. 901, 1

A-109
Y. Morita, *et al*.
Capacitor bank of power supply for J-PARC MR main magnets
Nucl. Instrum. Methods Phys. Res. Sect. A, Vol. 901, 156

A-110
M. Tomizawa, *et al*.
Slow extraction from the J-PARC main ring using a dynamic bump
Nucl. Instrum. Methods Phys. Res. Sect. A, Vol. 902, 51

A-111
M. Harada, *et al*.
Experimental validation of the brightness distribution on the surfaces of coupled and decoupled moderators composed of 99.8% parahydrogen at the J-PARC pulsed spallation neutron source
Nucl. Instrum. Methods Phys. Res. Sect. A, Vol. 903, 38-45

A-112
S. Itoh, *et al*.
Pendellosung interferometry by using pulsed neutrons
Nucl. Instrum. Methods Phys. Res. Sect. A, Vol. 908, 78

A-113
W. Guan, *et al*.
Optimization study on structural analyses for the J-PARC mercury target vessel
Nucl. Instrum. Methods Phys. Res. Sect. A, Vol. 894, 8-19

A-114
T. Fujiwara, *et al*.
Radiation imaging with glass gas electron multipliers (G-GEMs)

Nucl. Instrum. Methods Phys. Res., Sect. A, Vol. 878, 40-49

A-115
M.Teshigawara, *et al*.
Implementation of a low-activation Au-In-Cd decoupler into the J-PARC 1 MW short pulsed spallation neutron source
Nuclear Materials and Energy, Vol. 14, 14-21

A-116
T. Takamuku, *et al*.
Hydrogen bonds of the imidazolium-ring of ionic liquids with DMSO studied by NMR, soft X-ray spectroscopy, and SANS
Phys. Chem. Chem. Phys., Vol. 20, 12858

A-117
Y. Ishii, *et al*.
Pressure-induced stacking disorder in boehmite
Phys. Chem. Chem. Phys., Vol. 20, 16650

A-118
A. Doté, *et al*.
Fully coupled-channel study of K–pp resonance in a chiral SU(3)-based $\bar{K}N$ potential
Phys. Lett. B, Vol. 784, 405

A-119
P. K. Saha, *et al*.
Simulation, measurement, and mitigation of beam instability caused by the kicker impedance in the 3-GeV rapid cycling synchrotron at the Japan Proton Accelerator Research Complex
Phys. Rev. Accel. Beams, 21(2), 024203_1 - 024203_20

A-120
S. Bae, *et al*.
First muon acceleration using a radio-frequency accelerator
Phys. Rev. Accel. Beams, Vol. 21, 050101

A-121
Y. Shobuda, *et al*.
Reducing the beam impedance of the kicker at the 3-GeV rapid cycling synchrotron of the Japan Proton Accelerator Research Complex
Phys. Rev. Accel. Beams, Vol. 21, 061003

A-122
A. W. T. Gregg, *et al*.
Tomographic Reconstruction of Two-Dimensional Residual Strain Fields from Bragg-Edge Neutron Imaging
Phys. Rev. Appl., Vol. 10, 064034

A-123
H. Shishido, *et al*.
High-Speed Neutron Imaging Using a Current-Biased Delay-Line Detector of Kinetic Inductance
Phys. Rev. Appl., Vol. 18, 044044

A-124
S. Shamoto, *et al*.
Neutron scattering study of yttrium iron garnet
Phys. Rev. B, Vol. 97, 054429

A-125
K. Horigane, *et al*.
Magnetic phase diagram of Sr2–xLaxIrO4 synthesized by mechanical alloying
Phys. Rev. B, Vol. 97, 064425

A-126
T. Hattori
Is there a pressure-induced discontinuous volume change in liquid Cs?
Phys. Rev. B, Vol. 97, 100101®

A-127
I. Yamauchi, *et al*.
Local spin structure of the α-RuCl3 honeycomb-lattice magnet observed via muon spin rotation/relaxation
Phys. Rev. B, Vol. 97, 134410

A-128
S. Hayashida, *et al*.
Pressure-induced quantum phase transition in the quantum antiferromagnet CsFeCl3
Phys. Rev. B, Vol. 97, 140405®

A-129
T. Kim, *et al*.
Renormalization of spin excitations in hexagonal HoMnO3 by magnon-phonon coupling
Phys. Rev. B, Vol. 97, 201113®

A-130
N. Murai, *et al*.
Effect of electron correlations on spin excitation bandwidth in Ba0.75K0.25Fe2As2 as seen via time-of-flight inelastic neutron scattering
Phys. Rev. B, Vol. 97, 241112®

A-131
T. Nakajima, *et al*.
Phase-transition kinetics of magnetic skyrmions investidated by stroboscopic small-angle neutron scattering
Phys. Rev. B, Vol. 98, 014424

A-132
H. Okabe, *et al*.
Local electronic structure of interstitial hydrogen in iron disulfide
Phys. Rev. B, Vol. 98, 075210

A-133
P. Wu, *et al*.
Investigation of the electronic structure and lattice dynamics of the thermoelectric material Na-doped SnSe
Phys. Rev. B, Vol. 98, 094305

A-134
S. Lee, *et al*.
Magnetoelastic octahedral breathing mode in the ferrimagnetic La2CoIrO6 double perovskite
Phys. Rev. B, Vol. 98, 104409

A-135
S. Torigoe, *et al*.
Nanoscale ice-type structural fluctuation in spinel titanates
Phys. Rev. B, Vol. 98, 134443

A-136
H. Tamatsukuri, *et al*.
Gapless magnetic excitation in a heavily electron-doped antiferromagnetic phase of LaFeAsO0.5D0.5
Phys. Rev. B, Vol. 98, 174415

A-137
T. Moyoshi, *et al*.
Inelastic neutron scattering study on the electronic transition in (Pr1-yYy)1-xCaxCoO3 single crystals
Phys. Rev. B, Vol. 98, 205105

A-138
H. Kohri, *et al*.
Differential cross section and photon-beam asymmetry for the $\vec{\gamma}p \to \pi^+ n$ reaction at forward π^+ angles at E_γ = 1.5–2.95 GeV
Phys. Rev. C, Vol. 97, 015205

A-139
S. H. Shiu, *et al*.
Photoproduction of Λ and Σ0 hyperons off protons with linearly polarized photons at Eγ = 1.5–3.0 GeV
Phys. Rev. C, Vol. 97, 015208

A-140
M. Aaboud, *et al*.
Measurement of long-range multiparticle azimuthal correlations with the subevent cumulant method in pp and p+Pb collisions with the ATLAS detector at the CERN Large Hadron Collider
Phys. Rev. C, Vol. 97, 024904

A-141
T. Okudaira, *et al*.
Angular distribution of γ rays from neutron-induced compound states of 140La
Phys. Rev. C, Vol. 97, 034622

A-142
A. Konishi, *et al*.
Degenerate two-body and three-body coupled-channels systems: Renormalized effective Alt-Grassberger-Sandhas equations and near-threshold resonances
Phys. Rev. C, Vol. 97, 064001

A-143
A. Adare, *et al*.
Measurements of mass-dependent

azimuthal anisotropy in central p + Au, d + Au, and 3He + Au collisions at √sNN =200 GeV
Phys. Rev. C, Vol. 97, 064904

A-144
A. Adare, *et al*.
Lévy-stable two-pion Bose-Einstein correlations in √sNN =200 GeV Au+Au collisions
Phys. Rev. C, Vol. 97, 064911

A-145
A. Adare, *et al*.
Measurement of emission-angle anisotropy via long-range angular correlations with high-pT hadrons in d + Au and p + p collisions at√sNN = 200 GeV
Phys. Rev. C, Vol. 98, 014912

A-146
A. Adare, *et al*.
Low-momentum direct-photon measurement in Cu + Cu collisions at√sNN = 200 GeV
Phys. Rev. C, Vol. 98, 054902

A-147
C. Aidala, *et al*.
Production of π0 and η mesons in Cu + Au collisions at √sNN = 200 GeV
Phys. Rev. C, Vol. 98, 054903

A-148
K. Abe, *et al*.
First measurement of the νμ charged-current cross section on a water target without pions in the final state
Phys. Rev. D, Vol. 97, 012001

A-149
S. Kumano, *et al*.
Hadron tomography by generalized distribution amplitudes in the pion-pair production process γ * γ ! π0π0 and gravitational form factors for pion
Phys. Rev. D, Vol. 97, 014020

A-150
K. Abe, *et al*.
Measurement of the single π0 production rate in neutral current neutrino interactions on water
Phys. Rev. D, Vol. 97, 032002

A-151
C. C. Haddock, *et al*.
A Search for deviations from the inverse square law of gravity at nm range using a pulsed neutron beam
Phys. Rev. D, Vol. 97, 062002

A-152
K. Abe, *et al*.
Atmospheric neutrino oscillation analysis with external constraints in Super-Kamiokande I-IV
Phys. Rev. D, Vol. 97, 072001

A-153
A. Aguilar-Arevalo, *et al*.
Improved search for heavy neutrinos in the decay π → eν
Phys. Rev. D, Vol. 97, 072012

A-154
K. Abe, *et al*.
Measurement of inclusive double-differential νμ charged-current cross section with improved acceptance in the T2K off-axis near detector
Phys. Rev. D, Vol. 98, 012004

A-155
C. Aidala, *et al*.
Single-spin asymmetry of J/ψ production in p + p, p + Al, and p + Au collisions with transversely polarized proton beams at√sNN = 200 GeV
Phys. Rev. D, Vol. 98, 012006

A-156
K. Abe, *et al*.
Characterization of nuclear effects in muon-neutrino scattering on hydrocarbon with a measurement of final-state kinematics and correlations in charged-current pionless interactions at T2K
Phys. Rev. D, Vol. 98, 032003

A-157
A. Adare, *et al*.
Cross section and longitudinal single-spin asymmetry AL for forward W ± ! μ ± √ ν production in polarized p + p collisions at s = 510 GeV
Phys. Rev. D, Vol. 98, 032007

A-158
Z. Li, *et al*.
Measurement of the tau neutrino cross section in atmospheric neutrino oscillations with Super-Kamiokande
Phys. Rev. D, Vol. 98, 052006

A-159
C. Aidala, *et al*.
Nonperturbative transverse-momentum-dependent effects in dihadron and direct photon-hadron angular correlations in p + p collisions at√s = 200 GeV
Phys. Rev. D, Vol. 98, 072004

A-160
M. Aghasyan, *et al*.
Light isovector resonances in π-p →π-π-π+p at 190 GeV/c
Phys. Rev. D, Vol. 98, 092003

A-161
A. Adare, *et al*.
Measurement of φ-meson production at forward rapidity in p + p collisions at √ s = 510 GeV and its energy dependence from √ s = 200 GeV to 7 TeV
Phys. Rev. D, Vol. 98, 092006

A-162
R. Inoue, *et al*.
Experimental investigation of the glass transition of polystyrene thin films in a broad frequency range
Phys. Rev. E, Vol. 97, 012501

A-163
C. Aidala, *et al*.
Nuclear Dependence of the Transverse-Single-Spin Asymmetry for Forward Neutron Production in Polarized p + A Collisions at√sNN = 200 GeV
Phys. Rev. Lett., Vol. 120, 022001

A-164
C. Aidala, *et al*.
Measurements of Multiparticle Correlations in d +Au Collisions at 200, 62.4, 39, and 19.6 GeV and p +Au Collisions at 200 GeV and Implications for Collective Behavior
Phys. Rev. Lett., Vol. 120, 062302

A-165
S. B. Yang, *et al*.
First Determination of the Level Structure of an sd-Shell Hypernucleus, 19 F
Phys. Rev. Lett., Vol. 120, 132505

A-166
T. Xie, *et al*.
Neutron Spin Resonance in the 112-Type Iron-Based Superconductor
Phys. Rev. Lett., Vol. 120, 137001

A-167
H. Kohri, *et al*.
Differential Cross Section and Photon-Beam Asymmetry for the →γp ! π – Δ++(1232) Reaction at Forward π – Angles for Eγ=1.5–2.95 GeV
Phys. Rev. Lett., Vol. 120, 202004

A-168
C. Kachulis, *et al*.
Search for Boosted Dark Matter Interacting with Electrons in Super-Kamiokande
Phys. Rev. Lett., Vol. 120, 221301

A-169
T. Xie, *et al*.
Odd and Even Modes of Neutron Spin Resonance in the Bilayer Iron-Based Superconductor CaKFe4As4
Phys. Rev. Lett., Vol. 120, 267003

A-170
K. Kurashima, *et al*.
Development of Ferromagnetic Fluctuations in Heavily Overdoped (Bi,Pb)2Sr2CuO6+δ Copper Oxides
Phys. Rev. Lett., Vol. 121, 057002

A-171
J. Sugiyama, *et al*.
Nuclear magnetic field in solids detected with negative-muon spin rotation and relaxation
Phys. Rev. Lett., Vol. 121, 087202

A-172
K. Abe, *et al*.
Search for CP Violation in Neutrino and Antineutrino Oscillations by the T2K Experiment with 2.2 1021 Protons on Target
Phys. Rev. Lett., Vol. 121, 171802

A-173
A. Adare, *et al*.
Pseudorapidity Dependence of Particle Production and Elliptic Flow in Asymmetric Nuclear Collisions of p + Al, p + Au, d + Au, and 3He + Au at$\sqrt{}$sNN = 200 GeV
Phys. Rev. Lett., Vol. 121, 222301

A-174
Y. Sakaguchi, *et al*.
Kinetics of Silver Photodiffusion Into Amorphous Ge 20 S 80 Films: Case of Pre-Reaction
Phys. Status Solidi A, Vol. 215, 1800049

A-175
K. Ohoyama, *et al*.
White Neutron Holography in Pulsed Neutron Facilities
Phys. Status Solidi B, Vol. 225, 1800143

A-176
D. Ueta, *et al*.
Crystalline electric field level scheme of the non-centrosymmetric CePtSi3
Physica B, Vol. 536, 21-23

A-177
M. Yoshida, *et al*.
Magnetic and thermodynamic studies on the charge and spin ordering in the highly hole-doped La2-xSrxCoO4
Physica B, Vol. 536, 338-341

A-178
K. Matsuura, *et al*.
Magnetic excitations in the orbital disordered phase of MnV2O4
Physica B, Vol. 536, 372-376

A-179
K. Ikeuchi, *et al*.
Detailed study of the structure of the low-energy magnetic excitations in overdoped La1.75Sr0.25CuO4
Physica B, Vol. 536, 717-719

A-180
K. Nakajima, *et al*.
High-energy magnetic excitations in lightly oxygen-doped lanthanum nickel oxides
Physica B, Vol. 551, 142-145

A-181
S. Itoh, *et al*.
Magnetic excitations in metallic antiferromagnets Fe0.5Mn0.5 and Fe0.7Mn0.3
Physica B, Vol. 551, 21-23

A-182
N. L. Yamada, *et al*.
In-situ measurement of phospholipid nanodisk adhesion on a solid substrate using neutron reflectometry and atomic force microscopy
Physica B, Vol. 551, 222-226

A-183
Y. Kawakita, *et al*.
Anomaly of structural relaxation in complex liquid metal of bismuth - Dynamic correlation function of coherent quasi-elastic neutron scattering -
Physica B, Vol. 551, 291-296

A-184
M. Nakamura, *et al*.
Phonon dynamics of NaI investigated by G(r, E) analysis
Physica B, Vol. 551, 351-354

A-185
K. Iwasa, *et al*.
Inelastic neutron scattering study on 4 f -electron multipole system PrTr2X20 (Tr : transition metal, X : Al and Zn)
Physica B, Vol. 551, 37-40

A-186
M. Nakamura, *et al*.
Performances of oscillating radial collimator for the Fermi chopper spectrometer 4SEASONS at J-PARC
Physica B, Vol. 551, 480-483

A-187
H. Ninomiya, *et al*.
Neutron diffraction study of antiferromagnetic ErNi3Ga9 in magnetic fields
Physica B: Cond. Matter, Vol. 536, 392-396

A-188
Z. Tan, *et al*.
The investigation of magnetic phase transition in cobaltite perovskites byhigh-resolution neutron powder diffraction under 14 T magnetic field
Physica B: Cond. Matter, Vol. 551, 111-114

A-189
K. Hiroi, *et al*.
Study of the magnetization distribution in a grain-oriented magnetic steel using pulsed polarized neutron imaging
Physica B: Cond. Matter, Vol. 551, 146-151

A-190
M. Hirai, *et al*.
Macromolecular crowding effect on protein structure and hydration clarified by using X-ray and neutron scattering
Physica B: Cond. Matter, Vol. 551, 212-217

A-191
S. Ajito, *et al*.
Protective action of trehalose and glucose on protein hydration shell clarified by using X-ray and neutron scattering
Physica B: Cond. Matter, Vol. 551, 249-255

A-192
K. Akutsu, *et al*.
Penetration behavior of an ionic liquid in thin-layer silica coating: Ionic liquid deuteration and neutron reflectivity analysis
Physica B: Cond. Matter, Vol. 551, 262-265

A-193
M. Mizusawa, *et al*.
An electrochemical cell with vertical geometry for neutron reflectivity measurements
Physica B: Cond. Matter, Vol. 551, 270-273

A-194
J. Abe, *et al*.
Effect of gauge volume on strain measurement in rock materials using time-of-flight neutron diffraction
Physica B: Cond. Matter, Vol. 551, 283-286

A-195
W. R. Puspita, *et al*.
Temperature Dependence of Structural Disorder in Thermoelectric Clathrate Ba8Al16Ge30
Physica B: Cond. Matter, Vol. 551, 41-45

A-196
K. Sakurai, *et al*.
Hadamard coding of time-of-flight neutron reflectogram at grazing incidence
Physica B: Cond. Matter, Vol. 551, 426-430

A-197
K. Oikawa, *et al*.
Recent progress on practical materials study by Bragg edge imaging at J-PARC
Physica B: Cond. Matter, Vol. 551, 436-442

A-198
N. Miyata, *et al*.
Relatively thick (few micrometers) film structure estimated by back-incidence neutron reflectometry
Physica B: Cond. Matter, Vol. 551, 449-451

A-199
Y. Ishikawa, *et al*.
Z-MEM, Maximum Entropy Method software for electron/nuclear densitydistribution in Z-Code
Physica B: Cond. Matter, Vol. 551, 472-475

A-200
T. Kai, *et al*.
Characteristics of the 2012 model lithium-6 time-analyzer neutron detector (LiTA12) system as a high efficiency detector for resonance absorption imaging
Physica B: Cond. Matter, Vol. 551, 496-500

A-201
H. Iwase, *et al*.
Installation of a high-resolution position-sensitive scintillation detector in the small and wide angle neutron scattering instrument (TAIKAN), MLF, J-PARC
Physica B: Cond. Matter, Vol. 551, 501-505

A-202
Y. Seki, *et al*.
Effect of upstream beam collimation on neutron phase imaging with a Talbot-Lau interferometer at the RADEN beam line in J-PARC
Physica B: Cond. Matter, Vol. 551, 512-516

A-203
P. Wu, *et al*.
Crystal structure of high-performance thermoelectric materials by high resolution neutron powder diffraction
Physica B: Cond. Matter, Vol. 551, 64-68

A-204
S. Lee, *et al*.
Weak-ferromagnetism of CoF3 and FeF3
Physica B: Cond. Matter, Vol. 551, 94-97

A-205
H. Kumada, *et al*.
Development of LINAC-Based Neutron Source for Boron Neutron Capture Therapy in University of Tsukuba
Plasma Fusion Res., 13(0), 2406006-2406006

A-206
H. Takei, *et al*.
Beam Extraction by the Laser Charge Exchange Method Using the 3-MeV LINAC in J-PARC
Plasma Fusion Res., Vol. 13, 2406012

A-207
F. Maekawa, Transmutation Experiment Facility design Team
J-PARC transmutation experimental facility program
Plasma Fusion Res., Vol. 13, 2505045

A-208
K. Abe, *et al*.
Physics potentials with the second Hyper-Kamiokande detector in Korea
Prog. Theor. Exp. Phys., 2018, 063C01

A-209
N. Kawamura, *et al*.
New concept for a large-acceptance general-purpose muon beamline
Prog. Theor. Exp. Phys., 2018, 113G01

A-210
Y. Shobuda
Evaluation of the frequency dependence of the complex conductivity of a resistive chamber by comparing theoretical and measured S-matrices
Prog. Theor. Exp. Phys., Vol. 2018, Issue 12, 123G01

A-211
Y. Ashida, *et al*.
A new electron-multiplier-tube-based beam monitor for muon monitoring at the T2K experiment
PTEP, 2018, 103H01

A-212
M. Ishikado, *et al*.
High-energy spin fluctuation in low-Tc iron-based superconductor LaFePO0.9
Sci. Rep., Nol. 8, 16343

A-213
A. Sano-Furukawa, *et al*.
Direct observation of symmetrization of hydrogen bond in δ-AlOOH under mantle conditions using neutron diffraction
Sci. Rep., Vol. 8, 15520

A-214
M. Sales, *et al*.
Three Dimensional Polarimetric Neutron Tomography of Magnetic Fields
Sci. Rep., Vol. 8, 2214

A-215
V. Ukleev, *et al*.
Unveiling structural, chemical and magnetic interfacial peculiarities in ε-Fe2O3/GaN (0001) epitaxial films
Sci. Rep., Vol. 8, 8741

A-216
R. Kajimoto, *et al*.
Elastic and dynamical structural properties of La and Mn-doped SrTiO3 studied by neutron scattering and their relation with thermal conductivities
Sci. Rep., Vol. 8, 9651

A-217
K. Kataoka, *et al*.
Lithium-ion conducting oxide single crystal as solid electrolyte for advanced lithium battery application
Sci. Rep., Vol. 8, 9965

A-218
Y. Shobuda, *et al*
Rigorous formulation of space-charge wake function and impedance by solving the three-dimensional Poisson equation
Sci. Rep., Vol. 8, Article number: 12805

A-219
B. Wang, *et al*.
Deformation of CoCrFeNi high entropy alloy at large strain
Scr. Mater., Vol. 155, 54-57

A-220
J. J. Kang, *et al*.
Directed Vertical Diffusion of Photovoltaic Active Layer Components into Porous ZnO-based Cathode Buffer Layers
Small, Vol. 14, 04310

A-221
H. Tanoue, *et al*.
Thermoresponsive Dynamic Polymer Brush Fabricated by the Segregation of Amphiphilic Diblock Copolymers
Soft Matter, Vol. 14, 5930-5935

A-222
N. Ishida, *et al*.
Average and local structure analysis of metastable LixMn0.9Ti0.1O2 by synchrotron X-ray and neutron sources
Solid State Ion., Vol. 325, 209-213

Conference Reports and Books

B-001
T. Nakamura, *et al*.
A sub-millimeter spatial resolution scintillation neutron detector for time-of-flight neutron diffraction imaging
2018 IEEE NSS and MIC, conference record, N07-197

B-002
T. Okuda, *et al*.
Schottky specific heat of the lightly Mn-substituted electron-doped SrTiO3
AIP Advances, Vol. 8, 101339

B-003
K. Shinto, *et al*.
Present status of the J-PARC cesiated RF-driven H– ion source
AIP Conf. Proc. Vol. 2011, 050018-1 - 050018-3

B-004
T. Yokoo, *et al*.
Ready to Roll? Time to Launch POLANO
AIP Conf. Proc., Vol. 1969, 050001

B-005
S. Itoh, *et al*.
High Resolution Chopper Spectrometer HRC and Neutron Brillouin Scattering
AIP Conf. Proc., Vol. 1969, 050002

B-006
R. Kajimoto, *et al*.
Instrumental Resolution of the Chopper Spectrometer 4SEASONS Evaluated by Monte Carlo Simulation
AIP Conf. Proc., Vol. 1969, 050004

B-007
T. Shibata, *et al*.
Observation of plasma density oscillation with doubled value of RF frequency in J-PARC RF ion source
AIP Conf. Proc., Vol. 2011, 020008-1 - 020008-3

B-008
K. Shinto, *et al*.
Observation of beam current fluctuation extracted from an RF-driven H- ion source
AIP Conf. Proc., Vol. 2011, 080016-1 - 080016-3

B-009
K. Shinto, *et al*.
Progress of the J-PARC cesiated rf-driven negative hydrogen ion source
AIP Conf. Proc., Vol. 2052 00002-1 - 050002-7

B-010
A. Ueno, *et al*.
Solving Beam Intensity Bottlenecks and 100 mA Operation of J-PARC Cesiated RF-Driven H^- Ion Source
AIP Conf. Proc., Vol. 2052, 050003

B-011
K.Yamamoto, *et al*.
Activation in injection area of J-PARC 3-GeV rapid cycling synchrotron and its countermeasures
ANS RPSD 2018

B-012
S. Kumano, *et al*.
Tomography and gravitational radii for hadrons by three-dimensional structure functions
EPJ Web Conf., Vol. 181, 01025

B-013
J. Kamiya
Vacuum technologies in the high-power proton beam accelerator:J-PARC
Hydraulics & pneumatics, 2018.7., 44

B-014
T. Takayanagi, *et al*.
Development of a new modular switch using a next-generation semiconductor
IOP Conf. Ser.: J. Phys.: Conf. Ser., Vol. 1067 , 082019

B-015
K. Ikeuchi, *et al*.
Fe-impurity-induced magnetic excitations in heavily over-doped La1.7Sr0.3Cu0.95Fe0.05O4
IOP Conf. Ser.: J. Phys.: Conf. Ser., Vol. 969, 012024

B-016
K. Mochiki, *et al*.
Pulsed-neutron imaging by a high-speed camera and center-of-gravity processing
J. Instrum., Vol. 13, C01038

B-017
M. Tomizawa, *et al*.
Beam Optics Design of Stretcher Ring and Transfer Line for J-PARC Slow Extraction
J. Phys. Conf. Ser. Vol. 1067, 042004

B-018
K. Satou, *et al*.
A novel field cage design for the CPS IPM and systematic errors in beam size and emittance
J. Phys. Conf. Ser., Vol. 1067, 072008

B-019
D. Kawana, *et al*.
YUI and HANA: Control and Visualization Programs for HRC in J-PARC
J. Phys. Conf. Ser., Vol. 1021, 012014

B-020
S. Meigo, *et al*.
Target test facility for ADS and cross-section experiment in J-PARC
J. Phys. Conf. Ser., Vol. 1021, 012072

B-021
M. Tomizawa, *et al*.
Beam Optics Design of Stretcher Ring and Transfer Line for J-PARC Slow Extraction
J. Phys. Conf. Ser., Vol. 1067, 042004

B-022
J. Tamura, *et al*.
Low-Reflection RF Window for ACS Cavity in J-PARC Linac
J. Phys. Conf. Ser., Vol. 1067, 052009

B-023
M. Otani, *et al*.
Muon Profile Measurement After Acceleration With a Radio-Frequency Quadrupole linac
J. Phys. Conf. Ser., Vol. 1067, 052012

B-024
M. Otani, *et al*.
Muon Profile Measurement After Acceleration With a Radio-Frequency Quadrupole linac
J. Phys. Conf. Ser., Vol. 1067, 052012

B-025
M. Yamamoto, *et al*.
Conceptual design of a single-ended MA cavity for J-PARC RCS upgrade
J. Phys. Conf. Ser., Vol. 1067, 052014

B-026
M. Otani, *et al*.
Simulation of Surface Muon Beamline, UltraSlow Muon Production and Extraction for the J-PARC g-2/EDM Experiment
J. Phys. Conf. Ser., Vol. 1067, 052018

B-027
T. Shibata, *et al*.
The Development of a New Low Field Septum Magnet System for Fast Extraction in Main Ring of J-PARC
J. Phys. Conf. Ser., Vol. 1067, 052020

B-028
Y. Shobuda, *et al*.
Reduction of the Kicker Impedance Maintaining the Performance of Present Kicker Magnet at RCS in J-PARC
J. Phys. Conf. Ser., Vol. 1067, 062007

B-029
B. Yee-Rendon, *et al*.
Updated model of the resistive wall impedance for the main ring of J-PARC
J. Phys. Conf. Ser., Vol. 1067, 062009

B-030
P. K. Saha, *et al*.
ORBIT Simulation, Measurement and Mitigation of Transverse Beam Instability in the Presence of Strong Space Charge in the 3-GeV RCS of J-PARC
J. Phys. Conf. Ser., Vol. 1067, 062013

B-031
A. Miura, *et al*.
Tensile fracture test of metalic wire of beam profile monitors
J. Phys. Conf. Ser., Vol. 1067, 072007

B-032
K. Moriya, *et al*.
Study of a tuner for a high-accuracy bunch shape monitor
J. Phys. Conf. Ser., Vol. 1067, 072009

B-033
F. Tamura, *et al*.
Baseband simulation model of the vector rf voltage control system for the J-PARC RCS
J. Phys. Conf. Ser., Vol. 1067, 072030

B-034
M. Otani, *et al*.
Longitudinal Bunch Size Measurements with an RF Deflector at J-PARC LINAC
J. Phys. Conf. Ser., Vol. 1067, no. 6, 052008

B-035
A. Miura, *et al*.
Application of carbon nanotube wire for beam profile measurement of negative

hydrogen ion beam
J. Phys. Conf. Ser., Vol. 1067, no. 6, 072020

B-036
H. Takahashi, *et al*.
Improvement of motor control system in J-PARC linac and RCS
J. Phys. Conf. Ser., Vol. 1067, no. 6, 072022

B-037
H. Hotchi, *et al*.
Pulse-by-pulse switching of operational parameters in J-PARC 3-GeV RCS
J. Phys. Conf. Ser., Vol. 1067, no.6, 062013

B-038
T. Tanaka, *et al*.
High precision measurement of muonium hyperfine structure
J. Phys. Conf. Ser., Vol. 1138, 012008

B-039
C. Trippl, *et al*.
A New Silicon Drift Detector System for Kaonic Atom Measurements
J. Phys. Conf. Ser., Vol. 1138, 012013

B-040
K. Nakajima, *et al*.
Recent issues encountered by AMATERAS: A cold-neutron disk-chopper spectrometer
J. Phys.: Conf. Ser., Vol. 1021, 012031

B-041
Y. Inamura, *et al*.
Applications of the differential events reading method at MLF, J-PARC
J. Phys.: Conf. Ser., Vol. 1021, 012015

B-042
H. Matsuda, *et al*.
Measurement of activation cross sections of the target and the proton beam window materials at J-PARC
J. Phys.: Conf. Ser., Vol. 1021, 012016

B-043
H. Matsuda, *et al*.
The measurements of neutron energy spectrum at 180 degrees with the mercury target at J-
J. Phys.: Conf. Ser., Vol. 1021, 012017

B-044
H. Matsuda, S. Meigo, H. Iwamoto
The measurements of neutron energy spectrum at 180 degrees with the mercury target at J-PARC
J. Phys.: Conf. Ser., Vol. 1021, 012017

B-045
S. Itoh, *et al*.
Improvement for Neutron Brillouin Scattering Experiments on High Resolution Chopper Spectrometer HRC
J. Phys.: Conf. Ser., Vol. 1021, 012028

B-046
R. Kajimoto, *et al*.
Status report of the chopper spectrometer 4SEASONS
J. Phys.: Conf. Ser., Vol. 1021, 012030

B-047
T. Kai, *et al*.
Off-gas processing system operations for mercury target vessel replacement at J-PARC
J. Phys.: Conf. Ser., Vol. 1021, 012042

B-048
H. Iwamoto, H. Matsuda, S. Meigo
Shielding analysis of Transmutation Experimental Facility
J. Phys.: Conf. Ser., Vol. 1021, 012049

B-049
M. Teshigawara, *et al*.
Present fabrication status of spare moderators and reflector in J-PARC spallation neutron source
J. Phys.: Conf. Ser., Vol. 1021, 012061

B-050
T. Aso, *et al*.
Recovery of helium refrigerator performance for cryogenic hydrogen system at J-PARC MLF
J. Phys.: Conf. Ser., Vol. 1021, 012085

B-051
Y. Miki, *et al*.
Neutron signal features of Nb-based kinetic inductance detector with 10B convertor
J. Phys.: Conf. Ser., Vol. 1054, 012054

B-052
T. Koyama, *et al*.
Electrodynamic theory for the operation principle of a superconducting kinetic inductance stripline detector
J. Phys.: Conf. Ser., Vol. 1054, 012055

B-053
Y. Iizawa, *et al*.
Physical characteristics of delay-line current-biased kinetic inductance detector
J. Phys.: Conf. Ser., Vol. 1054, 012056

B-054
J. Kamiya, *et al*.
Non-destructive 2-D beam profile monitor using gas sheet in J-PARC LINAC
J. Phys.: Conf. Ser.,072006

B-055
S. Ohira-Kawamura, *et al*.
Magnetic Properties of One-Dimensional Quantum Spin System Rb2Cu2Mo3O12 Studied by Muon Spin Relaxation
JPS Conf. Proc., Vol. 21, 011007

B-056
M. Fujita, *et al*.
μSR Study of Magnetism in the As-Prepared and Non-Superconducting T*-La0.9Eu0.9Sr0.2CuO4
JPS Conf. Proc., Vol. 21, 011026

B-057
T. Sumura, *et al*.
Reduction Effects on the Cu-Spin Correlation in the Electron-Doped T'-Cuprate Pr1.3-xLa0.7CexCuO4+δ (x = 0.10)
JPS Conf. Proc., Vol. 21, 011027

B-058
K. Nishimura, *et al*.
Muon Spin Relaxation of an Al–3.4%Zn–1.9%Mg alloy
JPS Conf. Proc., Vol. 21, 011030

B-059
M. Mihara, *et al*.
μSR Study on Hydrogen Behavior in Palladium
JPS Conf. Proc., Vol. 21, 011031

B-060
T. Kiyotani, *et al*.
Visualization of proton and electron transfer processes of a biochemical reaction by μSR
JPS Conf. Proc., Vol. 21, 011037

B-061
A. D. Pant, *et al*.
Theoretical Calculations of Charge States and Stopping Sites of Muons in Glycine and Triglycine
JPS Conf. Proc., Vol. 21, 011038

B-062
G. Liu, *et al*.
Supercritical Water Experimental Setup for μSR
JPS Conf. Proc., Vol. 21, 011039

B-063
I. Umegaki, *et al*.
Detection of Li in Li-ion Battery Electrode Materials by Muonic X-ray
JPS Conf. Proc., Vol. 21, 011041

B-064
K. Ninomiya, *et al*.
Isotope Identification of Lead by Muon Induced X-ray and Gamma-ray Measurements
JPS Conf. Proc., Vol. 21, 011043

B-065
G. Yabu, *et al*.
Imaging of Muonic X-ray of Light Elements with a CdTe Double-Sided Strip Detector
JPS Conf. Proc., Vol. 21, 011044

B-066
G. Yoshida, *et al*.
Development of Muonic Atom Beam Extraction System and First Evaluation by Intense Negative Muon Beam of J-PARC MUSE

JPS Conf. Proc., Vol. 21, 011046

B-067
P. Strasser, *et al*.
Possibility of New Precise Measurements of Muonic Helium Atom HFS at J-PARC MUSE
JPS Conf. Proc., Vol. 21, 011046

B-068
Y. Miyake, *et al*.
J-PARC muon facility, MUSE
JPS Conf. Proc., Vol. 21, 011054

B-069
D. Tomono, *et al*.
Muon Beamline Commissioning and Feasibility Study for μSR at a New DC Muon Beamline, MuSIC-RCNP, Osaka University
JPS Conf. Proc., Vol. 21, 011057

B-070
S. Makimura, *et al*.
Perspective of Muon Production Target at J-PARC MLF MUSE
JPS Conf. Proc., Vol. 21, 011058

B-071
S. Matoba, *et al*.
Renovation of a Scraper Unit of a Muon Production Target at J-PARC
JPS Conf. Proc., Vol. 21, 011059

B-072
A. D. Pant, *et al*.
Transportation of Ultra Slow Muon on U-line, MLF, J-PARC
JPS Conf. Proc., Vol. 21, 011060

B-073
P. Strasser, *et al*.
Status of the New Surface Muon Beamline at J-PARC MUSE
JPS Conf. Proc., Vol. 21, 011061

B-074
K. M. Kojima, *et al*.
Development of General Purpose μSR Spectrometer ARTEMIS at S1 Experimental Area, MLF J-PARC
JPS Conf. Proc., Vol. 21, 011062

B-075
R. Katayama, *et al*.
Development of new neutron mirrors for measuring the neutron electric dipole moment
JPS Conf. Proc., Vol. 22, 011009

B-076
R. Maruyama, *et al*.
Effect of the interfacial roughness correlation on the reflectivity in a neutron multilayer mirror
JPS Conf. Proc., Vol. 22, 011011

B-077
J. D. Parker, *et al*.
Development of Energy-Resolved Neutron Imaging Detectors at RADEN
JPS Conf. Proc., Vol. 22, 011022

B-078
T. Uragaki, *et al*.
Evaluation of high-frame-rate camera with digital accumulation system combined with neutron color image intensifier for energy resolved neutron imaging
JPS Conf. Proc., Vol. 22, 011027

B-079
M. Segawa, *et al*.
Spatial Resolution Test Targets Made of Gadolinium and Gold for Conventional and Resonance Neutron Imaging
JPS Conf. Proc., Vol. 22, 011028

B-080
K. Hiroi, *et al*.
Development of a Polarization Analysis Method for Visualization of the Magnetic Field Distribution in a Small Electric Transformer using Pulsed Polarized Neutron Imaging
JPS Conf. Proc., Vol. 22, 011030

B-081
T. Kumada, *et al*.
Development of Dynamic Nuclear Polarization System for Spin-Contrast-Variation Neutron Reflectometry
JPS Conf. Proc., Vol. 22, 11015

B-082
T. Koyama, *et al*.
Deformation Analysis of Reinforced Concrete using Neutron Imaging Technique
Materials Research Proc., Vol. 4, 155-160

B-083
M. Kumagai, *et al*.
Convergence Behavior in Line Profile Analysis Using Convolutional Multiple Whole-Profile Software
Materials Research Proc., Vol. 6, 57-62

B-084
Y. Sato, *et al*.
Critical Conditions of Cold Cracking in High Strength Steel Weld Based on the Local Stress Distribution and Hydrogen Accumulation
Materials Scientific Forum, Vol. 941, 153-157

B-085
S. Satoh
Development of a Flat-Panel and Resistor-Type Photomultiplier Tube System for High Position-Resolution Two-Dimensional Neutron Detector
PFR, Vol. 13, 2405056

B-086
S. Meigo, H. Iwamoto, H. Matsuda
Cross section measurement in J-PARC for neutronics of the ADS
Proc. of AccApp2017 396-402 (2018).

B-087
S. Saito, *et al*.
Design of LBE spallation target for ADS target test facility (TEF-T) in J-PARC
Proc. of AccApp2017, 448-457 (2018)

B-088
K. Moriyama, *et al*.
Development of status analysis system based on ELK stack at J-PARC MLF
Proc. of ICALEPCS

B-089
F.A. Mavuso, *et al*.
Iron oxide-pluronic F127 polymer nanocomposites as carriers for doxorubicin drug delivery system
Proc. of ICRAMS

B-090
F.A. Mavuso, *et al*.
Synthesis and structural characterization of polymer-magnetic nanocomposites as carriers for drug delivery system
Proc. of ICRAMS

B-091
K.Yamamoto, *et al*.
Recent status of J-PARC rapid cycling synchrotron
Proc. of IPAC2018

B-092
K. Hasegawa, *et al*.
Performance and status of the J-PARC accelerators
Proc. of IPAC2018 (Internet), 1038-1040

B-093
Y. Kondo, *et al*.
Re-acceleration of Ultra Cold Muon in J-PARC Muon Facility
Proc. of IPAC2018 (Internet), 5041-5046

B-094
T. Takayanagi, *et al*.
New design and development for an ultrahigh-voltage short pulse switch power supply
Proc. of EAPPC

B-095
S. V. Cao
Latest results from T2K
Proc. of EW2018, 259

B-096
S. Meigo
Beam instruments for high power spallation neutron source and facility for ADS
Proc. of HB2018, pp., 99-103

B-097
P. Saha, *et al*.

Status of proof-of principle demonstration of 400 MeV H- stripping to proton by using only lasers at J-PARC
Proc. of HB2018 (Internet), 422-427

B-098
H. Hotchi
J-PARC RCS: Effects of emittance exchange on injection painting
Proc. of HB2018, 20-25

B-099
Y. Iwamoto, *et al*.
Radiation damage calculation in PHITS and benchmarking experiment for cryogenic-sample high-energy proton irradiation
Proc. of HB2018, 116-121

B-100
S. Igarashi
HIGH-POWER BEAM OPERATION AT J-PARC
Proc. of HB2018, 147

B-101
M. Tomizawa, *et al*.
STATUS AND BEAM POWER RAMP-UP PLANS OF THE SLOW EXTRACTION OPERATION AT J-PARC MAIN RING
Proc. of HB2018, 347

B-102
Y. Liu, *et al*.
60 mA BEAM STUDY IN J-PARC LINAC
Proc. of HB2018, 60

B-103
P.K. Saha, et al.
MEASUREMENT OF EACH 324 MHz MICRO PULSE STRIPPING EFFICIENCY FOR H– LASER STRIPPING EXPERIMENT IN J-PARC RCS
Proc. of IBIC2017 (Internet), 233-236(2017)

B-104
S. I. Meigo, *et al*.
Profile monitor on target for spallation neutron source
Proc. of IBIC2017, pp., 373-376 (2018)

B-105
H. Takei, *et al*.
Beam extraction by the laser charge exchange method using the 3-MeV linac in J-PARC
Proc. of IBIC2017, pp., 435-439 (2018)

B-106
N. Hayashi, *et al*.
ANALYSIS OF INTERLOCKED EVENTS BASED ON BEAM INSTRUMENTATION DATA AT J-PARC LINAC AND RCS
Proc. of IBIC2018, 219-223

B-107
K. Nakayoshi, *et al*.
DEVELOPMENT OF AN EXPERT SYSTEM FOR THE HIGH INTENSITY NEUTRINO BEAM FACILITY AT J-PARC
Proc. of IBIC2018, 154

B-108
K. Sakashita, *et al*.
UPGRADE OF THE MACHINE PROTECTION SYSTEM TOWARD 1.3MW OPERATION OF THE J-PARC NEUTRINO BEAMLINE
Proc. of IBIC2018, 18

B-109
S. Cao, *et al*.
OPTICAL SYSTEM OF BEAM INDUCED FLUORESCENCE MONITOR TOWARD MW BEAM POWER AT THE J-PARC NEUTRINO BEAMLINE
Proc. of IBIC2018, 505

B-110
M. Friend
BEAM PARAMETER MEASUREMENTS FOR THE J-PARC HIGH-INTENSITY NEUTRINO EXTRACTION BEAMLINE
Proc. of IBIC2018, 85

B-111
Y. Nakamura, *et al*.
In Situ Neutron Diffraction Study on Microstructure Evolution During Thermo-Mechanical Processing of Medium Manganese Steel
Proc. of ICOMAT, 155-158

B-112
N. Tsuchida, *et al*.
TRIP Effect in a Constant Load Creep Test at Room Temperature
Proc. of ICOMAT, 43-46

B-113
S. Meigo, *et al*.
MEASUREMENT OF DISPLACEMENT CROSS-SECTION FOR STRUCTURAL MATERIALS IN HIGH-POWER PROTON ACCELERATOR FACILITY
Proc. of IPAC2018, pp., 499-501

B-114
K. Yamamoto, *et al*.
Recent status of J-PARC rapid cycling synchrotron
Proc. of IPAC2018

B-115
K. Hasegawa, *et al*.
Performance and status of the J-PARC accelerators
Proc. of IPAC2018 (Internet), 1038-1040

B-116
Y. Kondo, *et al*.
Re-acceleration of Ultra Cold Muon in J-PARC Muon Facility
Proc. of IPAC2018 (Internet), 5041-5046

B-117
R. Kitamura, *et al*.
RESULT OF THE FIRST MUON ACCELERATION WITH RADIO FREQUENCY QUADRUPOLE
Proc. of IPAC2018, 1190

B-118
H. Iinuma, *et al*.
THREE-DIMENSIONAL SPIRAL BEAM INJECTION FOR A COMPACT STORAGE RING
Proc. of IPAC2018, 1673

B-119
S. Li, *et al*.
ADAPTIVE FEEDFORWARD CONTROL DESIGN BASED ON SIMULINK FOR J-PARC LINAC LLRF SYSTEM
Proc. of IPAC2018, 2187

B-120
N. Ogiwara, *et al*.
A NON-DESTRUCTIVE 2D PROFILE MONITOR USING A GAS SHEET
Proc. of IPAC2018, 2190

B-121
T. Toyama, *et al*.
MEASUREMENT OF TRANSVERSE DIPOLE AND QUADRUPOLE MOMENTS WITH THE BPMS IN THE J-PARC 3-50 BT
Proc. of IPAC2018, 2197

B-122
K. Futatsukawa, *et al*.
IMPROVEMENT OF THE CHOPPER SYSTEM FOR RF DEFLECTOR AT THE J-PARC LINAC
Proc. of IPAC2018, 2816

B-123
Y. Sato
HIGH POWER BEAM OPERATION OF THE J-PARC RCS AND MR
Proc. of IPAC2018, 2938

B-124
A. Miura, *et al*.
APPLICATION OF CARBON NANOTUBE WIRE FOR BEAM PROFILE MEASUREMENT OF NEGATIVE HYDROGEN ION BEAM
Proc. of IPAC2018, 5022

B-125
T. Koseki
UPGRADE PLAN OF J-PARC MR - TOWARD 1.3 MW BEAM POWER
Proc. of IPAC2018, 966

B-126
M. Otani, *et al*.
SIMULATION OF SURFACE MUON BEAM LINE, ULTRASLOW MUON PRODUCTION AND EXTRACTION FOR THE J-PARC G-2/EDM EXPERIMENT
Proc. of IPAC2018, 970

B-127
M. Otani, *et al*.
LONGITUDINAL BUNCH SIZE MEASUREMENTS WITH AN RF DEFLECTOR AT J-PARC LINAC

Proc. of IPAC2018, 974

B-128
M. Yoshii, *et al.*
PRESENT STATUS AND FUTURE UPGRADES OF THE J-PARC RING RF SYSTEMS
Proc. of IPAC2018, 984

B-129
K. Futatsukawa, *et al.*
DEVELOPMENT OF NEW LLRF SYSTEM AT THE J-PARC LINAC
Proc. of LINAC2018, 233

B-130
R. Kitamura, *et al.*
MUON ACCELERATION TEST WITH THE RFQ TOWARDS THE DEVELOPMENT OF THE MUON LINAC
Proc. of LINAC2018, 342

B-131
J. Y. Yoon, *et al.*
DESIGN STUDY OF A PROTOTYPE 325MHz RF POWER COUPLER FOR SUPERCONDUCTING CAVITY
Proc. of LINAC2018, 451

B-132
T. Shibata, *et al.*
NUMERICAL AND EXPERIMENTAL STUDY OF H- BEAM DYNAMICS IN J-PARC LEBT
Proc. of LINAC2018, 519

B-133
N. Oi, *et al.*
A Search for Possible Deviations from Newtonian Gravity at the nm Length Scale Using Neutron-Noble Gas Scattering
Proc. of NOP2017

B-134
S. Tada, *et al.*
Development of High Spatial Resolution Cold/Ultra-Cold Neutron Detector Using Nano Imaging Tracker
Proc. of NOP2017

B-135
K. Mishima, *et al.*
Fundamental physics activities with pulsed neutron at J-PARC(BL05)
Proc. of NOP2017

B-136
N. Sumi, *et al.*
Precise Neutron Lifetime Measurement with a Solenoidal Coil
Proc. of NOP2017

B-137
S. Imajo, *et al.*
Time-focus Experiment of Ultracold Neutron by Improved UCN Rebuncher at J-PARC/MLF
Proc. of NOP2017

B-138
Wan, T., Obayashi, H., Sasa, T.
Optimization of design of the LBE spallation target at JAEA
Proc. of NUTHOS-12 (USB flash memory), 14 pages

B-139
T. Kimura
DEVELOPMENT OF THE NEW SPILL CONTROL DEVICE for J-PARC MR
Proc. of PCaPAC2018, 192

B-140
N. Kamikubota, *et al.*
DEVELOPMENT OF TRIGGERED SCALER TO DETECT MISS-TRIGGER
Proc. of PCaPAC2018, 213

B-141
S. Kumano
Theoretical perspective for the future experiments on parton densities
Proc. of Science, DIS 2018, 245

B-142
T. Kumada, *et al.*
Development of closed-cycle dynamic nuclear polarization system for small-angle neutron scattering and neutron reflectometry
Proc. of Science, Vol. 324, 9

B-143
T. Takayanagi, *et al.*
Development of solid-state switch for power supply with SiC-MOSFET
Proc. of 15th Annual Meeting of PASJ (Internet)

B-144
A. Tokuchi, *et al.*
Research on accelerator applications of 13 kV high voltage SiC devices
Proc. of 15th Annual Meeting of PASJ (Internet), 1010-1014

B-145
H. Yasuda, *et al.*
DEVELOPMENT OF MUON SPIN ROTATOR FOR J-PARC MUON g - 2/EDM EXPERIMENT
Proc. of 15th Annual Meeting of PASJ (Internet), 1027-1030

B-146
T. Miyao, *et al.*
BEAM PROFILE MEASUREMENT USING CARBON NANOTUBE WIRES (3)
Proc. of 15th Annual Meeting of PASJ (Internet), 1031-1034

B-147
Y. Nakazawa, *et al.*
Commissioning of the diagnostic beam line for the muon RF acceleration with negative hydrogen ion beam derived from the ultraviolet light
Proc. of 15th Annual Meeting of PASJ (Internet), 1047-1050

B-148
Y. Sue, *et al.*
Development of the good time resolution monitor to measure the longitudinal structure of low-rate muon bunch for J-PARC E34 Experiment
Proc. of 15th Annual Meeting of PASJ (Internet), 1051-1054

B-149
N. Hayashi, *et al.*
MONITORING OF THE INJECTED BEAM TO THE J-PARC RCS AND BPM DESIGN FOR H0 DUMP LINE
Proc. of 15th Annual Meeting of PASJ (Internet), 1055-1059

B-150
F. Tamura, *et al.*
NEXT GENERATION LLRF CONTROL SYSTEM FOR J-PARC RCS
Proc. of 15th Annual Meeting of PASJ (Internet), 1131-1135

B-151
K. Hasegawa, *et al.*
STATUS OF J-PARC ACCELERATORS
Proc. of 15th Annual Meeting of PASJ (Internet), 1317-1321

B-152
M. Sato, *et al.*
Status report of the iBNCT accelerator
Proc. of 15th Annual Meeting of PASJ (Internet), 1350-1354

B-153
M. Otani, *et al.*
BEAM COMMISSIONING OF J-PARC MEBT1 FOR A HIGHER BEAM CURRENT
Proc. of 15th Annual Meeting of PASJ (Internet), 216-219

B-154
R. Kitamura, *et al.*
Demonstration of the muon RF acceleration with the negative muonium
Proc. of 15th Annual Meeting of PASJ (Internet), 239-243

B-155
K. Suganuma, *et al.*
Present status of water cooling system at J-PARC LINAC 2018
Proc. of 15th Annual Meeting of PASJ (Internet), 309-311

B-156
K. Hirano, *et al.*
STATUS OF 3MeV BEAM SCRAPERS FOR THE J-PARC LINAC
Proc. of 15th Annual Meeting of PASJ (Internet), 324-328

B-157
T. Shibata, *et al*.
Status of development on LaB6 filament multi-cusp ion source for iBNCT
Proc. of 15th Annual Meeting of PASJ (Internet), 385-387

B-158
Y. Kondo, *et al*.
Low power test of an L-band RFQ
Proc. of 15th Annual Meeting of PASJ (Internet), 421-424

B-159
S. Lim, *et al*.
An improvement of compact pulsed power supply for Ion source using 13kV-SiC-MOSFET
Proc. of 15th Annual Meeting of PASJ (Internet), 488-489

B-160
T. Watanabe, *et al*.
Development of beam energy position monitor system for RIKEN superconducting acceleration cavity
Proc. of 15th Annual Meeting of PASJ (Internet), 49-54

B-161
J. Kamiya, *et al*.
Upgrade of vacuum chamber at RCS beam injection area aimed at lower radiation and maintainability increase
Proc. of 15th Annual Meeting of PASJ (Internet), 645-648

B-162
P. K. Saha, *et al*.
PROGRESS STATUS OF PROOF-OF-PRINCIPLE DEMONSTRATION OF 400 MeV H- LASER STRIPPING AT J-PARC 3-GeV RCS
Proc. of 15th Annual Meeting of PASJ (Internet), 806-810

B-163
K. Ohkoshi, *et al*.
Operation Status of the J-PARC H- Ion Source
Proc. of 15th Annual Meeting of PASJ (Internet), 889-892

B-164
Y. Nakazawa, *et al*.
Performance test of Inter-digital H-mode drift-tube linac prototype with alternative phase focusing for muon linac
Proc. of 15th Annual Meeting of PASJ (Internet), 904-908

B-165
H. Takahashi, *et al*.
Standardization of Stepping Motor Control System in J-PARC Linac and RCS
Proc. of the 15th Annual Meeting of PASJ, 1105-1108

B-166
K. Akutsu, *et al*.
Development of new waterproof thin-layers for the magnetic alloy core and structural study by neutron reflectometry
Proc. of the 15th Annual Meeting of PASJ, 1198

B-167
H. Hotchi, *et al*.
J-PARC RCS: Effects of nonlinear field components of injection bump magnets on circulating beam
Proc. of the 15th Annual Meeting of PASJ, 371-375

B-168
Y. H. Chin, *et al*.
Chromaticity effects on head-tail instabilities for broadband impedance using two particle model, Vlasov analysis, and simulations
Proc. of the 15th Annual Meeting of PASJ, THP030

B-169
E. Yanaoka, *et al*.
The Improvement of forced synchronous trip system of bump magnet power supplies
Proc. of the 15th Annual Meeting of PASJ, WEP078

B-170
K. Miura, *et al*.
MAGNET POWER SUPPLY CALIBRATION WITH A PORTABLE CURRENT MEASURING UNIT AT THE J-PARC MAIN RING
Proc. of the 15th Annual Meeting of PASJ, 1015

B-171
H. Yasuda, *et al*.
DEVELOPMENT OF MUON SPIN ROTATOR FOR J-PARC MUON g - 2/EDM EXPERIMENT
Proc. of the 15th Annual Meeting of PASJ, 1027

B-172
T. Miyao, *et al*.
BEAM PROFILE MEASUREMENT USING CARBON NANOTUBE WIRES (3) - BEAM PROFILES IN HIGH ENERGY PART IN LINAC -
Proc. of the 15th Annual Meeting of PASJ, 1031

B-173
M. Okada, *et al*.
DUALIZE OF INTRA-BUNCH FEEDBACK SYSTEM IN J-PARC MR
Proc. of the 15th Annual Meeting of PASJ, 1044

B-174
Y. Nakazawa, *et al*.
COMMISSIONING OF THE DIAGNOSTIC BEAM LINE FOR THE MUON RF ACCELERATION WITH H- ION BEAM DERIVED FROM THE ULTRAVIOLET LIGHT
Proc. of the 15th Annual Meeting of PASJ, 1047

B-175
Y. Sue, *et al*.
J-PARC E34 EXPERIMENT: DEVELOPMENT OF THE GOOD TIME RESOLUTION MONITOR TO MEASURE THE LONGITUDINAL STRUCTURE OF LOW-RATE MUON BUNCH
Proc. of the 15th Annual Meeting of PASJ, 1051

B-176
K. Agari, *et al*.
TEMPERATURE MEASUREMENT OF BEAM DUMP AT J-PARC HADRON EXPERIMENTAL FACILITY
Proc. of the 15th Annual Meeting of PASJ, 1065

B-177
T. Sugimoto, *et al*.
MEASURES AGAINST BEAM LOSS DUE TO RESIDUAL MAGNETIZATION OF FERRITE FOR FAST EXTRACTION KICKER MAGNET OF J-PARC MAIN RING
Proc. of the 15th Annual Meeting of PASJ, 1082

B-178
Y. Tajima, *et al*.
DEVELOPMENT OF EPICS-BASED SOFTWARE OF TRIGGERED SCALER
Proc. of the 15th Annual Meeting of PASJ, 1091

B-179
K. Sato, *et al*.
DEMONSTRATIVE APPLICATIONS OF TRIGGERED SCALER IN J-PARC MR
Proc. of the 15th Annual Meeting of PASJ, 1095

B-180
T. Soma, *et al*.
APPLYING OF SYSTEM INVARIANT ANALYSIS TECHNOLOGY (SIAT) TO J-PARC ACCELERATOR SYSTEM
Proc. of the 15th Annual Meeting of PASJ, 114

B-181
Y. Kawabata, *et al*.
EXPERIMENTAL APPLICATION OF POSITIONING SENSOR NETWORK SYSTEM AND DISASTER PREVENTION APP IN J-PARC
Proc. of the 15th Annual Meeting of PASJ, 119

B-182
M. Uota, *et al*.
AFTER 10 YEARS, IS THERE ANY AGING DETERIORATION OF VACUUM SYSTEM AT J-PARC MR?
Proc. of the 15th Annual Meeting of PASJ, 1190

B-183
M. Otani, *et al*.
BEAM COMMISSIONING OF J-PARC MEBT1 FOR A HIGHER BEAM CURRENT
Proc. of the 15th Annual Meeting of PASJ, 216

B-184
Y. Sugiyama, *et al*.
THE FEEDBACK SYSTEM FOR THE LONGITUDINAL COUPLED BUNCH OSCILLATION IN J-PARC MR
Proc. of the 15th Annual Meeting of PASJ, 220

B-185
Y. Kurimoto, *et al*.
EVALUATION OF SLOW-EXTRACTED BEAM QUALITY WITH REAL-TIME BETATRON TUNE CORRECTION USING MAGNET CURRENT AT J-PARC MAIN RING
Proc. of the 15th Annual Meeting of PASJ, 225

B-186
Y. Fukao, *et al*.
MEASUREMENT OF PROTON BEAM PROFILE AT 8 GEV ACCELERATION COMMISSIONING FOR THE J-PARC COMET EXPERIMENT
Proc. of the 15th Annual Meeting of PASJ, 231

B-187
M. Tomizawa, *et al*.
8GeV-SLOW EXTRACTION TEST FOR MUON ELECTRON CONVERSION SEARCH EXPERIMENT
Proc. of the 15th Annual Meeting of PASJ, 235

B-188
R. Kitamura, *et al*.
DEMONSTRATION OF THE MUON RF ACCELERATION WITH THE NEGATIVE MUONIUM
Proc. of the 15th Annual Meeting of PASJ, 239

B-189
M. Shirakata, *et al*.
RADIATION MONITORING IN THE DOWNSTREAM AREA OF J-PARC MR COLLIMATORS
Proc. of the 15th Annual Meeting of PASJ, 267

B-190
R. Muto, *et al*.
BEAM COMMISSIONING OF SLOW EXTRACTION AT J-PARC MAIN RING
Proc. of the 15th Annual Meeting of PASJ, 305

B-191
K. Hara, *et al*.
STATUS REPORT OF DEVELOPMENT OF SECOND HARMONIC RF SYSTEM IN J-PARC MR
Proc. of the 15th Annual Meeting of PASJ, 312

B-192
Y. Morita, *et al*.
FUSE ARCING TEST FOR CAPACITOR BANK OF MAIN MAGNET POWER SUPPLY IN J-PARC MR
Proc. of the 15th Annual Meeting of PASJ, 319

B-193
Y. Arakaki, *et al*.
AN IMPROVEMENT AND HIGH VOLGAGE TEST OF TITANIUM-ESS IN J-PARC MR
Proc. of the 15th Annual Meeting of PASJ, 329

B-194
T. Yasui, *et al*.
MEASUREMENTS OF TUNE SHIFTS BY THE SPACE CHARGE EFFECT IN J-PARC MR
Proc. of the 15th Annual Meeting of PASJ,338

B-195
H. Watanabe, *et al*.
DESIGN OF BEAM WINDOW MADE OF BERYLLIUM AT J-PARC HADRON FACILITY
Proc. of the 15th Annual Meeting of PASJ, 388

B-196
H. Watanabe, *et al*.
DESIGN OF BEAM WINDOW MADE OF BERYLLIUM AT J-PARC HADRON FACILITY
Proc. of the 15th Annual Meeting of PASJ, 388

B-197
M. Furusawa, *et al*.
THE SPEEDUP FOR THE MACHINE PROTECTION SYSTEM ON THE RF ACCELERATING SYSTEM IN J-PARC MAIN RING
Proc. of the 15th Annual Meeting of PASJ, 480

B-198
D. Naito, *et al*.
PERFORMANCE ESTIMATION OF A NEW POWER SUPPLY WITH HIGH REPETITION RATE OPERATION IN J-PARC MR
Proc. of the 15th Annual Meeting of PASJ, 494

B-199
K. Okamura, *et al*.
DEVELOPMENT A PULSED POWER SUPPLY UTILISING 13 KV CLASS SIC-MOSFETS
Proc. of the 15th Annual Meeting of PASJ, 504

B-200
T. Shimogawa, *et al*.
DEVELOPMENT OF CHARGING CONTROL FOR FLOATING CAPACITOR METHOD
Proc. of the 15th Annual Meeting of PASJ, 508

B-201
T. Toyama, *et al*.
BEAM SIZE MEASUREMENT WITH THE BPMS IN THE J-PARC 3-50BT (2)
Proc. of the 15th Annual Meeting of PASJ, 537

B-202
S. Meigo, *et al*.
MEASUREMENT OF DISPLACEMENT CROSS SECTION OF PROTON FOR 0.4 - 3 GEV
Proc. of the 15th Annual Meeting of PASJ, 549

B-203
K. Okamura, *et al*.
A CONSIDERATION ON THE TRANSFER FUNCTION BETWEEN RQ FIELD AND SLOW EXTRACTION SPILL IN THE MAIN RING OF J-PARC
Proc. of the 15th Annual Meeting of PASJ, 558

B-204
K. Satou
GAMMA RAY IRRADIATION TEST OF PROTOTYPE CUIRCUIT OF THE PHOT-ODIODE BASED BEAM LOSS MONITOR FOR J-PARC MR
Proc. of the 15th Annual Meeting of PASJ, 569

B-205
N. Kamikubota, *et al*.
DEVELOPMENT OF SLOW-SAMPLING DIGITIZER FOR J-PARC MR
Proc. of the 15th Annual Meeting of PASJ, 587

B-206
A. Kobayashi, *et al*.
BUNCH TRAIN TUNE SHIFT STUDY FOR HIGHER BEAM POWER AT J-PARC MR
Proc. of the 15th Annual Meeting of PASJ, 60

B-207
A. Toyoda, *et al*.
DEVELOPMENT OF DATA ARCHIVE SYSTEM FOR J-PARC HADRON BEAMLINE(3)
Proc. of the 15th Annual Meeting of PASJ, 601

B-208
T. Kimura, *et al*.
DEVELOPMENT OF A MS-ABORT SYSTEM VIA J-PARC MR-MPS
Proc. of the 15th Annual Meeting of PASJ, 609

B-209
S. Yamada
REAL-TIME AND DETAILED PROVISION OF ACCELERATOR OPERATION INFORMATION FROM THE J-PARC ACCELERATOR CONTROL LAN TO THE J-PARC OFFICE LAN
Proc. of the 15th Annual Meeting of PASJ, 613

B-210
T. Michikawa, *et al*.
DEVELOPMENT OF WEB BASED ELECTRONIC LOG AND PICTURE LOG SYSTEMS
Proc. of the 15th Annual Meeting of PASJ, 617

B-211
H. Iinuma, *et al*.
DEVELOPMENT OF THREE-DIMENSIONAL SPIRAL BEAM INJECTION SCHEME WITH X-Y COUPLING BEAM FOR MRI SIZED COMPACT STORAGE RING CONFERENCES
Proc. of the 15th Annual Meeting of PASJ, 79

B-212
Y. Morita, *et al*.
DESIGN OF ACCELERATING CAVITY AND INPUT COUPLER FOR LONGITUDINAL EMITTANCE BLOW-UP IN J-PARC MR
Proc. of the 15th Annual Meeting of PASJ, 790

B-213
Y. Hashimoto, *et al*.
BEAM PROFILE MONITORS FOR SLOW EXTRACTED BEAM USING MULTI-LAYERED GRAPHENE IN THE J-PARC
Proc. of the 15th Annual Meeting of PASJ, 794

B-214
S. Igarashi, *et al*.
STUDY ON THE BEAM INTENSITY UPGRADE OF J-PARC MR
Proc. of the 15th Annual Meeting of PASJ, 799

B-215
H. Harada, *et al*.
DEVELOPMENT OF LASER SYSTEM FOR A PROOF-OF-PRINCIPLE EXPERIMENT OF LASER STRIPPING INJECTION
Proc. of the 15th Annual Meeting of PASJ, 811

B-216
H. Takahashi, *et al*.
DEVELOPMENT OF NEW PRODUCTION TARGET AT J-PARC HADRON EXPERIMENTAL FACILITY (2)
Proc. of the 15th Annual Meeting of PASJ, 879

B-217
T. Morishita, *et al*.
RF DESIGN AND TUNING OF THE J-PARC RFQ USING THREE-DIMENSIONAL MODELING
Proc. of the 15th Annual Meeting of PASJ, 914

B-218
M. Sawamura, *et al*.
DEVELOPMENT OF HOM COUPLER WITH C-SHAPED WAVEGUIDE
Proc. of the 15th Annual Meeting of PASJ, 934

B-219
Y. Yamamoto, *et al*.
RESEARCH ON CERAMIC AND COPPER PLATING FOR POWER COUPLERS
Proc. of the 15th Annual Meeting of PASJ, 938

B-220
K. Hasegawa, *et al*.
R&D STATUS OF 2ND HARMONIC RF CAVITIES WITH FT3M MA CORES AND A VACUUM CAPACITOR FOR J-PARC MR
Proc. of the 15th Annual Meeting of PASJ, 943

B-221
T. Shimogawa, *et al*.
STATUS OF NEW POWER SUPPLY FOR BENDING MAGNET IN J-PARC MAIN RING UPGRADE
Proc. of the 15th Annual Meeting of PASJ, 992

B-222
R. Kitamura, *et al*.
Muon acceleration test with the RFQ towards the development of the muon linac
Proc. of the 29th LINAC2018 (Internet), 342-345

B-223
M. Sato, *et al*.
Commissioning status of the linac for the iBNCT project
Proc. of the 29th LINAC2018(Internet), 174-176

B-224
Y. Nakazawa, *et al*.
Prototype of an Inter-digital H-mode drift-tube linac for muon linac
Proc. of the 29th LINAC2018(Internet), 180-183

B-225
K. Futatsukawa, *et al*.
Development of new LLRF system at the J-PARC linac
Proc. of the 29th LINAC2018(Internet), 233-235

B-226
H. Oguri
Approaches to high power operation of J-PARC accelerator
Proc. of the 29th LINAC2018(Internet), 29-34

B-227
T. Shibata, *et al*.
Numerical and experimental study of H– beam dynamics in J-PARC LEBT
Proc. of the 29th LINAC2018(Internet), 519-521

B-228
K. Hasegawa
Operation experiences of the J-PARC linac
Proc. of the 29th LINAC2018(Internet), 774-777

B-229
Y. Kondo, *et al*.
Low power measurement of a 1300-MHz RFQ cold model
Proc. of the 29th LINAC2018(Internet), 794-797

B-230
T. Morishita, *et al*.
Field tuning of a radio-frequency quadrupole using full 3D modeling
Proc. of the 29th LINAC2018(Internet), 798-801

B-231
M. Yoshimoto, *et al*.
Measurement of Radio-activation and Evaluation of Activated Nuclides due to Secondary Particles Produced in Stripper Foil in J-PARC RCS
Proc. of The 29th World Conference of the INTDS

B-232
M. Yoshimoto, *et al*.
Progress Status of Fabrication of Stripper Foils for 3 GeV RCS of J-PARC in Tokai-site
Proc. of The 29th World Conference of the INTDS

KEK Reports

C-001
T. Maruyama, *et al*.
12th KEK summer challenge in 2018
KEK Proc. 2018-8

JAEA Reports

D-001
H. Iwamoto, *et al*.
Assessment of Lead-bismuth-eutetic Leak at ADS Target Test Facility in Transmutation Experimental Facility of J-PARC
JAEA-Technol. 2017-029 (2018)

D-002
Safety Division
Annual Report on the Activities of Safety in J-PARC, FY2016
JAEA-Review 2017-033(2018)

Others

E-001
K. Shibata
The Implementaton of the dynamics analysis spetrometer DNA; The Pedigree of the backscattering neutron spectrometer
neutron network news

E-002
A. Dote
Book Reviews
Butsuri Vol. 73 No. 6, 401

D-003
M. Otani, *et al*.
RF Acceleration of Muon for the Realization of Precise
Measurements of Muon g–2/EDM
Butsuri Vol. 73 No. 8, 564

E-004
H. Suzuki, *et al*.
Non-Destructive Bond Stress Evaluation of Bending and Shear Deformed Reinforced Concrete Structure using Neutron Diffraction
journal of N.D.I

E-005
M. Inagaki
Muon Transfer Rates from Muonic Hydrogen Atoms to Gaseous Benzene and Cyclohexane
JNRS

E-006
M. Tomizawa
8 GeV Slow Extraction Beam Test for COMET Experiment
Journal of PASJ, Vol. 15, No. 3, 117

E-007
M. Otani, *et al*.
Muon Acceleration Using a Linac
Journal of PASJ, Vol. 15, No. 2, 60

E-008
H. Harada, and K. Sakaue
Young Researchers Association of the Japan Beam Physics Club
Journal of PASJ, Vol. 15, No. 3, 143

E-009
S. Sato, *et al*.
In-situ Observation of Dislocation Evolution in Ferritic and Austenitic Stainless Steels under Tensile Deformation by Using Neutron Diffraction
Tetsu-to-Hagane

J-PARC Annual Report 2018
Vol.1: Highlight

January 2020

J-PARC

JAPAN PROTON ACCELERATOR RESEARCH COMPLEX

High Energy Accelerator Research Organization (KEK)
Japan Atomic Energy Agency (JAEA)

2-4 Shirakata, Tokai-mura, Naka-gun, Ibaraki 319-1195, Japan

http://j-parc.jp/